Dissertation

submitted to the

Combined Faculties for the Natural Sciences and for Mathematics

of the Ruperto-Carola University of Heidelberg, Germany

for the degree of

Doctor of Natural Sciences

Presented by

M.Sc. Manuela Nickl

born in: Mühlacker, Germany

oral examination: 26.03.2019

Targeted cleavage of the HIV-1 genome in human cells using AAV-delivered CRISPR/Cas9

For my family

Summary

More than 30 years after the discovery of HIV-1 as the causative agent of AIDS, the disease can still not be cured and is responsible for around 940,000 deaths worldwide in 2017. Antiretroviral therapy, which was started in 1995, rapidly decreased mortality and increased life expectancy. ART is a life-long therapy since treatment interruption leads to rapid rebound of viral loads due to long-lived latently infected cells mainly represented by resting CD4$^+$ T cells. Since ART can have severe side effects and resistant viruses can evolve under suboptimal treatment, there is an urgent need for a cure, which can only be achieved by eradicating the latent reservoir. A promising strategy to do so is to functionally inactivate the latent HIV-1 provirus by mutating different sites of the proviral genome with the help of site-specific designer nucleases. In this work a CRISPR/Cas9 system was established, which is delivered into target cells with AAV vectors and allows simultaneous targeting of three sites of the HIV-1 proviral genome. The gRNAs designed for this purpose were shown to successfully edit the HIV-1 LTRs, *pol* and *gag* in a HeLaP4 reporter cell line (HeLaP4-NLtr) with an integrated HIV-1 provirus and in J-Lat T cells, which harbor a latent HIV-1 provirus. Different gRNA combinations were cloned into gRNA multiplexing constructs which allow the expression of up to three gRNAs. These constructs were shown to edit different sites of the provirus simultaneously and facilitate the excision of proviral fragments between different gRNA target sites in HeLaP4-NLtr and J-Lat cells. In J-Lat cells we could additionally show excision of the whole proviral sequence between the LTRs upon treatment with our constructs. Furthermore, the constructs protected HeLaP4 cells against HIV-1 infection and reduced the population of HIV-1 infected cells by up to 80 %. In addition, the amount of released infectious viral particles was reduced by up to 100-fold. To show that our system enables the functional inactivation of latent HIV-1, J-Lat T cells were treated with the gRNA multiplexing constructs and Cas9 followed by transcriptional activation of the provirus. Indeed, viral release was significantly reduced by up to 74 %. To enable the application of our CRISPR system in primary human CD4$^+$ T cells, different AAV serotypes were compared for efficient transduction and AAV6 was shown to enable transduction of up to 60 % of the cells. Nevertheless, pretreatment with our three most effective gRNA multiplexing constructs and Cas9 did not protect the cells against HIV-1 infection, which is possibly caused by low Cas9 expression levels observed in these cells. Collectively, we established a CRISPR/Cas9 system that enables simultaneous editing of up to three sites in the HIV-1 proviral genome, the excision of proviral fragments or of the whole proviral genome, thereby facilitating the protection against HIV-1 infection and functional inactivation of the latent provirus in human cell lines.

Zusammenfassung

Mehr als 30 Jahre nach der Identifizierung von HIV als Erreger von AIDS, gilt die Krankheit immer noch als unheilbar und hat im Jahr 2017 weltweit circa 940.000 Todesopfer gefordert. Die seit 1995 eingesetzte antiretrovirale Therapie (ART) hat zu einer schnellen Reduktion der Mortalität und zu einer gesteigerten Lebenserwartung geführt. Die Therapie muss jedoch ein Leben lang erfolgen, da eine Unterbrechung der Behandlung zu einer raschen Zunahme der Viruslast führt. Dies wird durch ein Reservoir latent infizierter Zellen mit einer langen Lebensdauer, hauptsächlich repräsentiert durch ruhende CD4$^+$ T-Zellen, verursacht. Da ART starke Nebenwirkungen haben kann und unter suboptimaler Behandlung resistente Viren entstehen können, herrscht ein dringender Bedarf nach einer heilenden Therapie, die nur durch die Beseitigung des latenten Reservoirs erzielt werden kann. Eine vielversprechende Strategie ist es, Mutationen an mehreren Stellen des proviralen Genoms mithilfe spezifischer Nukleasen einzubringen und so die funktionelle Inaktivierung des Provirus zu erzielen. In dieser Arbeit wurde ein CRISPR/Cas9-System entwickelt, das mittels AAV-Vektoren in die Zielzellen eingebracht wird und bis zu drei Stellen des HIV-1-Provirus gleichzeitig mutieren kann. Es wurde gezeigt, dass die für diesen Zweck entwickelten gRNAs die HIV-1 LTRs, *gag* und *pol* in einer HeLaP4 Reporterzelllinie mit einem integrierten HIV-1-Provirus und in J-Lat-Zellen, die ein latentes HIV-1-Provirus enthalten, mutieren können. Verschiedene gRNA-Kombinationen wurden in gRNA-Multiplexingkonstrukte kloniert, welche die bis zu drei gRNAs exprimieren. Wir konnten zeigen, dass diese Konstrukte sowohl das gleichzeitige Mutieren des HIV-1 Genoms an verschiedenen Stellen als auch das Ausschneiden proviraler Fragmente zwischen verschiedenen gRNA-Bindestellen in HeLaP4-NLtr- und J-Lat-Zellen ermöglichen. In J-Lat-Zellen konnten wir zudem das Ausschneiden der kompletten proviralen Sequenz zwischen den LTRs nach Behandlung mit unseren Konstrukten nachweisen. Außerdem bot die Vorbehandlung von HeLaP4-Zellen mit unseren Konstrukten schützende Wirkung gegen eine Infektion mit HIV-1 und reduzierte die Population HIV-infizierter Zellen um bis zu 80 %. Weiterhin wurde die Menge an freigesetzten infektiösen viralen Partikeln bis zu 100-fach reduziert. Um zu analysieren, ob unser System das latente Provirus funktionell inaktivieren kann, wurden J-Lat-Zellen mit unseren Konstrukten behandelt und darauffolgend die provirale Transkription aktiviert. Dies führte zu einer Reduktion freigesetzter viraler Partikel um bis zu 74 %. Um die Anwendung unseres CRISPR-Systems in primären humanen CD4$^+$ T-Zellen zu ermöglichen, wurden verschiedene AAV-Seroptypen bezüglich ihrer Transduktionseffizienz untersucht und es wurde gezeigt, dass AAV6 bis zu 60 % der Zellen transduziert. Dennoch konnte die Behandlung mit den drei effizientesten Konstrukten die Zellen nicht gegen eine

HIV-Infektion schützen, was möglicherweise auf ein geringes Cas9-Expressionlevel in diesen Zellen zurückzuführen ist. Zusammenfassend wurde in dieser Arbeit ein CRISPR/Cas9-System entwickelt, welches gleichzeitig bis zu drei Stellen im proviralen Genom editieren, provirale Fragmente und das vollständigen Provirus ausschneiden kann und somit sowohl den Schutz vor einer HIV-Infektion als auch die funktionelle Inaktivierung des latenten HIV-1-Provirus in humanen Zellen ermöglicht.

Contents

Figures

Tables

Abbreviations

AAP	Assembly-activating protein
AAV	Adeno-associated virus
AIDS	Acquired immunodeficiency syndrome
APC	Antigen-presenting cell
ART	Antiretroviral therapy
ATP	Adenosine Triphosphate
bGH	Bovine growth hormone
CA	Capsid
Cas	CRISPR-associated genes
CCR5	C-C Motif Chemokine Receptor 5
CD4	Cluster of differentiation 4
cDNA	Complementary DNA
ChIP-Seq	Chromatin immunoprecipitation sequencing
CMV	Cytomegalovirus
CRISPR	Clustered regularly interspaced short palindromic repeat
crRNA	CRISPR RNA
CXCR4	C-X-C Motif Chemokine Receptor 4
DARPin	Designed Ankyrin Repeat Proteins
dCas9	Cleavage-deficient Cas
ddPCR	Digital droplet PCR
DMEM	Dulbecco's Modified Eagle Medium
DNA	Deoxyribonucleic acid
dNTP	Deoxynucleoside triphosphate
dsDNA	Double-stranded DNA
DTT	Dithiothreitol
dUTP	Deoxyuridine triphosphate
EFS	Elongation factor 1α short
ELISA	Enzyme-Linked Immunosorbent Assay
Env	Envelope
EP	Error-prone PCR
ESCRT	Endosomal sorting complex required for transport

FBS	Fetal bovine serum
FISH	Fluorescence in situ hybridization
Gag	Group-specific antigen
GFP	Green fluorescent protein
gRNA	GuideRNA
GUIDE-Seq	Genome-wide Unbiased Identification of DSBs Enabled by Sequencing
HDAC	Histone deacetylase
HEK	Human embryonic kidney
Hela	Henrietta Lacks
HIV-1	Human immunodeficiency virus type 1
HR	Homologous recombination
HSPCs	Hematopoietic stem and progenitor cells
IN	Integrase
ITR	Inverted terminal repeats
LB	Lysogeny broth
LRA	Latency-reversing agent
LTR	Long terminal repeat
MA	Matrix
MHC	Major histocompatibility complex
min-polyA	Minimal polyadenylation signal
MOI	Multiplicity of infection
NC	Nucleocapsid
nCas9	Nickase Cas9
Nef	Negative factor
NFAT	Nuclear factor of activated T-cells
NF-κB	Nuclear factor kappa-light-chain-enhancer of activated B-cells
NHEJ	Non-homologous end joining
nt	Nucleotides
ORF	Open reading frame
PAM	Protospacer-adjacent motif
PBS	Phosphate-buffered saline
PCR	Polymerase chain reaction
PEI	Polyethylenimine
PGK	Phosphoglycerate kinase

PHA	Phytohemagglutinin
Pol	Polymerase
PR	Protease
Rev	Regulator of expression of virion proteins
RNA	Ribonucleic acid
RNP	Ribonucleoprotein
RPMI	Roswell Park Memorial Institute
RPP30	Ribonuclease P protein subunit p30
RSV	Respiratory syncytial virus
RT	Room temperature; reverse transcriptase
SFFV	Spleen focus-forming virus
shCMV promoter	Short cytomegalovirus promoter
SV40	Simian virus 40
Syn	Synapsin
TALEN	Transcription activator-like effector nuclease
TAR	Trans-activation response
Tat	Trans-activator of transcription
TK	Thymidine kinase
TNFα	Tumor necrosis factor alpha
TPA	12-O-Tetradecanoylphorbol-13-acetate
tracrRNA	Trans-activating crRNA
v/v	Volume per volume
Vg	Viral genomes
Vif	Viral infectivity factor
VP	Viral (capsid) protein
Vpr	Viral protein R
Vpu	Viral protein U
w/v	Weight per volume
YFP	Yellow fluorescent protein
ZFN	Zinc-finger nuclease

1. Introduction

1.1 The Human Immunodeficiency Virus type 1

1.1.1 Genome and life cycle

The human immunodeficiency virus (HIV) is the causative agent of the human acquired immunodeficiency syndrome (AIDS) and belongs to the genus *Lentivirus* of the family *Retroviridae* [1, 2]. Its genome consists of two identical single-stranded RNA molecules and is composed of the three major genes *gag* (group-specific antigen), *pol* (polymerase) and *env* (envelope), that encode structural proteins, and of genes encoding the regulatory and accessory proteins Vif (viral infectivity factor), Vpr (viral protein R), Vpu (viral protein U), Tat (trans-activator of transcription), Rev (regulator of expression of virion proteins) and Nef (negative factor) [3, 4] (figure 1.1). The coding regions are flanked by two long terminal repeats (LTRs), which are important for reverse transcription, packaging, integration and also have promoter functions. *Env* encodes the glycoproteins gp41 and gp120 that bind to receptors on the host cell and mediate fusion with the viral membrane. *Pol* encodes the integrase (IN), the protease (PR) and the reverse transcriptase (RT) and *gag* encodes the matrix (MA) protein p17, the capsid (CA) protein p24, the nucleocapsid (NC) protein p7 and the budding protein p6 [3, 4].
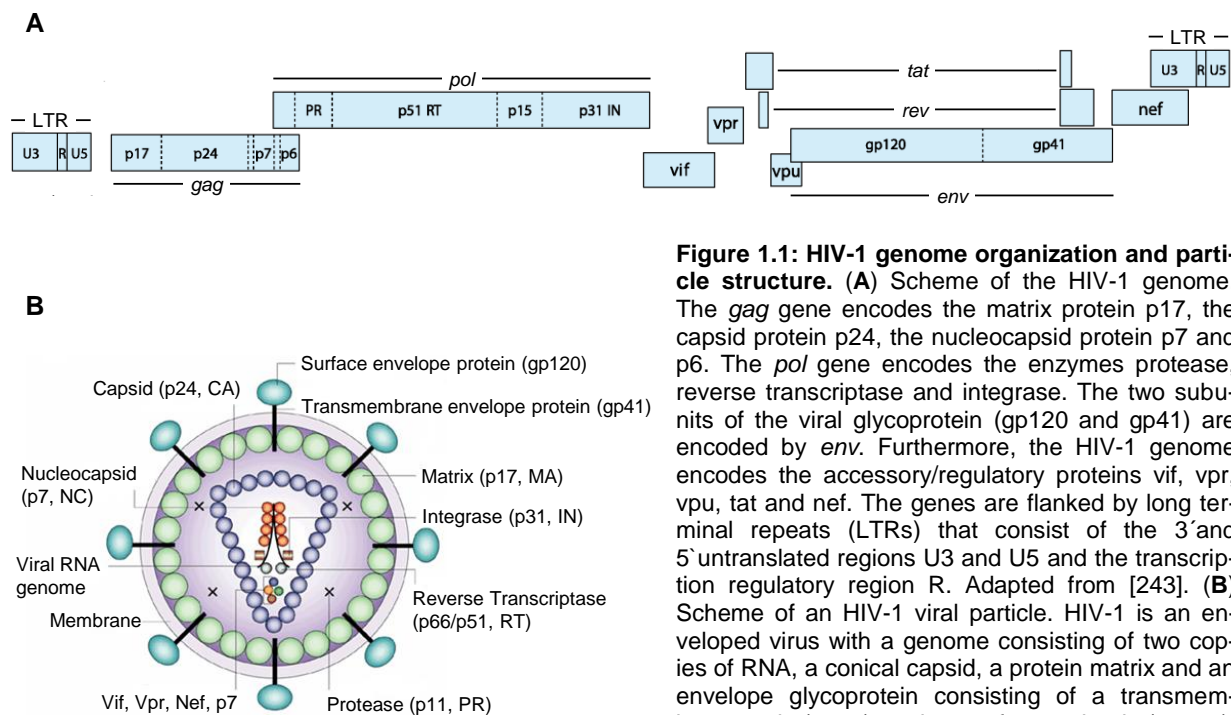
Figure 1.1: HIV-1 genome organization and particle structure. (**A**) Scheme of the HIV-1 genome. The *gag* gene encodes the matrix protein p17, the capsid protein p24, the nucleocapsid protein p7 and p6. The *pol* gene encodes the enzymes protease, reverse transcriptase and integrase. The two subunits of the viral glycoprotein (gp120 and gp41) are encoded by *env*. Furthermore, the HIV-1 genome encodes the accessory/regulatory proteins vif, vpr, vpu, tat and nef. The genes are flanked by long terminal repeats (LTRs) that consist of the 3´and 5`untranslated regions U3 and U5 and the transcription regulatory region R. Adapted from [243]. (**B**) Scheme of an HIV-1 viral particle. HIV-1 is an enveloped virus with a genome consisting of two copies of RNA, a conical capsid, a protein matrix and an envelope glycoprotein consisting of a transmembrane unit (gp41) and a surface subunit (gp120). Adapted from [244].

The HIV-1 life cycle is composed of different steps: Entry, reverse transcription of the viral RNA, integration of the viral genome into the host genome, transcription and translation of the viral genes and assembly and budding of new viral particles (figure 1.2). The HIV-1 infection starts with the binding of gp120 to CD4 (cluster of differentiation 4) and to one of the co-receptors CXCR4 (C-X-C Motif Chemokine Receptor 4) or CCR5 (C-C Motif Chemokine Receptor 5) on its target cells and the subsequent fusion of the viral and cellular membranes [5]. After fusion, the viral core is released into the cytoplasm and the viral genome is reversely transcribed into dsDNA by the viral RT [6]. This DNA is then transported to the nucleus together with the integrase and other proteins. The integrase processes the 3´ ends of the viral DNA thereby creating sticky ends and cuts the host DNA. Finally, it joins the ends of the viral and the host DNA together [7].
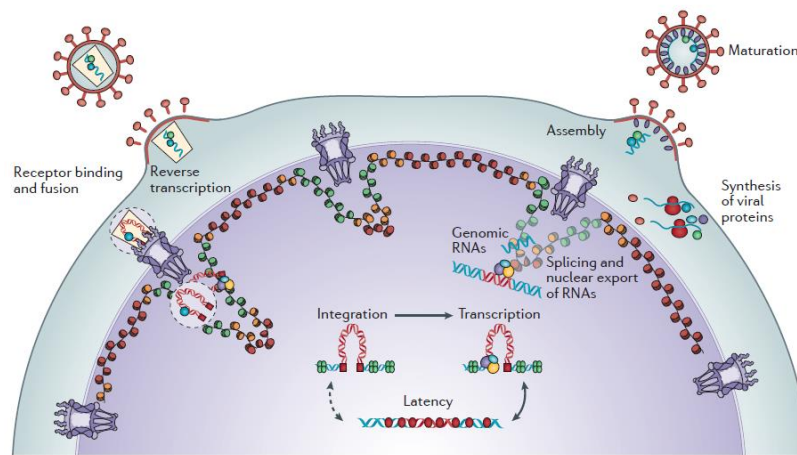
Figure 1.2: HIV-1 life cycle. After binding of the viral envelope protein to CD4 and co-receptors on the target cell, the viral membrane fuses with the cellular membrane and the capsid enters the cytoplasm. The RNA genome is reversely transcribed into double-stranded DNA and imported to the nucleus where it integrates into the cellular genome with the help of the viral integrase. In the case of latency the transcription of the integrated viral DNA (provirus) is blocked by several mechanisms. Otherwise the provirus is transcribed, the RNAs are exported to the cytoplasm and translated. Viral proteins assemble at the cellular membrane and new viral particles bud from the cell. After maturation through cleavage of the Gag precursor protein by the viral protease the particles can infect other cells. Taken from [7].

The stably integrated viral genome, also called "provirus", stays in a transcriptionally silent state in case of a latent infection or is transcribed by the cellular RNA polymerase II in case of a productive infection. The initial transcription results in the production of short fully spliced mRNAs that encode Nef, Rev and Tat [8]. Tat binds the trans-activation response (TAR) element of the LTR and enhances its promoter function by promoting the production of longer transcripts encoding Env, Vif, Vpu, Vpr and the Gag-Pol-polyprotein [9–12]. These longer transcripts are then exported to the cytoplasm with the help of Rev and are translated [13]. The mRNA encoding Gag and Pol can be translated into a Gag precursor containing CA, MA, NC and p6 domains or due to a frameshift event into a Gag-Pol-precursor protein, which additionally contains the viral

enzymes [14]. Env is also translated as a precursor protein from ribosomes associated with the endoplasmic reticulum. The precursor protein gp160 is cleaved by a cellular protease in the Golgi apparatus into gp41 and gp120 [15, 16]. After translation of the viral proteins, Env, the Gag- and Gag-Pol-precursor proteins are recruited to the cell membrane. NC interacts with the viral RNA thereby facilitating its packaging into the viral particles [17] and p6 recruits the cellular ESCRT (endosomal sorting complex required for transport) machinery that mediates the release of viral particles [18, 19]. During viral release the viral protease cleaves Gag and the Gag-Pol-precursor at several sites, which leads to a rearrangement of the proteins in the viral particle and thereby to the formation of mature particles that can infect other cells [20–23].

1.1.2 Antiretroviral therapy and latency

After over 30 years of HIV research there is still no cure available against HIV-1 infections. However, since the middle of the 1990s HIV-1 infections can be treated with so called combination antiretroviral therapy (ART) [24]. This therapy uses at least three drugs that target different steps of the viral life cycle thereby inhibiting the infection of new cells. ART decreases the viral load below detection limit and leads to a decreased mortality and improved life quality among HIV-1-infected patients [25–28]. Although ART effectively decreases viremia, interruption of treatment leads to a rapid rebound of viral loads [29, 30]. The rebound of viral loads after treatment interruption is thought to come from reservoirs of long-lived latently infected cells. In 1995, Chun et al. [31] isolated resting CD4$^+$ T cells from HIV-1-infected patients and showed that they contain HIV-1 DNA. Furthermore, they showed that this provirus was replication competent after activation of the cells. Over 20 years later, resting CD4$^+$ T cells are still considered to be the largest latent HIV-1 reservoir. Even if it is probable that other cells like macrophages serve additionally as latent reservoirs for HIV-1, this has not been finally proven [32]. As HIV-1 does not efficiently infect resting CD4$^+$ T cells [33–35], the current model for the establishment of the latent reservoirs is, that HIV-1 infects activated CD4$^+$ T cells and some of them survive long enough to revert to a resting state and persist as memory cells. These cells have only low levels of the transcription factors NFAT (nuclear factor of activated T-cells) and NF-κB (nuclear factor kappa-light-chain-enhancer of activated B-cells) and of deoxynucleosides, which are necessary for the transcription of the HIV provirus [36–41]. Other mechanisms contributing to the latent state of HIV-1 in resting CD4$^+$ T cells include epigenetic modifications through histone deacetylases (HDACs) [42, 43] and DNA methylation of CpG islands at the HIV-1 transcription start site [44, 45].

The HIV-1 latent reservoir is very stable with a half-life of 44 months [31, 46, 47]. As a large fraction of HIV-1 proviruses in patients on ART have identical sequences [48, 49] and as this was also reported for replication deficient proviral sequences [48, 50], it is believed that proliferation of latently infected cells is one mechanism that contributes to the stability of the reservoir. Several studies indicate that this proliferation is mediated by integration of HIV-1 into genes associated with cell growth and oncogenesis [51–53]. Furthermore, it is suggested that homeostatic proliferation, which is induced by cytokines like IL-7 and IL-15, plays a role in maintaining the size of the reservoir [54–56]. Due to the remarkable stability of the HIV-1 latent reservoir, its clearance under ART might take around 73 years [46, 47]. Hence, ART is not curative and lifelong treatment is required. As ART can have serious side effects [57, 58] and resistance can occur under suboptimal treatment [59], the development of a cure against HIV-1 infections, which eliminates the latent HIV-1 reservoir, is of great interest.

1.1.3 Strategies to cure HIV-1 infections

Different strategies have been developed to eliminate or reduce the size of the latent reservoir and thereby achieve a cure for HIV-1 infections. The so-called "shock and kill" strategy uses latency-reversing agents (LRAs) to reactivate the transcription of the provirus in latently infected cells which corresponds to the "shock". Next, these cells are recognized and killed by the immune system or killed through viral cytopathic effects. LRAs include reagents influencing histone modifications like HDAC inhibitors [60–62] and reagents that activate cellular transcription factors like Prostratin which releases NF-κB from inactivating complexes [63]. However LRAs alone do not significantly decrease the size of the latent reservoir in HIV-1-infected patients [62, 64, 65] because the immune system is not efficient enough to kill the reactivated cells. Hence, it is suggested that LRAs should be combined with reagents enhancing the immune system like therapeutic vaccines, interferon or broadly neutralizing antibodies [32, 66].

The only reported patient who has ever been cured from HIV-1, is the so-called Berlin patient [67, 68]. He received an allogenic stem cell transplant from a donor with a homozygous 32 bp depletion in the CCR5 gene, a mutation that confers resistance against HIV infection [69]. Based on this case, other strategies for an HIV-1 cure attempt to isolate hematopoietic stem and progenitor cells (HSPCs) or CD4$^+$ T cells from HIV infected patients, disrupt the CCR5 locus with the help of designer nucleases like zinc-finger nucleases (ZFNs) and then reinfuse the cells back to the patient. Even if this strategy is very promising and clinical studies have been initiated, there are still open questions remaining, like for example how big the portion of CCR5-modified

cells needs to be to circumvent the further propagation of the virus and the opportunity to switch to X4 tropism or when to remove ART after transplantation to test for viral rebound [70].

Another strategy to cure HIV infections is to deliver recombinases or designer nucleases to the patient to excise the provirus from latently infected cells or to functionally inactivate it by introduction of double strand breaks at functionally or structurally important proviral sites. Karpinski et al. [71] developed Brec-1, a recombinase that specifically recognizes a highly conserved site in the HIV-1 LTRs and mediates the precise excision of the proviral genome from infected cells. Furthermore, they showed that engraftment of mice with CD4$^+$ T cells from HIV infected patients treated with lentiviral vectors encoding Brec-1 reduced the viral load below detection limit. In addition to the recombinase Brec-1, designer nucleases like ZFNs and transcription activator-like effector nucleases (TALENs) have been shown to facilitate excision or editing of the HIV-1 provirus in different human cell lines [72–76]. However, most studies that show editing of the HIV-1 provirus with site directed nucleases are based on CRISPR/Cas9. As this system can be very easily adapted to target a desired DNA sequence, it has become very popular for gene editing strategies including targeting the HIV-1 proviral genome. Three *in vivo* studies [77–79] in different mice models, which found that CRISPR/Cas9 enables excision of HIV-1 proviral DNA in several tissues and reduces viral loads, show the great potential of the system for targeting the HIV-1 provirus in infected individuals and give hope for the development of a CRISPR/Cas9-based cure against HIV-1 infections.

1.2 CRISPR/Cas

1.2.1 Origin

Clustered regularly interspaced short palindromic repeat (CRISPR) DNA sequences are part of a defense system against viral or plasmid invaders found in bacteria. These repeat sequences are interspaced by non-repetitive sequences called "spacers", which represent DNA sequences from past invaders that were integrated into the bacterial genome [80, 81], [82] (figure 1.3). Adjacent to the CRISPR sequences, well conserved CRISPR-associated genes (Cas) that encode a RNA-guided endonuclease are localized.

The spacer and repeat sequences are transcribed into CRISPR RNAs (crRNAs), loaded on the Cas proteins and guide the enzyme to complementary DNA sequences (protospacers), thereby mediating double strand cleavage and inactivation of invading sequences [83, 84]. Depending

on differences in the components and their functionality CRISPR systems from different bacteria can be divided into two classes [85–87]. Due to the simplicity of the class II system, which uses only one Cas protein (Cas9), it is the most commonly used system for gene editing. This chapter will focus only on the class II CRISPR system as this system was used in the following work.
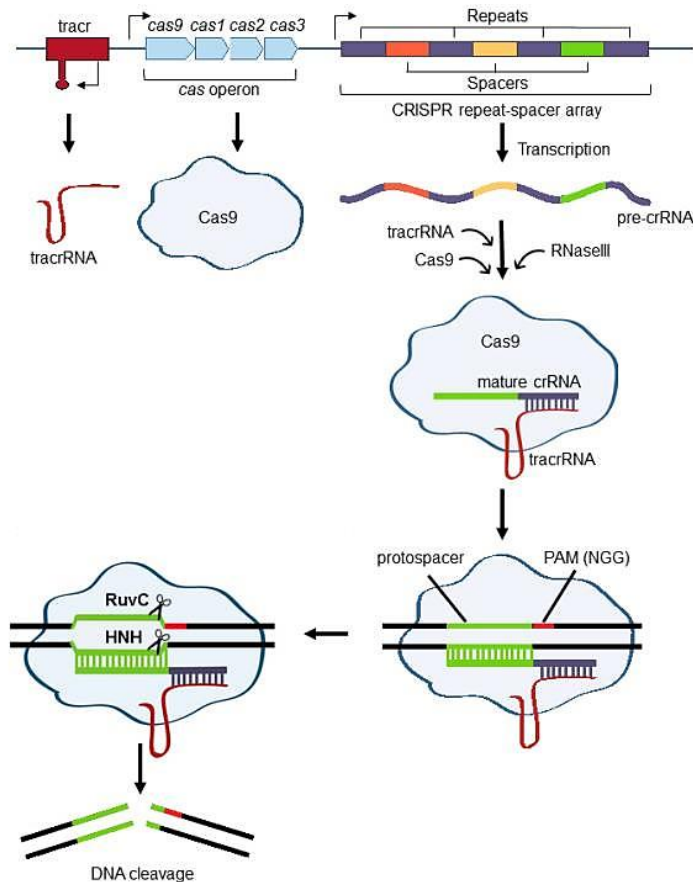
Figure 1.3: The class II CRISPR system. The CRISPR repeat and spacer sequences are transcribed into a pre-crRNA which is processed by a complex of Cas9 tracrRNA and RNaseIII to a mature crRNA consisting of only one spacer and one repeat. The tracrRNA hybridizes with the repeat of the crRNA and the tracrRNA interacts with the Cas9. Cas9 is guided to DNA that is complementary to the spacer sequence of the crRNA and adjacent to a PAM. Both DNA strands are cut by the RuvC and HNH (histidine-asparagine-histidine) domains of Cas9. Taken from [245].

In addition to the crRNA the class II CRISPR systems uses transactivating crRNAs (tracrRNAs) that hybridize with the repeat region of the crRNAs and mediate binding of the tracrRNA-crRNA complex to Cas9 [83, 88]. Cas9 only cleaves target sequences when they are adjacent to a so-called "protospacer-adjacent motif" (PAM) [89] that differs between CRISPR systems of different species. The most commonly used class II CRISPR system from *Streptococcus pyogenes* uses a 5´-NGG-3´ PAM and also recognizes a 5´-NAG-3´ PAM but with lower efficiency [90]. The cleavage of the protospacer sequence is mediated approximately 3 nucleotides away from the PAM [83, 84].

6

1.2.2 Gene editing with CRISPR/Cas9

To simplify the application of the CRISPR system for gene editing, Jinek *et al.* [83] showed that the tracrRNA-crRNA complex can be fused to one single guideRNA (gRNA). The resulting system consisting of only two components can be easily adapted to recognize any DNA sequence adjacent to the required PAM. In comparison to other designer nucleases used for gene editing like TALENs [91, 92] or ZFNs [93, 94], which are recognizing their target sequences trough protein-DNA interactions, CRISPR/Cas9 is based on Watson-Crick base pairing between the gRNA and the target DNA sequence and can thereby be easily adapted to target another sequence. Furthermore, by using more than one gRNA (gRNA multiplexing) CRISPR/Cas9 enables simultaneous editing at several target sites [95].

CRISPR/Cas9 can be used for different gene editing applications depending on which mechanism is used to repair the induced DNA double strand break (figure 1.4). The break can either be repaired by non-homologous end joining (NHEJ) or homologous recombination (HR) in eukaryotic cells.
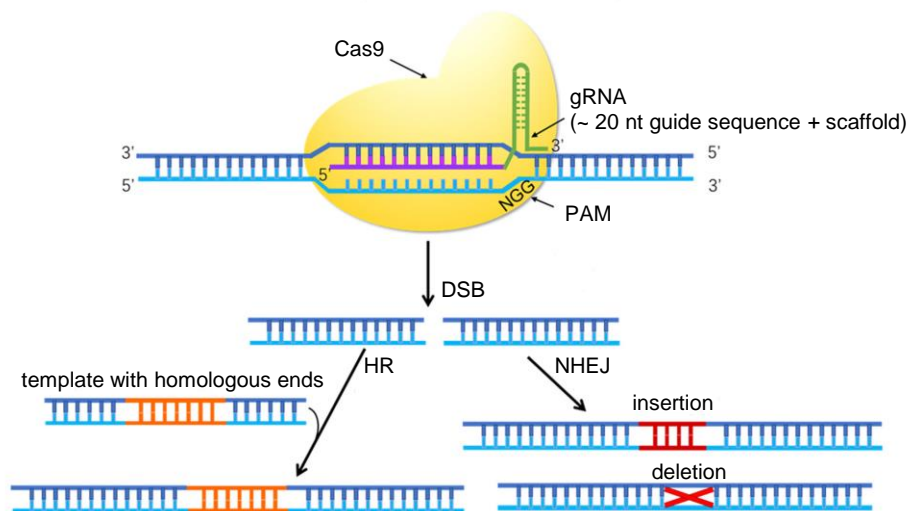
Figure 1.4: CRISPR/Cas9 as a tool for genome engineering. To simplify the application of CRISPR/Cas9 for genome engineering the tracrRNA and crRNA were fused to one single guideRNA (gRNA) consisting of an approximately 20 nt long guide sequence (purple) complementary to the target sequence and a scaffold (green) that is bound by Cas9. The DNA double strand break mediated by Cas9 can either be repaired by homologous recombination (HR) or non- homologous end joining (NHEJ). NHEJ leads to insertions or deletions at the target site. HR uses homologous templates to repair the break without any mutations. This repair pathway can be used to specifically integrate certain sequences at the target site. Adapted from [96].

NHEJ rejoins the break ends without the use of large homologies and usually leads to insertions or deletions at the cutting site [97]. Hence, this repair pathway can be used to knockout genes

by introducing a frameshift mutation or by mutating a structurally or functionally important region of the encoded protein. Furthermore, by using several gRNAs it is also possible to generate large deletions. For example, several studies have shown the deletion of several megabases in mice using CRISPR/Cas9 [98, 99]. In contrast to NHEJ, HR uses a homologous template (for example the sister chromatid) to repair the break without any mutations [97]. By offering a template with sequences homologous to the cutting site, this mechanism can be used to introduce reporter genes or site-specific mutations for example.

1.2.3 Targeting specificity of CRISPR/Cas9

As CRISPR/Cas9 is a very interesting tool for gene therapy applications, it is important to analyze the safety of the system with regard to unwanted off-target mutations, which could for example cause cancer or could have other unpredictable consequences.

Different methods have been established to detect cleavage at off-target sites. One example is chromatin immunoprecipitation sequencing (ChIP-Seq), a method for the analysis of DNA-Protein interactions, that has been adapted to identify binding sites of a cleavage-deficient Cas (dCas9) to genomic DNA [100–102]. Other methods tag DNA double strand breaks with known sequences, which allows the amplification of those sites with PCR and subsequent sequencing. For example, GUIDE-Seq (Genome-wide Unbiased Identification of DSBs Enabled by Sequencing) is based on the integration of short double-stranded oligonucleotides via the cell`s own DNA repair machinery [103]. After shearing of the DNA, adapter ligation and amplification with primers binding the integrated oligo and the adapters, the PCR products are sequenced. Another method, that can be applied *in vivo*, tags DNA double-strand breaks using integrase-defective lentiviral vectors, that are integrated in DNA double strand breaks via NHEJ [104]. As an alternative to such sequencing-based methods fluorescence in situ hybridization (FISH) has also been described for the detection of CRISPR off-targets [105]. For this purpose DNA double strand breaks were marked with short DNA fragments, that were integrated via the cell`s DNA repair pathways, and later on these fragments were hybridized with fluorescently labelled probes.

A general rule about how many mismatches are tolerated by Cas9 does not seem to exist. While it has been shown that some target sites with 6 mismatches can still be cleaved by Cas9 [95, 106], others with only one mismatch are not cleaved anymore [107, 108]. It has been demonstrated by many studies that in general mismatches of nucleotides distal from the PAM are better tolerated than mismatches proximal to the PAM [83, 90, 109]. This is also in line with the

model that Cas9 scans the genome for PAM sequences and then unwinds the DNA starting at the PAM proximal region [110].

Several different strategies have been developed to reduce off-target effects of CRISPR/Cas9. For example, it has been reported that shortening the region complementary to the target site by 2 or 3 nt improves the on-target specificity, probably because less mismatches are tolerated by these truncated gRNAs [111]. Furthermore, addition of two unpaired guanines at the 5´ end of the gRNA has been shown to reduce off-target effects [112].

Another strategy is to develop re-engineered Cas9 variants with increased targeting specificity. For example, Kleinstiver et al. [113] changed four residues of SpCas9 that mediate contact to the phosphate backbone of DNA and thereby created SpCas9-HF1, which shows reduced cleavage at off-target sites. Slaymaker et al. [114] mutated residues in a groove of Cas9 that stabilizes DNA unwinding and created the more specific variants eSpCas9(1.0) and eSpCas9(1.1.).

Additionally, CRISPR-based double-nicking strategies have been developed to reduce cleavage at off-target sites. Using two gRNAs binding close to each other and recognizing opposite DNA strands in combinations with a nickase Cas9 (nCas9), which only cleaves one DNA strand, has been shown to decrease off-target effects [107, 115] . Also a fusion of a dCas9 and the endonuclease FokI in combination with two gRNAs targeting opposite DNA strands has been shown to reduce off-target activity [116, 117].

1.2.4 Delivery of the CRISPR/Cas9 system

The two components of the CRISPR/Cas9 system, the gRNA and Cas9, can be delivered into target cells in different forms. One possibility is to deliver DNA, for example a plasmid, that encodes Cas9 and the gRNA. In this case it is important to choose the right promoter according to the desired cell type. Furthermore, to ensure efficient expression of Cas9, the codons need to be optimized according to the organism from which the target cells originated. In addition Cas9 and the gRNA can also be delivered as RNAs. It was shown that RNA delivery results in a faster start of gene editing compared to the DNA delivery strategy probably because the transcription step is skipped with RNA delivery [118]. However, mRNA is less stable than DNA and can thereby be rapidly degraded. The third possibility is to deliver Cas9 and gRNA as ribonucleoprotein (RNP) [119, 120]. Here additionally the translation step is skipped making the process even

faster than with RNA delivery [118]. However it is challenging to deliver Cas9 as a protein due to the large size and the charge of the protein.

Several methods have been used so far to deliver the CRISPR components into the target cells. These methods can be divided into three groups: physical delivery, chemical delivery and viral delivery. The physical methods include electroporation, microinjection and hydrodynamic injection. Electroporation has been successfully used to transfer the CRISPR components as RNA, DNA and RNP but cell death can be induced [121–123]. Microinjection allows the precise dosage and localization of the CRISPR components in the cell but is time consuming and therefore not suited for high-throughput applications [124–126]. Hydrodynamic injection is a technique where high volumes of a DNA solution are injected intravenously with high pressure, which causes pores in the blood vessels allowing the DNA to reach the target tissue. The method has been successfully used to deliver Cas9 and gRNA into different tissues of mice [127–129] but as a volume of approximately 10 % of the body weight is needed, the method is currently restricted to the use with small animals.

Important chemical delivery methods include the encapsidation of the CRISPR components with lipid-based or polymeric carriers, that are positively charged and thereby bind the negatively charged DNA enabling the DNA to come close to the negatively charged cell membrane and finally being taken up by the cell via endocytosis [119, 130]. Also the delivery of Cas9 RNP complexed with gold nanoparticles via a membrane fusion based process has been described [131].

Although the previously described physical and chemical methods are suited for the work with cell culture, tissues or animal models, they cannot be used for therapeutic applications in humans. For this purpose, viral vectors have been used for decades. Therapeutic viral vectors represent viral particles that do not carry genes necessary for viral replication but instead carry a transgene of interest. Hence, the viral vector is able to enter the cell and deliver the transgene but cannot spread to other cells. The most popular viral vectors are based on lentiviruses and adeno-associated viruses (AAVs) and several studies have used these vectors for delivery of CRISPR/Cas9 [132]. Lentiviral vectors have a packaging capacity of around 9-10 kb and are able to infect dividing and non-dividing cells. Furthermore they integrate into the host genome enabling stable transgene expression but also bearing the risk of insertional mutagenesis [133]. AAV vectors are single-stranded DNA viruses with a packaging capacity of around 5 kb that do not integrate into the host genome, they show low immunogenicity, enable the transduction of dividing and non-dividing cells and are non-pathogenic [134]. As many serotypes are available, this vector system can be used for the transduction of various cell types. In addition, different

techniques have been developed to engineer new capsid variants thereby even broadening the host range [135].

1.3 Adeno-associated viruses (AAVs)

1.3.1 AAV life cycle

AAVs were first discovered in 1965 as a contaminant of adenovirus preparations [136]. AAVs belong to the family of *Parvoviridae* and are non-enveloped viruses with an icosahedral capsid and a single-stranded DNA genome [137, 138]. The genome has a size of approximately 4.7 kb and is composed of three open reading frames (*rep*, *cap*, AAP) that are flanked by two inverted terminal repeats (ITRs) with a length of around 145 bp (figure 1.5). The *rep* ORF encodes the four proteins Rep78, Rep68, Rep52 and Rep40, which are involved in the replication and packaging of the viral genome [139–141]. The *cap* ORF encodes the three proteins VP1, VP2 and VP3, which assemble to the AAV capsid in a VP1:VP2:VP3 ratio of approximately 1:1:10 [142–144]. The third ORF overlaps with *cap* and encodes the assembly-activating protein (AAP), which is involved in assembly of AAV particles. The two flanking ITRs are required for packaging and replication [145, 146].
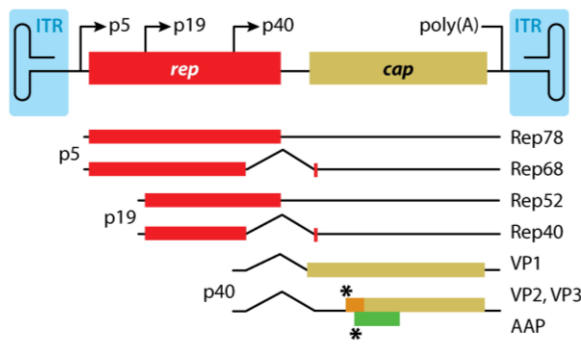
Figure 1.5: The AAV genome. The wildtype AAV genome consists of the two genes *rep* and *cap,* which are flanked by two inverted terminal repeats, that fold into hairpin structures. The promoter p5 drives the expression of mRNAs encoding Rep78 (unspliced) and Rep68 (spliced). The Rep52 (unspliced) and Rep40 (spliced) encoding mRNAs are expressed by the promoter p19. The p40 promoter drives the expression of mRNAs coding the capsid proteins VP1, 2 and 3 and the assembly activating protein AAP. VP2, VP3 and AAP are translated from the same mRNA. VP3 under the usage of a conventional AUG start codon, VP2 from a weak ACG start codon (asterisk) and AAP from a weak CTG start codon (asterisk). Taken from [159].

AAVs enter the cell via interactions with carbohydrates and different receptors on the cell surface. The sugar and receptor binding preferences differ among the 13 serotypes identified so far, due to differences in the capsid sequences [147]. After binding to the cell surface, the virus is taken up via endocytosis (figure 1.6). It has been shown that AAV seems to use different endocytic pathways like clathrin-mediated endocytosis [148], caveolae-mediated endocytosis [149] or

the Clathrin-Independent Carriers/GPI-Enriched Endocytic Compartment (CLIC/GEEC) endocytic pathway [150]. After entering the cell, AAV traffics to the Golgi apparatus [151–153] where it accumulates before it is released and enters the nucleus where the genome is uncoated [154, 155].
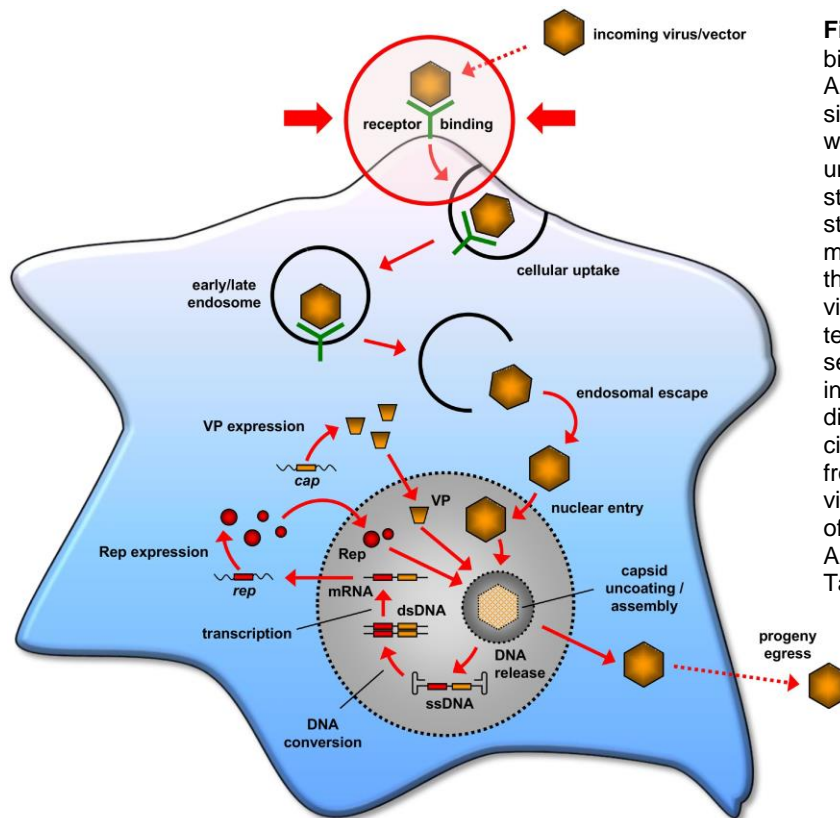
Figure 1.6: The AAV life cycle. After binding to receptors on the target cell, AAV is taken up by the cell via endocytosis and released into the cytoplasm from where it enters the nucleus where the uncoating takes place. The single-stranded DNA is converted to a double stranded DNA that is transcribed. The mRNA is exported from the nucleus to the cytoplasm and translated into the viral Rep and Cap proteins. These proteins enter the nucleus again and assembly of new viral particles takes place in the nucleolus. The light gray circle displays the nucleus and the dark gray circle displays the nucleolus. All steps from replication of the viral genome to viral release are only taking place in case of an infection with wildtype virus since AAV vectors do not encode viral proteins. Taken from [246].

If no helper virus, such as Adenovirus or Herpes simplex virus, is present in the cell, Rep mediates integration of the AAV genome into a certain locus of chromosome 19 where it stays transcriptionally silent [156–158]. However, in case of a co-infection with a helper virus AAV actively replicates. The AAV genome replicates via a so-called rolling hairpin mechanism during which the ITRs form a hairpin that creates a 3´-OH primer for second strand synthesis by the cellular DNA polymerase. Nicking of the double stranded DNA by Rep78 and Rep68 followed by single-strand displacement synthesis results in a newly formed double stranded molecule, which can be nicked again, starting a new cycle of DNA replication, and a displaced single strand, that can be packaged into capsids [159]. The assembly of the AAV capsid takes place in the nucleoli [146, 160]. The assembled capsids enter the nucleus and single-stranded DNA genomes are

pumped through a pore into the capsid by the helicases Rep52 and Rep40 [141]. Finally, the viral particles traffic to the cytoplasm and are released by helper virus induced cell lysis.

1.3.2 AAV vectors

AAV vectors usually contain a transgene flanked by ITRs. These vectors can either be produced by transfection or with packaging cell lines. For the transfection approach usually HEK293T cells are transfected with three plasmids. One containing the transgene flanked by ITRs, one containing genes of a helper virus and one encoding the Rep and Cap proteins [161–163]. Packaging cell lines contain one or more of the genetic components needed for AAV production stably integrated allowing large scale AAV production [164, 165].

Even if AAV vectors offer many advantages, there are also some limitations of these vectors and many strategies have been developed to overcome them. One such limitation is for example the second strand synthesis of the viral genome needed for transgene expression [166, 167]. This step, that slows down the initiation of transgene expression, can be overcome by using self-complementary (sc) AAV vectors [168]. These vectors can be produced by simply mutating the ITR so that nicking by Rep68 and Rep78 cannot be performed and double-stranded genomes will be packaged. ScAAV vectors have been shown to mediate faster initiation of transgene expression but only transgenes with half of the size of the conventional AAV genome can be expressed from these vectors [168]. Another limitation of AAV vectors is the packaging limit of around 5 kb [169–171]. To enable the expression of larger transgenes dual overlapping AAV vectors have been used [172, 173]. To generate such vectors, the two halves of a transgene with an overlapping part are packaged into separate particles. Inside the cell the full-length transgene can be restored through HR. In addition to these AAV genome engineering strategies also capsid engineering strategies have been developed to improve transduction efficiency and specificity or to reduce immunogenicity. Capsid engineering strategies can be divided into rational design approaches and directed evolution approaches.

Rational design approaches are based on knowledge about interaction of the capsid with certain ligands. For example, capsid residues that are marked for proteasomal degradation by certain enzymes have been exchanged to improve transduction efficiencies [174, 175]. Furthermore, Designed Ankyrin Repeat Proteins (DARPins) which are binding certain ligands, like CD4 for example, can be introduced into the capsid to specifically target the vectors to certain cell types [176].

Directed evolution strategies use libraries of capsid mutants to infect cells. Mutants able to produce progeny are enriched by several further rounds of infections and characterized by sequencing. The mutants are produced either by DNA shuffling, Error-prone PCR (EP) or AAV peptide display [124, 135]. DNA shuffling is based on the digestion of *cap* genes of many serotypes with nucleases. The fragments are then annealed based on sequence homologies and a primerless PCR is performed. The Error-prone PCR strategy uses a polymerase without proofreading activity to randomly introduce mutations into the *cap* gene. In the AAV peptide display method peptides of a random sequence are integrated into surface exposed positions of the capsid. This method resulted in the identification of many new serotypes with improved transduction efficiencies or altered tropism [135].

1.3.3 AAV vectors as a tool for gene therapy

To date, AAV vectors have been used in several preclinical and clinical gene therapy studies as they offer several properties that are advantageous for therapeutic applications. For example, AAV vectors have been used to recover vision in patients with homozygous recessive rpe65 deficiency that causes blindness in low light [177]. Furthermore the blood clotting disorder hemophilia B, that is caused by deficiency of the serum protein factor IX, has been treated using AAV vectors [178]. As AAV vectors don`t encode Rep, they don`t specifically integrate at chromosome 19 like the wildtype virus and preferentially stay episomal. Although random insertions have been reported, these only occur at a low rate of 0.1 % to 1 %, which makes AAV vectors safe in regard to deleterious insertional mutagenesis [179–181]. Furthermore, AAVs are not pathogenic and only cause a mild immune response [182, 183]. Even though AAVs do not stably integrate into the host genome, it has been shown that they mediate long-term transgene expression. For example in hemophilia B patients transgene expression was still detectable after 4 years in muscle and liver cells after one single treatment with AAV vectors [184] and in dogs treated with liver directed vectors transgene expression was still detectable after more than 8 years [185]. Although AAV vectors offer many advantageous properties for use in gene therapy, there are some hurdles that need to be overcome. For example as most humans (> 70%) are seropositive for different AAV serotypes [186, 187], neutralizing anti-AAV antibodies, which affect the efficient gene transfer, are a major limitation for the application in humans. However, by choosing an AAV serotype that is not highly prevalent in the human population or by engineering new capsid variants (chapter 1.3.2) that are resistant to neutralizing antibodies the limitations caused by pre-existing immunity can be overcome.

1.4 Aim of the thesis

The objective of this thesis was to develop a CRISPR/Cas9 system, which is delivered into HIV-1-infected cells using recombinant gene transfer vectors derived from AAVs, to target different regions in the proviral genome, thereby inhibiting the production of functional virions. The project is divided into three parts:

Part 1: CRISPR tool development

In this part of the project gRNAs targeting different sites in the HIV-1 provirus should be designed and cloned into AAV vectors mediating the expression of single gRNAs, kindly provided by Florian Schmidt (Grimm Group). Functional editing with the gRNAs in a HeLaP4 reporter cell line carrying an HIV-1 NL4-3 provirus stably integrated (HeLaP4-NLtr cells) and in J-Lat T cells that carry a GFP-tagged latent HIV-1 provirus [188] should be tested with T7 assay and functional gRNAs should be cloned into gRNA multiplexing AAV vectors that allow the expression of three gRNAs.

Part 2: Technology validation

Here, the previously established gRNA multiplexing vectors should be tested for editing and functional inactivation of the HIV-1 provirus in cell lines. Simultaneous editing at different proviral target sites should be analyzed in J-Lat cells and HeLaP4-NLtr cells using T7 assay. To further investigate if our system is able to functionally inactivate the HIV-1 provirus, J-Lat cells should be treated with our CRISPR/Cas9 vectors and imaged after activation of proviral transcription. Moreover, SG-PERT should be used to analyze the amount of viral particles released. Furthermore, HeLaP4 cells should be treated with our CRISPR/Cas9 vectors prior to HIV-1 infection to see if our system provides a protective effect against HIV-1 infection.

Part 3: Application in primary cells

Finally, the three best performing multiplexing constructs should be used to work with primary human $CD4^+$ T-cells. For this purpose different AAV serotypes should be tested for efficient transduction of these cells. Next, in a first proof of concept experiment, the cells should be treated with our CRISPR/Cas9 vectors prior to HIV-1 infection. To analyze the infection rate, cells should be stained for p24 and analyzed by FACS.

2. Materials and Methods

2.1 Materials

2.1.1 Antibodies

Table 2.1: Primary antibodies.

Name	Antigen	Host Species	Dilution	Manufacturer
KC57-FITC	HIV-1 p24	mouse	1:100	Beckman Coulter (Brea, USA)
MAK 183	HIV-1 p24	mouse	1:1000	Exbio Antibodies (Prague, Czech Republic)
Rabbit anti capsid	HIV-1 p24	rabbit	1:1000	Kräusslich and Müller lab, Centre for Infectious Dis-eas-es/ Virology Heidelberg
Sheep anti capsid	HIV-1 p24	sheep	1:500	Kräusslich and Müller lab, Centre for Infectious Dis-eases/ Virology Heidelberg

Table 2.2: Secondary antibodies.

Name	Host Species	Dilution	Manufacturer
Alexa Fluor® 647 anti-sheep IgG (H+L)	donkey	1:250	Thermo Fisher Scientific (Waltham, USA)
Peroxidase AffiniPure Goat Anti-Rabbit IgG (H+L)	goat	1:2000	Jackson Immu-noResearch (Ely, UK)

2.1.2 Bacterial strains

Table 2.3: Bacterial strains.

Name	Description	Source
E. coli ccdB SurvivalTM T1R	chemically competent	Life Technologies GmbH (Paisley, UK)
E. coli MAX Efficiency DH5aTM	chemically competent	Life Technologies GmbH (Paisley, UK)

2.1.3 Buffers

Table 2.4: Buffers.

Name	Composition	
Benzonase buffer (pH 8.5)	50 mM	Tris-HCl (pH 8.5)
	150 mM	NaCl
	2 mM	MgCl
10 x Dilution buffer for SG-PERT	50 mM	$(NH_4)_2SO_4$
	200 mM	KCl
	200 mM	Tris-HCl (pH 8.0)
Iodixanol (15 %)	25 % (v/v)	Iodixanol (Optiprep)
	75 % (v/v)	PBS-MK-NaCl
Iodixanol (25 %)	41.56 % (v/v)	Iodixanol (Optiprep)
	58.19 % (v/v)	PBS-MK
	0.25 % (v/v)	phenol red solution
Iodixanol (40 %)	66.67 % (v/v)	Iodixanol (Optiprep)
	33.33 % (v/v)	PBS-MK
Iodixanol (60 %)	99.75 % (v/v)	Iodixanol (Optiprep)
	0.25 % (v/v)	phenol red solution

Name	Composition	
Luciferase assay buffer	25 mM	Glycylglycine
	15 mM	KPO_4 buffer (pH 7.8)
	15 mM	$MgSO_4$
	4 mM	EGTA
Renilla Quenching buffer	1.1 M	NaCl
	2.2 mM	Na_2EDTA
	0.22 M	K_xPO_4 (pH 5.1)
	0.44 mg/ml	BSA
	1.3 mM	NaN_3
2 x Lysis buffer for SG-PERT	50mM	KCl
	100mM	Tris-HCl (pH 7.4)
	40 % (v/v)	Glycerol
	0.25 % (v/v)	Triton-X100
Lysogeny broth (LB) agar	1 % (w/v)	tryptone
	0.5 % (w/v)	yeast extract
	1 % (w/v)	NaCl
	1.5 % (w/v)	agar
Lysogeny broth (LB) media	1 % (w/v)	tryptone
	0.5 % (w/v)	yeast extract
	1 % (w/v)	NaCl
PBS (1x)	137 mM	NaCl
	3 mM	KCl
	10 mM	Na_2HPO_4
	2 mM	KH_2PO_4
PBS-MK	1x	PBS
	1 mM	$MgCl_2$
	2.5 mM	KCl
PBS-MK-NaCl	1x	PBS

Name	Composition	
	1 mM	MgCl$_2$
	2.5 mM	KCl
	1 M	NaCl
2 x Reaction buffer for SG-PERT	1x	Dilution buffer
	10 mM	MgCl$_2$
	2x	BSA
	400 µM	dNTPs
	7 pmoles/ml	MS2 RNA
	1:10.000	SYBR Green
	1 µM	primer RT-Assay-fwd
	1 µM	primer RT-Assay-rev
	2 % (w/v)	tryptone
	0.5 % (w/v)	yeast extract
	0.05 % (w/v)	NaCl
SOB media	2.5 mM	KCl
	10 mM	MgCl$_2$
	10 mM	MgSO$_4$
	2 % (w/v)	tryptone
	0.5 % (w/v)	yeast extract
	0.05 % (w/v)	NaCl
SOC media	2.5 mM	KCl
	10 mM	MgCl$_2$
	10 mM	MgSO$_4$
	20 mM	glucose
	2 M	Tris
	50 mM	EDTA
	1 M	acetic acid
TAE buffer (50x, pH 8.3)	2 M	Tris

Name	Composition	
	50 mM	EDTA
	5.71 % (v/v)	acetic acid

2.1.4 Cell culture media and additives

Table 2.5: Cell culture media, additives and transfection reagents.

Product	Company
12-O-Tetradecanoylphorbol 13-acetate (TPA)	Sigma-Aldrich (St. Louis, USA)8<
Dulbecco's Modified Eagle Medium (DMEM) with 4.5g/L D-Glucose and Glu-taMAX™	Thermo Fisher Scientic (Waltham, USA)
Dynabeads® Human T-Activator CD3/CD28	Thermo Fisher Scientic (Waltham, USA)
Fetal bovine serum (FBS)	
Interleukin-2, human (hIL-2) (10.000U/ml)	Sigma-Aldrich (St. Louis, USA)
Penicillin/Streptomycin (100x) (10.000 U/ml Penicillin and 10mg/ml Streptomycin)	Capricorn Scientific GmbH (Ebsdorfergrund, Germany)
Phytohemagglutinin-M (PHA-M)	Sigma-Aldrich (St. Louis, USA)
Polyethylenimine (PEI, linear, MW~25000)	Polyscience (Warrington, USA)
Recombinant Human TNF-alpha Protein	R & D Systems (Minneapolis, USA)
Roswell Park Memorial Institute (RPMI) medium 1640 with GlutaMAX™	Thermo Fisher Scientic (Waltham, USA)
TurboFect Transfection Reagent	Thermo Fisher Scientic (Waltham, USA)

2.1.5 Cell lines

Table 2.6: Cell lines.

Name	Origin	Description	Reference
C8166	*H. sapiens*	Human T cell leukemia cells containing a defective HTLV-1 genome. Derived by phusion of primary umbilical cord blood cells with a HTLV-1 producing line from an adult T cell leukemia lymphoma patient	[189]
HEK293T	*H. sapiens*	Human embryonic kidney cells expressing the SV40 large T-antigen	[190]
HeLaP4	*H. sapiens*	Cervical cancer epithelial cells isolated in 1951 from the patient Henrietta Lacks expressing CD4 and CXCR4	[191]
HeLaP4-pNltr	*H. sapiens*	Derivative of HeLaP4 cells carrying a replication-incompetent NL4-3 HIV-1 genome with deletions in *env*, *nef* and *tat* and a *gfp* reporter gene at the *nef* open reading frame	Provided by Dr, Jens Bohne
J-Lat	*H. sapiens*	Derivative of Jurkat T cell leukemia cells infected with HIV-R7/E-/GFP, which is a full length HIV-1 genome with a non-functional *env* due to a frameshift, and GFP in place of *nef*.	[188]
MT4	*H. sapiens*	HTLV-1 transformed human T cells isolated from a patient with adult T-cell leukemia	[192]

2.1.6 Chemicals and reagents

Table 2.7: Chemicals and reagents

Product	Company
3,3',5,5'-Tetramethylbenzidine	SERVA Electrophoresis (Heidelberg, Germany)
Adenosintriphosphat	Sigma-Aldrich (St. Louis, USA)
Agarose	Biozym Scientifc GmbH (Hessisch Oldendorf, Germany)
Albumin fraction V (BSA)	Roth (Karlsruhe, Germany)
Ammonium sulfate ($(NH)_4SO_4$)	Thermo Fisher Scientific (Waltham, USA)
Ampicillin	Roth (Karlsruhe, Germany)
Ampicillin	Roth (Karlsruhe, Germany)
Bacto^{TM} Agar	BD (Franklin Lakes, USA)
Bacto^{TM} Trypton	BD (Franklin Lakes, USA)
Bacto^{TM} Yeast Extract	BD (Franklin Lakes, USA)
Biocoll	VWR (Radnor, USA)
Bromophenol blue	Waldeck GmbH (Münster, Germany)
CellTiter 96® AQueous One Solution reagent	Promega (Madison, USA)
Chloramphenicol	Roth (Karlsruhe, Germany)
Coelenterazine	PJK GmbH (Kleinblittersdorf, Germany)
Dipotassium hydrogenphosphate (K_2HPO_4)	AppliChem (Darmstadt, Germany)
Dithiothreitol (DTT)	Sigma-Aldrich (St. Louis, USA)
D-Luciferin	PJK GmbH (Kleinblittersdorf, Germany)
dNTPs (dATP, dCTP, dGTP, dTTP)	Fermentas (St. Leon-Rot, Germany)
D-Sucrose	Roth (Karlsruhe, Germany)
Ethanol	Sigma-Aldrich (St. Louis, USA)
Ethidium bromide	Roth (Karlsruhe, Germany)
Ethylene glycol tetraacetic acid (EGTA)	Sigma-Aldrich (St. Louis, USA)
Ethylenediaminetetraacetic acid (EDTA)	Sigma-Aldrich (St. Louis, USA)

Product	Company
Ethylenediaminetetraacetic acid disodium salt dihydrate (Na$_2$EDTA)	Sigma-Aldrich (St. Louis, USA)
Gel Loading Dye, Purple (6X)	NEB (Frankfurt am Main, Germany)
Gelatine	Sigma-Aldrich (St. Louis, USA)
Glycerol	VWR (Radnor, USA)
Glycylglycin	Sigma-Aldrich (St. Louis, USA)
HEPES	Roth (Karlsruhe, Germany)
Hoechst 33258	Invitrogen / Life Technologies (Paisley, UK)
Hydrochloric acid (HCl)	Sigma-Aldrich (St. Louis, USA)
Iodixanol (OptiprepTM)	Axis-Shield (Oslo, Norway)
Isopropanol	Sigma-Aldrich (St. Louis, USA)
Magnesium chloride	AppliChem (Darmstadt, Germany)
Magnesium sulfate	Merck (Darmstadt, Germany)
MS2 RNA	Merck (Darmstadt, Germany)
Paraformaldehyde	Sigma-Aldrich (St. Louis, USA)
Passive Lysis 5X Buffer	Promega (Madison, USA)
Phenol red	Merck (Darmstadt, Germany)
Poly-L-lysine solution 0.1 % (w/v) in H$_2$O	Sigma-Aldrich (St. Louis, USA)
Potassium chloride (KCl)	AppliChem (Darmstadt, Germany)
Potassium dihydrogen phosphate (KH$_2$PO$_4$)	AppliChem (Darmstadt, Germany)
RiboLock RNase Inhibitor	Thermo Fisher Scientific (Waltham, USA)
Sodium azide (NaN$_3$)	Sigma-Aldrich (St. Louis, USA)
Sodium chloride (NaCl)	Sigma-Aldrich (St. Louis, USA)
Sodium hydroxide (NaOH)	Sigma-Aldrich (St. Louis, USA)
SYBR™ Green Nucleic Acid Gel Stain, 10,000X concentrate	Thermo Fisher Scientific (Waltham, USA)
TE buffer	Invitrogen / Life Technologies (Paisley, UK)

Product	Company
Tris	Roth (Karlsruhe, Germany)
Tris-HCl	Roth (Karlsruhe, Germany)
Triton-X100	Merck (Darmstadt, Germany)
Trypan blue solution 0.4 %	Sigma-Aldrich (St. Louis, USA)
Tween-20	Roth (Karlsruhe, Germany)

2.1.7 Consumables

Table 2.8: Consumables.

Name	Company
96-well black cell culture plates	Corning (New York, USA)
96-well cell culture plates with V-bottom	Corning (New York, USA)
96-well ddPCR plates	BioRad (Hercules, USA)
Cell culture dishes (Ø 6cm, 15cm)	Greiner Bio-One (Frickenhausen, Germany)
Cell culture flasks (25 cm^2 / 75 cm^2 / 175 cm^2)	Greiner Bio-One (Frickenhausen, Germany)
Cell culture plates with flat bottom (6-well /24-well/ 96-well)	Greiner Bio-One (Frickenhausen, Germany)
Cell lifter (18 cm)	Corning (New York, USA)
Centrifuge tubes (15 ml / 50 ml / 500 ml)	Greiner Bio-One (Frickenhausen, Germany), Corning (New York, USA)
DG8 cartridges and gaskets	BioRad (Hercules, USA)
Erlenmeyer flasks	Fisher Scientific (Schwerte, Germany)
Filter tips	Sorenson Bioscience (Murray, USA)
Glass bottles	DURAN Group (Wertheim/Main,

Name	Company
	Germany)
Glass culture tubes (16 x 160 mm)	DURAN Group (Wertheim/Main, Germany)
Microplates PS 96-well, F-bottom, white, LU-MITRAC™	Greiner Bio-One (Frickenhausen, Germany)
Needles (0.8 x 40 mm / 0.9 x 40 mm)	BD (Franklin Lakes, USA)
Nunc MaxiSorp™ flat-bottom 96-well plates	Thermo Fisher Scientific (Waltham, USA)
Open-Top Polyallomer tubes	Seton Scientific (Petaluma, USA)
Pasteur capillary pipettes (230 mm)	NeoLab (Heidelberg, Germany)
PCR tubes 0.5ml	Sarstedt (Nümbrecht, Germany)
Pierceable PCR plate heat foil	BioRad (Hercules, USA)
Reaction tubes (0.5 / 1.5 / 2 / 5 ml)	Sarstedt (Nümbrecht, Germany)
SepMate™-50	Stemcell Technologies (Vancouver, Kanada)
Serological pipettes	Sarstedt (Nümbrecht, Germany)
Steritop filter (0.22 µm)	Merck (Darmstadt, Germany)
SW 32 Ti Swinging-Bucket Rotor	Beckman Coulter (Brea, USA)
Syringe filter units (0.2 / 0.45 µm pore size)	Whatman / GE Healthcare (Buckinghamshire, UK)
Syringes (3 ml / 50 ml)	BD (Franklin Lakes, USA)
Ultracentrifuge tubes - iodixanol purification (16x76 mm)	Seton Scientific (Petaluma, USA)
Ultracentrifuge tubes - iodixanol purification (25x89 mm)	Beckman Coulter (Brea, USA)

2.1.8 Devices

Table 2.9: Devices.

Name	Supplier
Allegra X-12 Benchtop Centrifuge	Beckman Coulter (Brea, USA)
Bacterial incubator Heraeus Function Line	Thermo Fisher Scientific (Waltham, USA)
BD FACSVerse™ Flow Cytometer	BD Biosciences (Franklin Lakes, USA)
C1000 Touch™ Thermal Cycler	BioRad (Hercules, USA)
Centrifuge 5430 R	Eppendorf (Hamburg, Germany)
CFX96™ Real-Time PCR Detection System	BioRad (Hercules, USA)
Dual Block Thermocycler Mastercycler® nexus GX2	Eppendorf (Hamburg, Germany)
Eclipse Ti inverted microscope	Nikon (Tokyo, Japan)
Fixed angle JA-10 rotor	Beckman Coulter (Brea, USA)
Fixed angle type 70 Ti rotor	Beckman Coulter (Brea, USA)
Fixed angle type 70.1 Ti rotor	Beckman Coulter (Brea, USA)
Flow cytometer FC500 MPL	Beckman Coulter (Brea, USA)
Galaxy Mini Centrifuge C12xx	VWR (Radnor, USA)
Gel DocTM XR	BioRad (Hercules, USA)
GloMax 96 Microplate Luminometer	Promega (Madison, USA)
HERAcell 150 CO_2 Incubator	Thermo Fisher Scientific (Waltham, USA)
HERAsafe® sterile workbench	Thermo Fisher Scientific (Waltham, USA)
Inverted microscope CKX41	Olympus (Hamburg, Germany)
Microwave	Sharp Electronics (Hamburg, Germany)
MINI-SUB CELL GT	BioRad (Hercules, USA)
Mixing block MB-102	Biozym Scientific GmbH (Hessisch Oldendorf, Germany)
Multiskan Ascent Platereader	Thermo Fisher Scientific (Waltham, USA)
NanoDrop 2000 UV-Vis Spectrophotometer	Thermo Fisher Scientific (Waltham, USA)

Name	Supplier
Pipettes	Eppendorf (Hamburg, Germany)
PX1™ PCR Plate Sealer	BioRad (Hercules, USA)
QX200™ Droplet Generator	BioRad (Hercules, USA)
QX200™ Droplet Reader	BioRad (Hercules, USA)
Rotamax 120	Heidolph Instruments (Schwabach, Germany)
Rotor-Gene 6000	QIAGEN (Hilden, Germany)
ScanR microscope	Olympus (Hamburg, Germany)
Shaking Incubator Multitron	INFORS HT (Basel, Switzerland)
SUB CELL GT	BioRad (Hercules, USA)
Thermostatic waterbath	Fried Electric (Haifa, Israel)
Ultracentrifuge Optima L-90K	Beckman Coulter (Brea, USA)
Ultracentrifuge Optima LE80K	Beckman Coulter (Brea, USA)
Ultrasonic bath	BANDELIN (Berlin, Germany)
UV transilluminator UST-30M-8E	Biostep GmbH (Burkhardtsdorf, Germany)
Vortex mixer 7-2020	neoLab (Heidelberg, Germany)

2.1.9 DNA ladders

Table 2.10: DNA ladders.

Name	Supplier
1 Kb Plus DNA Ladder	Thermo Fisher Scientific (Waltham, USA)
100 bp DNA Ladder	Thermo Fisher Scientific (Waltham, USA)

2.1.10 Enzymes

Table 2.11: Enzymes.

Name	Supplier
Benzonase	Merck (Darmstadt, Germany)
GoTaq Hot Start DNA Polymerase	Promega (Madison, USA)
Phusion Hot Start Flex DNA Polymerase	NEB (Frankfurt am Main, Germany)
Restriction enzymes	NEB (Frankfurt am Main, Germany), Thermo Fisher Scientific (Waltham, USA)
T4 DNA Ligase	NEB (Frankfurt am Main, Germany)
T7 Endonuclease I	NEB (Frankfurt am Main, Germany)

2.1.11 GRNA constructs

Table 2.12: GRNA constructs.

Internal number	Name	Description
#3	H1Cas9_gRNA3	ssAAV vector for the expression of Cas9 from the 224bp CMV promoter and gRNA3 with standard scaffold from the H1 promoter
#5	H1Cas9_gRNA5	ssAAV vector for the expression of Cas9 from the 224bp CMV promoter and gRNA5 with standard scaffold from the H1 promoter
#6	H1Cas9_gRNA6	ssAAV vector for the expression of Cas9 from the 224bp CMV promoter and gRNA6 with standard scaffold from the H1 promoter
#7	H1Cas9_gRNA7	ssAAV vector for the expression of Cas9 from the 224bp CMV promoter and gRNA7 with standard scaffold from the H1 promoter

Internal number	Name	Description
#21	U6_gRNA3	scAAV vector for the expression of gRNA3 with standard scaffold from the U6 promoter
#23	U6_gRNA5	scAAV vector for the expression of gRNA5 with standard scaffold from the U6 promoter
#24	U6_gRNA6	scAAV vector for the expression of gRNA6 with standard scaffold from the U6 promoter
#25	U6_gRNA7	scAAV vector for the expression of gRNA7 with standard scaffold from the U6 promoter
#28	U6_E+F_gRNA3	scAAV vector for the expression of gRNA3 with F+E scaffold from the U6 promoter
#29	U6_E+F_gRNA5	scAAV vector for the expression of gRNA5 with F+E scaffold from the U6 promoter
#30	U6_E+F_gRNA6	scAAV vector for the expression of gRNA6 with F+E scaffold from the U6 promoter
#31	U6_E+F_gRNA7	scAAV vector for the expression of gRNA7 with F+E scaffold from the U6 promoter
#32	U6_gag17 (E+F)	scAAV vector for the expression of the gRNA p17 with F+E scaffold from the U6 promoter
#33	U6_gag24 (E+F)	scAAV vector for the expression of the gRNA p24_1 with F+E scaffold from the U6 promoter
#73	gagp24_1 (E+F)	scAAV vector for the expression of the gRNA p24_2 with F+E scaffold from the U6 promoter
#78	pol_3 (E+F)	scAAV vector for the expression of the gRNA int3 with F+E scaffold from the U6 promoter
#79	pol_4 (E+F)	scAAV vector for the expression of the gRNA int4 with F+E scaffold from the U6 promoter
#80	pol_5 (E+F)	scAAV vector for the expression of the gRNA int5 with F+E scaffold from the U6 promoter
#214	U6 gag1 E+F	scAAV vector for the expression of the gRNA gag1 with F+E scaffold from the U6 promoter
#215	M1	scAAV gRNA multiplexing vector for the expression of

Internal number	Name	Description
		g6 from the U6 promoter, int4 from the H1 promoter and gag1 from the 7SK promoter (named MP11 in this work)
#216	M2	scAAV gRNA multiplexing vector for the expression of p24_2 from the U6 promoter, int4 from the H1 promoter and gag1 from the 7SK promoter (named MP10 in this work)
#217	M3	scAAV gRNA multiplexing vector for the expression of gag1 from the U6 promoter, int4 from the H1 promoter and p24_2 from the 7SK promoter (named MP9 in this work)
#218	M4	scAAV gRNA multiplexing vector for the expression of g5 from the U6 promoter, int4 from the H1 promoter and gag1 from the 7SK promoter (named MP8 in this work)
#219	M5	scAAV gRNA multiplexing vector for the expression of gag1 from the U6 promoter, g3 from the H1 promoter and int4 from the 7SK promoter (named MP7 in this work)
#220	M6	scAAV gRNA multiplexing vector for the expression of gag1 from the U6 promoter, g5 from the H1 promoter and int4 from the 7SK promoter (named MP6 in this work)
#221	M7	scAAV gRNA multiplexing vector for the expression of gag1 from the U6 promoter, g6 from the H1 promoter and int4 from the 7SK promoter (named MP5 in this work)
#225	M9_Multi	scAAV gRNA multiplexing vector for the expression of g5 from the U6 promoter, g6 from the H1 promoter and gag1 from the 7SK promoter (named MP4 in this work)
#182	Multi_TRISPR/Cas_Flo gR6, gR6,gRgag17 (E+F)	scAAV gRNA multiplexing vector for the expression of g6 from the U6 promoter, p17 from the H1 promoter and g6 from the 7SK promoter (named MP3 in this work)
#183	Multi_TRISPR v2/K17	scAAV gRNA multiplexing vector for the expression of g6 from the U6 promoter, p24_2 from the H1 promoter

Internal number	Name	Description
		and g3 from the 7SK promoter (named MP2 in this work)
#184	Multi_TRISPR v2/K18	scAAV gRNA multiplexing vector for the expression of g6 from the U6 promoter, p24_2 from the H1 promoter and g5 from the 7SK promoter (named MP1 in this work)

2.1.12 Kits

Table 2.13: Kits.

Name	Supplier
Invisorb RNA Cell HTS 96-Kit	Stratec Molecular (Berlin, Germany)
Invisorb Spin Plasmid Mini Two	Stratec Molecular (Berlin, Germany)
InviTrap Spin Universal RNA Mini Kit	Stratec Molecular (Berlin, Germany)
NucleoBond AX 500	Macherey-Nagel (Düren, Germany)
NucleoBond PC 100	Macherey-Nagel (Düren, Germany)
PeqGOLD Tissue DNA Mini Kit	VWR (Radnor, USA)
Plasmid Plus Midi	QIAGEN (Hilden, Germany)
QIAquick Gel Extraction Kit	QIAGEN (Hilden, Germany)
QIAquick Nucleotide Removal Kit	QIAGEN (Hilden, Germany)
SensiMixTM II Probe No-ROX Kit	Bioline (London, UK)
Verso cDNA synthesis Kit	Thermo Fisher Scientific (Waltham, USA)
TURBO DNA-free™ Kit.	Thermo Fisher Scientific (Waltham, USA)

2.1.13 Oligonucleotides

Table 2.14: Oligonucleotides.

Name	Sequence (5´→3´)
958	CGGCGGGATCCTTAAGCTTGCTCGGCTCTTAGAG
g1for	cacc AGAACTACACACCAGGGCCA
g1rev	aaac TGGCCCTGGTGTGTAGTTCT
g2for	cacc GATATCCACTGACCTTTGGA
g2rev	aaac TCCAAAGGTCAGTGGATATC
g3for	cacc AGAGAGAAGTGTTAGAGTGG
g3rev	aaac CCACTCTAACACTTCTCTCT
g5for	cacc GGTTAGACCAGATCTGAGCC
g5rev	aaac GGCTCAGATCTGGTCTAACC
g6for	cacc GGGAGCTCTCTGGCTAACTA
g6rev	aaac TAGTTAGCCAGAGAGCTCCC
g7for	cacc GCCCGTCTGTTGTGTGACTC
g7rev	aaac GAGTCACACAACAGACGGGC
gagfor	cacc GAGGCTAGAAGGAGAGAGAT
Gagp24_forward	GTCCTCTATTGTGTGCATCAAAGG
Gagp24_reverse	CCATCTTCCTGGCAAATTCATTTC
gagrev	aaac ATCTCTCTCCTTCTAGCCTC
HIVamp	CCTTGATCTGTGGATCTACCACAC
HIV-Ex-1	CTTAATACCGACGCTCTCGCAC
int3for	cacc GGGATTGGGGGGTACAGTGC
int3rev	aaac GCACTGTACCCCCCAATCCC
int4for	cacc AAGCTCCTCTGGAAAGGTGA
int4rev	aaac TCACCTTTCCAGAGGAGCTT
int5for	cacc GATTATGGAAAACAGATGGC
int5rev	aaac GCCATCTGTTTTCCATAATC

Name	Sequence (5´→3´)
Jlatgag24for	ACCCTCTATTGTGTGCATCAAAGG
Jlatgag24rev	CATCTTCCTGGCAAACTCATTTC
Jlatpolfor2	GGGCAGCTAACAGGGAGACT
Jlatpolrev	GGCTTGTTCCATCTATCCTCTGTC
LTRpsirev	GAACCA<u>GCTAGC</u>TTTGGCGTACTCACCAGTCG
NcoIrev1	GACTGA<u>CCATGG</u>TGGCGTCGACGCTCGGAGGACTGGCGC
p17for	cacc GATGGGTGCGAGAGCGT
p17rev	aaac ACGCTCTCGCACCCATC
P2	TAATTTCAGTTGTCCTTATTGGAAGGG
p24_1for	cacc GACAGCATGTCAGGGAG
p24_1rev	aaac CTCCCTGACATGCTGTC
p24_2for	cacc AGAAATGATGACAGCATGTC
p24_2rev	aaac GACATGCTGTCATCATTTCT
P3	GACTTGGTGGAAAAGGTGGA
P7	TGTTGGGCTTGACAGCAGTTAC
PacI for	ATGCCA<u>TTAATTAA</u>CAGCTAGCTAGCTGCAGTAACGCC
Pol_for1	GGGGCAGCCAATAGGGAAAC
Pol_rev1	GCTTGTTCCATCTGTCCTCTGTC
primer1ShalemCas	CCAGAAGGGACAGAAGAACAG
primer2ShalemCas	TGCAGGTAGTACAGGTACAG
psiJBAsclfor	GTTGGT<u>GGCGCGCC</u>TGGAAGGGCTAATTTGGTCC
psioligoasclfor	GTTGGT<u>AGATCT</u>TTGGGTGGCGCGCCGTTGGTGCTAGCTGGTTG
psioligoasclrev	CAACCA<u>GCTAGC</u>ACCAACGGCGCGCCACCCAAAGATCTACCAAC
qPCR GFP FOR	GAGCGCACCATCTTCTTCAAG
qPCR GFP REV	TGTCGCCCTCGAACTTCAC
RPP30-Fw	GATTTGGACCTGCGAGCG
RPP30-Rv	GCGGCTGTCTCCACAAGT
RT-Assay-fwd	TCCTGCTCAACTTCCTGTCGAG

Name	Sequence (5´→3´)
RT-Assay-rev	CACAGGTCAAACCTCCTAGGAATG
U6for	AATGCTTTCGCGTCGCGCAG
U6rev	TTGCCTGCGCGTCTTTCCAC

Overhangs are written in small letters
Restriction sites are underlined

2.1.14 Plasmids

Table 2.15: Plasmids.

Name	Description	Source (internal plasmid number)
#48_GGC_1+2_pBSU6(long)ccdB_FE_Scaffold	Plasmid expressing a single gRNA with F+E scaffold from the U6 promoter for cloning of gRNA multiplexing constructs	Grimm lab, Centre for Infectious Diseases/ Virology Heidelberg (#1589)
#48_GGC_2+3_pBSH1_ccdB_FE_Scaffold	Plasmid expressing a single gRNA with F+E scaffold from the H1 promoter for cloning of gRNA multiplexing constructs	Grimm lab, Centre for Infectious Diseases/ Virology Heidelberg (#1592)
#48_GGC_3+4_pBS7SK_ccdB_FE_Scaffold	Plasmid expressing a single gRNA with F+E scaffold from the 7SK promoter for cloning of gRNA multiplexing constructs	Grimm lab, Centre for Infectious Diseases/ Virology Heidelberg (#1595)
#552-EFS	scAAV vector for the expression of YFP from the EFS promoter	Grimm lab, Centre for Infectious Diseases/ Virology Heidelberg (#1563)
#552-SFFV	scAAV vector for the expression of YFP from the SFFV promoter	Grimm lab, Centre for Infectious Diseases/ Virology Heidelberg

Name	Description	Source (internal plasmid number)
		(#1641)
AAV TRISPR 2.0 ccdB GGC 1+4_YFP Assembly Vector 2nd Generation	Assembly AAV plasmid for the expression of three gRNAs with F+E scaffold from U6, H1 and 7SK promoters	Grimm lab, Centre for Infectious Diseases/ Virology Heidelberg (#1600)
AAV TRISPR 2.0, pBS7SKccdB_FE_Scaffold	AAV plasmid for the expression of one gRNA with F+E scaffold from the 7SK promoter	Grimm lab, Centre for Infectious Diseases/ Virology Heidelberg (#1583)
AAV TRISPR 2.0, pBSH1ccdB_FE_Scaffold	AAV plasmid for the expression of one gRNA with F+E scaffold from the H1 promoter	Grimm lab, Centre for Infectious Diseases/ Virology Heidelberg (#1580)
AAV TRISPR 2.0, pBSU6(long)ccdB_FE_ Scaffold	AAV plasmid for the expression of one gRNA with F+E scaffold from the U6 promoter	Grimm lab, Centre for Infectious Diseases/ Virology Heidelberg (#1577)
Adeno helper plasmid	Helper plasmid with Ad5 genes E2A, E4, VA RNA	Grimm lab, Centre for Infectious Diseases/ Virology Heidelberg (#1111)
EFS_Zhang/Shalem_Cas9_ 60bp-Poly(A)	AAV plasmid for the expression of SpCas9 from the EFS promoter	Grimm lab, Centre for Infectious Diseases/ Virology Heidelberg (#1602)
EFS_Zhang/Shalem_Cas9_ bGH-Poly(A)	AAV plasmid for the expression of SpCas9 from the EFS promoter with a bGH-Poly(A) site	Dr. Kathleen Börner, Centre for Infectious Diseases/ Virology Heidelberg (#119)
pAAV-FZ-SpCas9	AAV plasmid for the expression of SpCas9 from a 224bp CMV promoter	Grimm lab, Centre for Infectious Diseases/ Virology Heidelberg

Name	Description	Source (internal plasmid number)
		(#1451)
pBS-sds-H1-gRNA scaffold	AAV plasmid for the expression of one gRNA with standard scaffold from the H1 promoter	Grimm lab, Centre for Infectious Diseases/ Virology Heidelberg (#1197)
pBS-sds-U6-gRNA scaffold	AAV plasmid for the expression of one gRNA with standard scaffold from the U6 promoter	Grimm lab, Centre for Infectious Diseases/ Virology Heidelberg (#1196)
pBSUF3rev-YFP-sds	scAAV vector for the expression of YFP from the CMV promoter	Grimm lab, Centre for Infectious Diseases/ Virology Heidelberg (#552)
pcDNA-Tat	Tat expression plasmid	Müller lab, Centre for Infectious Diseases/ Virology Heidelberg (#197), [193]
pCHIV	Non-replication competent HIV provirus derivative	[194]
PGK_Zhang/Shalem_Cas9_60bp-Poly(A)	AAV plasmid for the expression of SpCas9 from the PGK promoter with a 60bp Poly(A) site	Dr. Kathleen Börner, Centre for Infectious Diseases/ Virology Heidelberg (#111)
PGK_Zhang/Shalem_Cas9_bGH-Poly(A)	AAV plasmid for the expression of SpCas9 from the PGK promoter with a bGH-Poly(A) site	Dr. Kathleen Börner, Centre for Infectious Diseases/ Virology Heidelberg (#121)
pNL4-3	Prototype X4-HIV-1 proviral construct	Kräusslich lab, Centre for Infectious Diseases/ Virology Heidelberg,[195]
psiCheck^{TM}-2	Plasmid expressing Renilla and Firefly lu-	Promega, Germany

Name	Description	Source (internal plasmid number)
	ciferases	
pSSV9_shortCMV-Cas9-H1 gRNA	AAV plasmid for the expression of spCas9 from a 224bp CMV promoter and one gRNA with standard scaffold from the H1 promoter	Grimm lab, Centre for Infectious Diseases/ Virology Heidelberg (#1296)
scAAV_U6_BbsI(x2)_F+E scaffold_RSV:GFP	AAV plasmid for the expression of one gRNA with F+E scaffold from the U6 promoter	Grimm lab, Centre for Infectious Diseases/ Virology Heidelberg (#1529)
SFFV-Cas	AAV plasmid for the expression of SpCas9 from the SFFV promoter	Cloned in this work (#254)
SV40_Zhang/Shalem_Cas9 _bGH-Poly(A)	AAV plasmid for the expression of SpCas9 from the SV40 promoter with a bGH-Poly(A) site	Dr. Kathleen Börner, Centre for Infectious Diseases/ Virology Heidelberg (#124)
synP_Zhang/Shalem_Cas9_ bGH-Poly(A)	AAV plasmid for the expression of SpCas9 from the synP promoter with a bGH-Poly(A) site	Dr. Kathleen Börner, Centre for Infectious Diseases/ Virology Heidelberg (#122)
TK_Zhang/Shalem_Cas9_60 bp-Poly(A)	AAV plasmid for the expression of SpCas9 from the TK promoter with a 60bp Poly(A) site	Grimm lab, Centre for Infectious Diseases/ Virology Heidelberg (#1604)
TK_Zhang/Shalem_Cas9_b GH-Poly(A)	AAV plasmid for the expression of SpCas9 from the TK promoter with a bGH-Poly(A) site	Dr. Kathleen Börner, Centre for Infectious Diseases/ Virology Heidelberg (#123)
WHc6 WT	AAV helper plasmid encoding rep and AAV6 cap	Grimm lab, Centre for Infectious Diseases/ Virology Heidelberg (#1764)

Name	Description	Source (internal plasmid number)
WHc9 A2	AAV helper plasmid encoding rep and cap. Chimeric capsid variant with peptide insertion (Börner et al. manuscript in preparation)	Grimm lab, Centre for Infectious Diseases/ Virology Heidelberg (#1790)

2.1.15 Probes

Table 2.16: Probes

Name	Sequence (5´→3´)	Labeling
EGFP	ACGACGGCAACTACA	5´6-FAM; 3´BHQ1
RPP30	CTGACCTGAAGGCTCT	5´6-FAM; 3´BHQ1
ShalemCas	AGAGAATGAAGCGGATCGAAGAGGGCATCAA	5´6-FAM; 3´BHQ1
		5´HEX; 3´BHQ1
U6	TGAGTAAGAGCCCGCGTCTGAACCCTCC	5´6-FAM; 3´BHQ1

2.1.16 Software

Table 2.17: Software.

Name	Application	Company/Reference
Ascent™ Software	Plate reader software	Thermo Fisher Scientific (Waltham, USA)

Name	Application	Company/Reference
CFX Manager™ Software	qPCR software	BioRad (Hercules, USA)
FACSuite Acquisition Software	Flow cytometry software	BD Biosciences (Franklin Lakes, USA)
Flowing Software 2	analysis of flow cytometry data	(Perttu Terho, Turku Centre for Biotechnology, Finland; www.flowingsoftware.com)
GATCViewer 1.00	visualization of chromato-grams from sequencing data	GATC Biotech (Konstanz, Germany)
GloMax®-96 Microplate Lumi-nometer Software	Luminometer software	Promega (Madison, USA)
GraphPad Prism	graphic illustration and statisitical analysis of data	GraphPad Software, Inc. (La Jolla, USA)
ImageJ	analysis of microscopy im-ages and gel images	
MXP software	Flow cytometry software	Beckman Coulter (Brea, USA)
QuantaSoft™ Software	ddPCR software	BioRad (Hercules, USA)
Quantity One 1-D Analysis Software 4.6.9	gel documentation software	BioRad (Hercules, USA)
Rotor Gene 6000 Series Software 1.7	qPCR software	QIAGEN (Hilden, Germany)
ScanR acquisition software	microscopy software	Olympus (Hamburg, Germany)

Name	Application	Company/Reference
SnapGene Viewer	visualization of plasmid maps	GSL Biotech (Chicago, USA)

2.2 Cell biological methods

2.2.1 Cell culture

All cells were cultured at 37 °C and 5 % CO_2. HEK293T, HeLaP4 and HeLa-pNLtr cells were cultured in DMEM supplemented with 10 % FBS, 100 U/ml Penicillin and 100 µg/ml Streptomycin. J-Lat, MT4 and C8166 cells were cultured in RPMI 1640 with GlutaMAX™ supplemented with 10 % FBS, 100 U/ml Penicillin and 100 µg/ml Streptomycin. Primary CD4$^+$ T cells were cultured in RPMI 1640 with GlutaMAX™ supplemented with 10 % heat inactivated FBS (heated for 30 min at 56 °C), 100 U/ml Penicillin, 100 µg/ml Streptomycin and 20 U/ml IL-2.

2.2.2 Isolation of CD4$^+$ T cells from Buffy coats and activation

500 µl of RosetteSep™ Human CD4$^+$ T Cell Enrichment Cocktail were added to 10 ml blood from uncooled buffy coats not older than 24 hours and the tube was inverted several times. After incubation for 20 minutes at RT, 10 ml 1 x PBS, sterile filtered using a membrane with 0.22 µm pore size, were added. 15 ml Ficoll were pipetted into a SepMate™ tube and 17 ml of the blood/PBS mixture were added slowly on top without mixing the phases. The tube was then centrifuged 20 min at 1200 g. After centrifugation, a white ring containing the CD4$^+$ T cells appears at the interface between plasma and Ficoll. Approximately two thirds of the plasma were carefully removed using a 10 ml pipette. The rest of the plasma and the white ring were transferred into a new 50 ml tube, sterile filtered PBS was added up to 45 ml and the tube was centrifuged at 1100 rpm for 10 min. The PBS was removed completely with a pipette and the cells were resuspended in 20 ml fresh PBS. 5 µl of this cell suspension were added to 20 µl trypan blue and cells were counted using a Neubauer counting chamber. After counting, another 25 ml of PBS were added to the cell suspension and the cells were centrifuged again at 1100 rpm for 10 min. The PBS was removed completely and the cells were resuspended in RPMI supplemented with 20 U/ml IL-2 and heat inactivated FBS (heated at 56 °C for 30 min) to reach a cell density of 2 -

5×10^6 cells/ml. To activate the cells, Dynabeads were washed with medium once and 60 µl of the beads were added per 10 million cells. The cells were incubated three days at 37 °C and 5 % CO_2. Then, the Dynabeads were removed using a DynaMag-2 magnet. For activation with PHA, instead of Dynabeads PHA was added at a final concentration of 2 µg/ml to the cells and incubated three days at 37 °C and 5 % CO_2.

2.2.3 MTS assay

40 h after activation, the viability of untransduced or transduced J-Lat cells (chapter 2.3.10) was measured with a MTS assay (CellTiter 96® AQueous One Solution Cell Proliferation Assay, Promega) according to manufacturer`s instructions. Briefly, 20 µl cellsuspension of a 24-well were transferred to a 1.5 ml tube and centrifuged at 1200 rpm. The old medium was replaced by 100 µl fresh medium and the cells were transferred to a 96-well plate and 20 µl of the CellTiter 96® AQueous One Solution reagent were added. The plate was incubated 1 h at 37 °C and 5 % CO_2. To stop the reaction, the suspension was transferred to a white plate with 25 µl 10 % SDS per well. Finally, the absorbance at 490 nm was measured with a luminometer.

2.3 Microbiological methods

2.3.1 Transformation of chemo-competent bacteria

Usually, 5 µl of ligation mix or in case of a re-transformation 1 µl plasmid were added to 50 µl of chemo-competent bacteria. After 15 min incubation on ice, the heat shock was performed at 42 °C for 50 sec followed by an incubation step on ice for 2 min. The bacteria were then plated on LB agar plates containing 100 µg/ml ampicillin and incubated overnight at 37 °C. For plasmids with a chloramphenicol resistance, 800 µl SOC media were added after the 2 min incubation step on ice and bacteria were shaked 1 h at 37 °C. Afterwards, the bacteria were centrifuged 5 min at 400 g, approximately 700 µl supernatant were discarded and the bacteria were plated on LB agar plates containing 25 µg/ml chloramphenicol and incubated at 37 °C overnight.

2.3.2 Transfection and harvesting of HEK293T for AAV crude lysate production

Per well 50,000 HEK293T cells were seeded in 4 ml DMEM on a 6-well plate. The day after, every well was transfected with a mix containing 390 µl DMEM without supplements, 8 µl TurboFect, 1.3 µg of an adeno-viral helper plasmid, 1.3 µg of a cap encoding plasmid and 1.3 µg of a plasmid carrying the transgene flanked by ITRs. The mix was vortexed well, incubated 20 min at RT and added dropwise to the cells. 72 h after transfection, the cells were collected in 15 ml tubes and centrifuged at 2500 rpm for 15 min. The medium was removed and the cell pellet was resuspended in 150 µl PBS per 6-well and transferred to 1.5 ml tubes. To lyse the cells, they were frozen in liquid nitrogen for 5 min and thawed in a water bath at 37 °C for 5 min. This procedure was repeated 5 times. Afterwards, the cell lysate was centrifuged at 13,200 rpm for 5 min and the supernatant was collected, aliquoted and frozen at -80 °C.

2.3.3 Transfection and harvesting of HEK293T cells for production of purified AAVs

For large scale AAV production, 4 million HEK293T cells were seeded in 22 ml DMEM on 15 cm dishes two days before transfection. For the transfection of one dish, 14.7 µg of an adeno-viral helper plasmid, 14.7 µg of a cap encoding plasmid and 14.7 µg of a plasmid carrying the transgene flanked by ITRs were mixed with water to a final volume of 790 µl. In parallel, 352 µl PEI were mixed with 438 µl water. Directly before usage, 790 µl 300 mM NaCl were added to the PEI solution and to the DNA solution. After inverting both solutions, the PEI mixture was added dropwise into the DNA mixture. The transfection mix was vortexed, incubated 10 min at RT and added dropwise to each dish. Three days after transfection, the cells were harvested with a cell lifter and centrifuged 15 min at 400 g. The medium was removed, the cell pellet was resuspended in PBS and centrifuged again 15 min at 400 g. The PBS was removed and the cell pellet was resuspended in either 5 ml benzonase buffer for purification using a small iodixanol gradient or in 20 ml benzonase buffer for purification using a big iodixanol gradient. These cell suspensions were either stored at -80 °C or directly further processed as described in chapter 2. 3.4.

2.3.4 Iodixanol purification of AAVs

The cells resuspended in benzonase buffer (see chapter 2.3.3) were 5 times frozen in liquid nitrogen and thawed in a waterbath at 37 °C. Afterwards, the samples were sonicated 1 min. 50 U/ml benzonase were added, the samples were incubated 1 hour in a waterbath at 37 °C and

inverted every 10 min. Next, the samples were centrifuged at 4000 g for 15 min. The supernatant was transferred to a new tube and centrifuged again at 4000 g for 15 min. To prepare the gradient, the supernatants were filled through a pasteur pipette into ultracentrifugation tubes and 15 % iodixanol, 25 % iodixanol, 40 % iodixanol and 60 % iodixanol were added. For the preparation of a small gradient, 1.5 ml of each iodixanol solution were added. For the preparation of a big gradient, 7 ml 15 % iodixanol, 5 ml 25 % iodixanol, 4 ml 40 % iodixanol and 4 ml 60 % iodixanol were added. The Pasteur pipette was removed carefully, the tubes were completely filled with benzonase buffer, sealed and centrifuged with an Optima L-90K ultracentrifuge. Small gradients were centrifuged at 50,000 rpm for 2 h at 4 °C using a 70.1Ti rotor. Big gradients were centrifuged at 50,000 rpm for 2.5 h at 4 °C using a 70Ti rotor. After centrifugation, the 40 % iodixanol phase was collected using a syringe. The virus was aliquoted and stored at -80 °C.

2.3.5 Titration of purified AAVs

To measure the titer of the iodixanol purified AAVs, 10 µl of virus were diluted with 10 µl of TE buffer. Then, 20 µl 2 M NaOH were added, the sample was mixed and incubated for 30 min at 56 °C to lyse the viral particles. After that, 38 µl 1 M HCl were added for neutralization and 922 µl H_2O were added in addition. To avoid inhibition of the PCR by iodixanol, the samples were further diluted 1:10 with water. To prepare a standard curve, a suitable plasmid was diluted at a range of 3.5×10^{11} to 3.5×10^6 molecules/ml in 10^{-1} steps. The following formula was used to determine the amount of molecules/ml:

$$\frac{\text{DNA concentration} \left(\frac{\text{g}}{\text{mL}}\right)}{660 \times \text{size of plasmid in bp}} \text{ x } 6.02 \text{x} 10^{23}$$

Samples and standards were measured in triplicates. The final PCR mix contained 1 x SensiMix[TM] II Probe No-Rox, 0.4 µM of each primer and 0.1 µM probe. Water was added to reach a final volume of 10 µl. The reaction was performed using a Rotor-Gene 6000 machine and the program shown in table 2.18.

Table 2.18: QPCR program for the titration of AAVs.

Step	Temperature	Time	Number of cycles
Initial activation	95 °C	10 min	1
Denaturation	95 °C	10 sec	40
Annealing	60 °C	20 sec	

To create the standard curve, the Ct values of the standards were plotted on the y-axis and the logarithm of the number of molecules per ml was plotted on the x-axis. Using the linear equation of the standard curve and the Ct values of the samples the x-values for the samples were calculated. As the samples were diluted 1:1000 with water after neutralization, the x-values were multiplied with 1000 to determine the number of viral genomes per ml. For single-stranded AAV constructs this value has to be multiplied by two as the plasmid used to create the standard curve is double-stranded.

2.3.6 HIV-1 NL4-3 production

HIV-1 used in this work was produced from MT4 co-culture. This co-culture was started by infecting 10 to 20 ml of MT4 cells in a 25 cm^2 flask with 1 ml supernatant from HEK293T cells transfected with pNL4-3. These cells were passaged twice a week 1:10 or 1:20 at the beginning and 1:200 routinely. For the production of HIV-1, three days after passaging 2 ml of the co-culture were added to 18 ml MT4 cells at a density of 5 x 10^5 cells/ml. At the same day 180 ml MT4 cells were prepared at a density of 3-5 x 10^5 cells/ml. 36 h later, the 20 ml infected MT4 cells were added to the 180 ml of non-infected cells. 2 days later, the cells were transferred to 50 ml tubes and centrifuged 5 min at 2500 rpm. The supernatant was filtered through a syringe filter with a pore size of 0.45 µm. 30-33 ml of this supernatant were added carefully on top of 6 ml of a sucrose cushion (20 % sucrose (w/v) in PBS) and centrifuged at 28,000 rpm for 2 h at 4 °C in a Optima LE80K ultracentrifuge using a SW32 rotor. The virus pellet was taken up in RPMI with 20 mM Hepes. The titers of the HIV-1 stocks used in this work are listed in table 2.19.

Table 2.19: Titers of HIV-1 stocks used in this work.

Name	pU RT/µl (SG-PERT)	µg p24/ml (ELISA)	infectious units/ml (C8166 titration)
NL4-3_1	2.32×10^{11}	96.11	3.16×10^{8}
NL4-3_2	2.25×10^{11}	384.15	3.16×10^{9}

2.3.7 Titration of HIV-1 NL4-3 on C8166 cells

4×10^{4} cells were seeded in 100 µl RPMI with 10 % FBS and 1 % penicillin/streptomycin on a 96-well plate. Supernatants from infected HeLaP4 cells (chapter 2.3.9) or HIV-1 produced from MT4 co-culture were diluted at a range of 10^{-2} to 10^{-11} with medium and 100 µl of these dilutions were added per well to the C8166 cells. 4 wells were infected in parallel with one dilution. Seven days post infection, the cells were checked for syncytia formation indicative for HIV-1 infection. The number of infectious units per ml was calculated with the following formula:

$$\text{Infectious units/ml} = 10^{-1 \times (L - (d \times (s - 0.5))} \times 10$$

L = log of the highest dilution where all 4 wells are positive

d = log of the dilution factor

s = sum of the number of all positive wells (beginning at the highest dilution where all 4 wells are positive) divided by the number of replicates analyzed per dilution

2.3.8 AAV transduction of HeLaP4-PNLtr cells

2,500 cells were seeded in 100 µl medium on a 96-well plate and 10 µl of each crude AAV vector or 5 µl of each iodixanol-purified AAV vector were added per well. Two days later, the medium was removed, replaced by 100 µl fresh medium and again 10 µl of each crude AAV vector or 5 µl of each iodixanol-purified AAV vector were added per well. Two days later, the medium was removed and 140 µl of DirectPCR® Lysis Reagent Cell (VWR) diluted 1:2 with water and supplemented with 11.4 U/ml proteinase K (NEB) were added per well. The plates were incubated at 55 °C for 5-16 h under continuous shaking and the lysates were frozen at -20 °C.

2.3.9 AAV transduction and HIV-1 infection of HeLaP4 cells

2,500 cells were seeded per well in 100 µl medium on a 96-well plate and 5 µl of each AAV vector were added. Three days later, the medium was removed and 50 µl fresh medium supplemented with 48 ng of the viral stock HIV-1 NL4-3_1 (table 2.19) were added per well. Additionally, 5 µl of each AAV vector were added per well. After 36 h, the medium was removed and the cells were fixed with 100 µl 4 % PFA for 90 minutes at RT. After fixation, the cells were stained and imaged (chapter 2.4.19). To analyze Cas9 expression in HeLaP4 cells, the cells were lysed three days after the first transduction and RNA was extracted (chapter 2.4.10).

2.3.10 AAV transduction and activation of J-Lat cells

50,000 cells were seeded in 500 µl medium per well on a 24-well plate and 10 µl of each AAV vector were added per well. After 54 h, the cells were transferred to 1.5 ml tubes and centrifuged at 1200 rpm. The medium was removed and 700 µl fresh medium were added. 320 µl of the cell suspension were transferred to a 24-well plate and 10 µl of each AAV vector were added per well. 21 h later, 350 µl medium supplemented with 2.7 µg/ml TPA and 20 ng/ml TNFα were added per well. 5-6 h later, the cells were transferred to 1.5 ml tubes and centrifuged at 1200 rpm. The medium was removed, 500 µl fresh medium were added and the cells were transferred to a 24-well plate again. After 40 h, 200-300 µl of the cells were transferred to 1.5 ml tubes and centrifuged at 1200 rpm. The medium was removed and frozen at -20 °C for later analysis with SG-PERT (chapter 2.4.14). To isolate genomic DNA for T7 assay analysis (chapter 2.4.15), 400 µl DNA Lysis Buffer T (PeqGOLD Tissue DNA Mini Kit, VWR) supplemented with 20 µl Proteinase K and 15 µl RNase A were added to the cell pellet and shaked 30 min at 50 °C. The samples were further processed according to manufacturer`s instructions. The other 200-300 µl of the cells were also transferred to 1.5 ml tubes and centrifuged at 1200 rpm. The medium was removed, the cells were stained with Hoechst and imaged (chapter 2.4.20). To validate the functionality of single gRNAs in J-Lat cells, 50,000 cells were seeded in 500 µl medium per well on a 24-well plate and 20 µl of each crude AAV vector were added per well. After 48 h, the cells were transferred to 1.5 ml tubes and centrifuged at 1200 rpm. The old medium was removed and 1 ml fresh medium was added to the cell pellet. 500 µl of the cell suspension were added on a 24-well plate and 20 µl of each crude AAV vector were added per well. Three days later, the genomic DNA was isolated using the PeqGOLD Tissue DNA Mini Kit (VWR) following the manufacturer`s instructions.

2.3.11 AAV transduction and HIV-1 infection of primary human CD4$^+$ T cells

50,000 cells were seeded in 100 µl medium per well on a 96-well V-bottom plate and 10 µl of each AAV vector were added. Two days later, the cells were centrifuged 5 min at 1200 rpm. The old medium was removed, 100 µl fresh medium and 10 µl of each AAV vector were added per well. After one additional day, the cells were centrifuged again 5 min at 1200 rpm, the old medium was removed and 50 µl medium containing 6.1 x 10^{-6} to 3.7 x 10^{-5} ng NL4-3_2 (table 2.19) per cell were added per well. Subsequently, the plates were sealed with a sterile sealing tape and centrifuged 1.5 h at 2000 rpm and 37 °C. Afterwards, the sealing tape was removed and the cells were incubated 5-6 h at 37 °C and 5 % CO$_2$. After the incubation, 100 µl fresh medium were added to the cells and the plates were centrifuged 5 min at 1200 rpm. The medium was removed and replaced by 100 µl fresh medium. Three days post infection, the cells were stained with a viability dye, fixed, stained with a FITC-labeled anti-capsid antibody and analyzed with flow cytometry (chapter 2.4.18). Cells that were only transduced with a YFP-encoding AAV vector and not infected with HIV-1, were fixed 72 h after the first transduction and then analyzed with flow cytometry. To analyze Cas9 expression in primary CD4$^+$ T cells, the cells were lysed one day after the second transduction and RNA was extracted (chapter 2.4.10).

2. 4 Molecular biological methods

2.4.1 Isolation of plasmid DNA

For isolation of plasmid DNA from transformed *E. coli* bacteria, the following Kits were used: Plasmid Plus Midi (Qiagen), NucleoBond AX 500 (Macherey Nagel), Invisorb Spin Plasmid Mini Two (Stratec). Plasmid DNA used for test digestions was isolated by isopropanol precipitation using buffers S1-3 from the NucleoBond PC 100 kit. Briefly, 2 ml of bacterial culture were centrifuged at 13,000 rpm for 3 min. Then, the bacteria were resuspended with 300 µl buffer S1 and lysed by addition of 300 µl buffer S2 and incubation at RT for 5 min. For neutralization, 300 µl buffer S3 were added and samples were incubated 5 min at RT. After that, samples were centrifuged at 13,000 rpm. The supernatant was mixed thoroughly with 600 µl isopropanol and centrifuged at 13,000 rpm. The supernatant was removed and the pellet was washed with 70 % Ethanol. The pellet was dried at 65 °C for 10 min and resuspended in 60 µl water.

2.4.2 Restriction enzyme digestion

In most cases (unless stated otherwise) enzymes from NEB and the corresponding buffers were used. For test digestions, usually 400-800 ng of plasmid DNA were mixed with 0.5 µl enzyme, 1 µl buffer and water to a final volume of 10 µl. The reaction was incubated at the recommended temperature for 1 h. For cloning, either 1 µg of plasmid DNA or the complete eluate of a gel extraction or nucleotide removal was mixed with 1 µl of enzyme and 5 µl of the appropriate buffer. Water was added up to a final volume of 50 µl. The mix was incubated at the recommended temperature overnight.

2.4.3 Ligation reaction

For ligation of PCR products or annealed oligonucleotides into plasmids a mix was prepared containing 50 ng of the digested plasmid, 1 µl T4 DNA Ligase Buffer (NEB) and 0.5 µl T4 DNA Ligase (NEB). The digested PCR product or annealed oligonucleotides were added at a molar vector to insert ratio of 1:3. Water was added to reach a final volume of 20 µl. The reaction was incubated 1 h at RT.

2.4.4 Cloning of SFFV-Cas

To clone an SFFV-driven Cas9 AAV vector, the plasmid #1641 was used for the amplification of the SFFV promoter with the primers PacI for and NcoI rev1. The reaction was performed as described in chapter 2.4.8 with an annealing temperature of 68 °C. The PCR product was purified using the QIAquick Nucleotide Removal Kit (Qiagen) according to manufacturer`s instructions. The PCR product and the plasmid #1451 were digested with NcoI and PacI and ligated.

2.4.5 Cloning of single gRNA constructs

For cloning of AAV vectors expressing a single gRNA either with standard or E+F scaffold from the U6 promoter, the plasmids #1196 or #1529 were digested with BbsI. For cloning of the "all-in-one" vectors expressing a single gRNA and Cas9, the plasmid #1296 was digested with BsmbI. GRNA oligonucleotides listed in table 2.14 were annealed and ligated into the plasmid backbones. For the annealing reaction, 5 µl of each oligonucleotide at a concentration of 100 pmol/µl were mixed with 5 µl NEBuffer 2 (New England Biolabs) and 35 µl water. The mix

was heated to 95 °C for 5 min in a heating block, that was then turned off to allow the mix to slowly cool down to RT.

2.4.6 Cloning of gRNA multiplexing constructs

To clone plasmids expressing three gRNAs from the promoters U6, 7SK and H1, first donor plasmids encoding one single gRNA were produced using Golden Gate cloning. For that purpose, the annealed gRNA oligonucleotides (chapter 2.4.5) were diluted 1:200 with water. 1 µl of the oligonucleotides was then mixed with 40 fmol of the recipient plasmid (#1589, # 1592, #1595) and with ATP and DTT 1 mM each, 1 µl 10 x FastDigest Buffer (Thermo Scientific), 1 µl T4 DNA ligase (400 U/µl) (NEB), 0.75 µl FastDigest Esp3 (Thermo Scientific) and water up to a final volume of 10 µl. Using a Mastercycler Nexus GX2 (Eppendorf) the reaction was performed as shown in table 2.20.

Table 2.20: Golden Gate cloning program.

Step	Temperature	Time	Number of cycles
Digestion	37 °C	3 min	
			30
Ligation	16 °C	5 min	
	37 °C	15 sec	1
Heat inactivation	65 °C	20 min	1

To assemble the multiplexing constructs, 20 fmol of each donor plasmid and the recipient plasmid #1600 were mixed with 0.75 µl BpiI (Thermo Scientific), 2 µl 10 x buffer G (Thermo Scientific), ATP and DTT 1 mM each, 0.5 µl T4 DNA Ligase (2000 U/µl) (NEB) and water to a final volume of 20 µl. The reaction was performed as shown in table 2.20.

2.4.7 Cloning of LTR driven luciferase constructs

To analyze promoter activity of CRISPR modified LTRs, the SV40 promoter driving Renilla luciferase expression was removed by digestion of the plasmid psiCheck™-2 with the enzymes BglII

and NheI-HF. To create an AscI digestion site, the oligonucleotides psioligoasclfor and psioligo-asclrev were annealed, sequentially digested with NheI and BglII and ligated into the digested psiCheck^TM-2. LTR sequences from HeLaP4-NLtr cell lysates were PCR amplified as described in chapter 2.4.8 with an annealing temperature of 64 °C using the primers LTRpsirev and psiJBAsclfor. The PCR product was purified using the QIAquick Nucleotide Removal Kit (Qiagen) according to manufacturer`s instructions. The PCR product and the modified psiCHECK-2 were digested with NheI-HF and AscI. After purification of the PCR product with the aforementioned nucleotide removal kit and after purification of the plasmid with QIAquick Gel Extraction Kit (Quiagen), the ligation reaction was performed. The cloned constructs were sequenced using the primer HIVamp and the TAR loop structures were predicted using the RNAfold web server (rna.tbi.univie.ac.at/cgi-bin/RNAWebSuite/RNAfold.cgi).

2.4.8 Polymerase chain reaction

For most purposes, (unless stated otherwise) a 25 µl PCR mix was prepared to amplify genomic or plasmid DNA. This mix contained 7.5 pmol of each primer, 5 pmol dNTPs, 3 % DMSO, 1 x HF buffer (NEB), 0.5 µl of Phusion Hot Start Flex (NEB) and 5 µl template DNA. Water was added to reach the final volume of 25 µl. The reaction was performed with a Mastercycler Nexus GX2 (Eppendorf) as shown in table 2.21.

Table 2.21: Standard PCR program.

Step	Temperature	Time	Number of cycles
Initial denaturation	98 °C	30 sec	1
Denaturation	98 °C	10 sec	
Annealing	variable	15 sec	40
Extension	72 °C	30 sec	
Final extension	72 °C	10 min	1
Hold	4 °C	∞	1

2.4.9 Agarose gel electrophoresis

T7 assay cleavage products, restriction enzyme digested DNA or PCR products were separated using agarose gel electrophoresis. To separate T7 assay cleavage products, usually a 2 % agarose gel (2 % agarose (w/v) in 1 x TAE buffer) was prepared were dissolved in for all other purposes a 1 % agarose gel (1 % agarose (w/v) in 1 x TAE buffer) was used. To visualize the DNA after the run, the gels were supplemented with 1 µg/ml ethidiumbromide. Prior to loading, the samples were mixed with 6 x purple gel loading dye. The gels were usually run at 100-120 V for 30-60 min. DNA was visualized with a Gel DocTM XR (BioRad).

2.4.10 RNA extraction

To extract RNA from primary human CD4$^+$ T cells, the cells were centrifuged in the 96-well plate at 1200 rpm, the medium was removed and 50 µl Lysis solution S (Stratec Molecular) were added. Plates were then stored at -80 °C. After thawing, another 300 µl of Lysis solution S were added and RNA was extracted according to manufacturer`s instructions using the InviTrap® RNA Cell HTS 96 Kit/ C (Stratec Molecular). For RNA extraction from HeLaP4 cells, the medium was removed, 50 µl Lysis solution S were added per well and plates were also stored at -80 °C. After thawing another 300 µl Lysis solution R were added per well and RNA was extracted using the InviTrap® Spin Cell RNA Mini Kit according to manufacturer`s instructions.

2.4.11 DNase digestion of RNA samples

To remove AAV DNA from RNA samples of transduced primary CD4$^+$ T cells or HeLaP4 cells, a DNA digestion was performed using the TURBO DNA-free™ Kit (Thermo Fisher Scientific). Briefly, 1.8 µl 10 x TURBO DNase Buffer and 0.75 µl TURBO DNase were added to 15 µl RNA and the sample was incubated at 37 °C for 30 min. Afterwards, 3.75 µl DNase Inactivation Reagent were added and the sample was incubated 2 min at RT. Subsequently, the sample was centrifuged 1 min at 10,000 rpm and the supernatant was transferred into a new tube.

2.4.12 CDNA synthesis

For cDNA synthesis the Verso cDNA Synthesis Kit (Thermo Fisher Scientific) was used. 10 µl of RNA solution were mixed with 4 µl 5 x RT buffer, 2 µl 10 mM dNTP mix, 1 µl random hexamer

primers, 1 µl RT enhancer, 1 µl enzyme mix and 1 µl nuclease free water. The reaction was per-formed as shown in table 2.22.

Table 2.22: cDNA synthesis program.

Step	Temperature	Time	Number of cycles
cDNA synthesis	32 °C	30 min	1
inactivation	95 °C	2 min	1

2.4.13 Digital droplet PCR

For one sample a 22 µl mix was prepared containing 5.5 µl sample, 11 µl ddPCR™ Supermix for Probes (No dUTP) (BioRad), 3.3 µl water, 1.1 µl 100 µM RPP30 probe and 1.1 µl 100 µM Cas9 probe. For droplet generation 20 µl of this mix were added to the middle row of a DG8™ car-tridge (BioRad) and 70 µl droplet generation oil for probes (BioRad) were added to the row be-low. The cartridge was covered with a gasket and droplets were generated using a QX200™ Droplet Generator (BioRad). 40 µl of the droplets were transferred to a PCR plate, the plate was sealed with Pierceable PCR plate heat foil (BioRad) using a PX1 PCR Plate Sealer (BioRad) and the reaction was run as shown in table 2.23 using a C1000 Touch™ Thermal Cycler (Bio-Rad). After PCR the positive droplets were detected using the QX200™ Droplet Reader (Bio-Rad) and QuantaSoft™ Software (BioRad).

Table 2.23: DdPCR program.

Step	Temperature	Time	Number of cycles
Initial denaturation	95 °C	10 min	1
Denaturation	94 °C	30 sec	
			40
Annealing and extension	57 °C	1 min	
	98 °C	10 min	1
Hold	4 °C	∞	

2.4.14 SG-PERT

The standard curve was created by diluting the plasmid pCHIV with 1 x dilutionbuffer at a range from 5.09×10^9 pUnits RT/µl to 5.09×10^3 pUnits RT/µl in 10^{-1} steps. 5 µl of culture supernatant or standard were mixed with 5 µl 2 x lysisbuffer and incubated for 10 min at RT. Afterwards, 90 µl of 1 x dilutionbuffer were added. For PCR, 10 µl 2 x reaction mix were added to 10 µl of lysed sample or lysed standard. The reaction was run on a BioRad CFX 96 using the program shown in table 2.24.

Table 2.24: SG-PERT program.

Step	Temperature	Time	Number of cycles
Reverse transcription	42 °C	20 min	1
Taq activation	95 °C	2 min	1
Denaturation	95 °C	5 sec	
Annealing	60 °C	5 sec	
			39
Extension	72 °C	15 sec	
Acquisition	80 °C	7 sec	
Melting curve	65 °C	31 sec	60
	65 °C + 0.5 °C/cycle	5 sec	

2.4.15 T7 assay

To detect cleavage and mutations caused by CRISPR/Cas at different gRNA target sites, a T7 endonuclease assay was performed. First, the target region was PCR amplified as described in chapter 2.4.8. The primers and annealing temperatures used are listed in table 2.25. After PCR amplification of the target region, the sample was denatured for 5 min at 95 °C and then cooled

down to 25 °C in steps of -5 °C and 5 min per step. Then 5 U of T7 Endonuclease (NEB) were added to 25 µl PCR sample and incubated for 20 min at 37 °C.

Table 2.25: Primers and annealing temperatures for T7 assay.

Cells	Target site	Primers	Annealing temperature/ extension time
HeLaP4-PNLtr/JLat	5´LTR	HIVamp/HIV-Ex-1	68 °C/30 s
HeLaP4-PNLtr	3´LTR	HIVamp/HIV-3.2	68 °C/30 s
HeLaP4-PNLtr/JLat	5´LTR/gag	HIVamp/958	68 °C/30 s
HeLaP4-PNLtr	gag p24	Gagp24_forward/ Gagp24_reverse	65 °C/50 s
JLat	gag p24	Jlatgag24for/ Jlatgag24rev	61 °C/30 s
HeLaP4-PNLtr	pol	Pol_for1/ Pol_rev1	65 °C/50 s
JLat	pol	Jlatpolfor2/ Jlatpolrev	64 °C/50 s

The cleavage efficiency was calculated using ImageJ. First, the background was subtracted using a rolling ball of radius of 10-20. The different lanes were marked with the rectangular selection and plotted. Then, the area under the curve was determined using the wand tool and the cleavage efficiency was calculated using the following formula described by Ran *et al.* [196].

$$\% \text{ cleavage efficiency} = 100 \times \left(1 - \sqrt{1 - (\text{fcut})} \right)$$

$$\text{fcut} = \frac{\text{sum of areas under the curve from T7 cleavage bands}}{\text{sum of areas under the curve from all bands}}$$

2.4.16 Enzyme-Linked Immunosorbent Assay (ELISA)

To measure the p24 amount of the produced HIV-1 NL4-3 stocks, an ELISA was performed. First, the anti-capsid antibody MAK183 was diluted 1:1000 in 1 x PBS, 100 µl were added per well on a Maxisorb 96-well plate and the plate was incubated overnight at RT in a moisture

chamber. Then, the plate was washed two times with 0.05 % Tween-20 in 1 x PBS and 150 µl 10 % FBS in 1 x PBS were added per well and incubated for 2 h at 37 °C for blocking. The standard was prepared by diluting purified capsid protein at a range from 5 ng/ml to 0.078 ng/ml in 1 x PBS supplemented with 0.1 % Tween-20. Viral particles were inactivated by adding 18 µl 1 x PBS and 1 µl 5 % Triton X-100 to 1 µl of the viral stock. This 1:20 dilution of the viral particles was then further diluted with 0.1 % Tween-20 in 1 x PBS at a range from 1:2,000 to 1:2,000,000. After incubation, the blocking buffer was removed from the plate and 100 µl per well of each dilution of the standard or the samples were added. Each dilution was measured in duplicates. The plate was incubated overnight at RT in a moisture chamber. Then, the plate was washed 2 times with 0.05 % Tween-20 in 1 x PBS. 100 µl rabbit anti-capsid antibody diluted 1:1000 in 1 x PBS supplemented with 10 % FBS and 0.1 % Tween-20 were added to each well and incubated at 37 °C 1 h. Afterwards, the plate was washed again two times with 0.05 % Tween-20 in 1 x PBS and 100 µl of a horseradish-peroxidase coupled goat anti-rabbit IgG diluted 1:2000 in 1 x PBS supplemented with 10 % FBS and 0.01 % Tween-20 were added per well and incubated 1 h at 37 °C. Then, the plate was washed twice with 0.05 % Tween-20 in 1 x PBS and then three times with water. Subsequently, 100 µl substrate (0.1 M NaOAc pH6.0 supplemented with 0.1 mg/ml Tetramethylbenzidine and 0.006 % (v/v) H_2O_2) were added per well and incubated 5 min at RT to visualize the bound antibody. The reaction was stopped by adding 50 µl 0.5 M H_2SO_4 per well and the absorbance at 405 nm was measured using a Multiskan Ascent Platereader (Thermo Fisher Scientific).

2.4.17 Luciferase assay

25,000 HEK293T cells were seeded on a 96-well plate in 100 µl medium. The day after, the cells were transfected using 100 ng of modified psiCheck-2, 100 ng of pcDNA-Tat and 0.4 µl TurboFect (Thermo Fisher Scientific) per well. 48 hours later, the cells were lysed by addition of 40 µl 1 x Passive Lysis Buffer (Promega) per well and shaking the plate for 15 min at RT. 10 µl of the lysates were transferred to a white 96-well plate (Greiner). Renilla and Firefly luciferase activities were measured using homemade buffers. Before use, the luciferase assay buffer was supplemented with DTT to a final concentration of 1 nM, with ATP to a final concentration of 400 nM and with D-Luciferin to a final concentration of 5 mM. Furthermore, 1.43 µM Coelenterazin was diluted 1:666 in Renilla Quenching buffer before use. The assay was performed using a Glomax 96 Microplate luminometer (Promega) injecting first 40 µl luciferase assay buffer per well followed by injection of 40 µl Renilla quenching buffer. Delaytime between the meas-

urements was set to 2 seconds and integration time to 10 seconds. After background subtraction, Firefly luciferase signals were used for normalization of the Renilla luciferase values.

2.4.18 Flow Cytometry

To analyze the HIV-1 infection rate of primary CD4$^+$ T cells, the cells were stained with the viability eFluor450 (Thermo Fisher Scientific) 72 h post infection. Briefly, 50 µl of the dye diluted 1:1000 in 1 x PBS were added per well. After incubation at 4 °C for 30 min, the cells were washed with 150 µl PBS and fixed with 50 µl 4 % PFA for 90 min. After fixation, the cells were washed again with 150 µl PBS and 50 µl KC57-FITC diluted 1:100 in 1 x PBS supplemented 0.1 % Triton and 0.01 % BSA were added. After incubation at 4 °C for 30 min, the cells were washed with 150 µl PBS and resuspended in 200 µl PBS with 1 % FCS. For flow cytometry analysis a BD FACSVerse (BD Biosciences) or a FC500 MPL flow cytometer (Beckman Coulter) was used. Usually, 10,000 events were acquired or the measurement was stopped after 2 min.

2.4.19 Immunostaining and microscopy of AAV-transduced and HIV-infected HeLaP4 cells

36 h post infection, HeLaP4 cells were fixed 90 minutes with 100 µl 4 % PFA per 96-well. Then, cells were permeabilized with 100 µl 0.1 % Triton for 10 min at RT and washed with 150 µl PBS. After that, 150 µl blocking buffer (5 % (v/v) FBS in PBS) were added and the plate was incubated either overnight at 4 °C or 30 min at RT on a shaker. The blocking buffer was removed and the cells were stained at 4 °C overnight with 50 µl sheep anti-capsid antibody diluted 1:500 in blocking buffer. The next day, the cells were washed three times with 150 µl PBS and stained 2 h at RT on a shaker with 50 µl blocking buffer supplemented 1:250 with donkey anti-sheep Alexa Fluor® 647 and 1:3000 with Hoechst stain 33258. Afterwards, the cells were washed three times with 150 µl PBS and imaged using a ScanR Inverted Microscope (Olympus) with an Olympus UPlanSApo 10x/0.40na objective. Per well 12 images were acquired. The number of nuclei and p24 positive cells as well as the infection ratio were determined with automated image segmentation using a matlab script provided by Dr. Kathleen Börner. Stained uninfected cells were used to determine the threshold for the calculation of p24 positive cells and the mean of all 12 infection rate values per well was calculated.

2.4.20 Microscopy of AAV-transduced and activated J-Lat cells

40 h after activation of the proviral transcription, the cells were incubated 1 h at 37 °C in a 96-well plate with 100 µl Hoechst stain 33258 diluted 1:100 in RPMI supplemented with 10 % FBS and 1 % Penicillin-Streptomycin. After the incubation, the cells were transferred to 1.5 ml tubes, 500 µl 1x PBS were added and the cells were centrifuged at 1200 rpm. The supernatant was removed and cells were resuspended in fresh medium and transferred to 8-well Lab-Tek chamber slides coated with 0.01 % (w/v) Poly-l-lysine in water. For the coating the Lab-Tek chamber slides were incubated with 200 µl Poly-L-lysine per well at RT. Then, the Poly-L-lysine was removed and each well was washed one time with 200 µl 1 x PBS. Images were acquired using a Nikon Eclipse Ti microscope with a CFI Plan Fluor DL10X (N.A. 0.3, W.D. 15.2mm) objective. At least 10 images were acquired per well. To quantify the percentage of GFP positive cells, the images were processed with ImageJ. Hoechst or GFP positive cells were determined using the Yen autothresholding algorithm. The median filter option was used to remove little dots and the watershed method was applied to separate cell clumps. The number of positive cells was counted with the "analyze particles" command. Objects with a size of at least 50 pixel units and a circularity of 0.5 to 1.0 were counted.

3. Results

The overall goal of this work was to establish a HIV-1-targeting CRISPR/Cas9 system, which is delivered into target cells with AAV vectors. For this purpose, we first designed a set of gRNAs targeting the HIV-1 LTRs, *gag* and *pol* (chapter 3.1). These were then tested with T7 assay for their functionality in HeLaP4-NLtr cells carrying an HIV-1 NL4-3 provirus (chapter 3.2) and in J-Lat cells harboring a latent HIV-1 HXB2 provirus (chapter 3.3). To enable simultaneous editing at different proviral sites and thereby to increase the chance to functionally inactivate the provirus, a subset of gRNAs was cloned into gRNA multiplexing constructs, which express three gRNAs simultaneously. These constructs were then analyzed for their ability to protect HeLaP4 cells against HIV-1-infection and to functionally inactivate the latent provirus integrated in J-Lat cells. After having proven the functionality of our CRISPR/Cas9 system in human cell lines, the three most effective constructs were chosen to test if the HIV-1-targeting CRISPR/Cas9 system can protect human primary CD4$^+$ T cells against HIV-1 infection (chapter 3.4).

3.1 GRNA design and *in silico* characterization of conservation and off-targets

For the establishment of our HIV-1-targeting CRISPR/Cas9 system, first of all, different gRNAs binding at the HIV-1 LTRs, *gag* or *pol* were designed (figure 3.1). Nine of the gRNAs are targeting the LTRs (g1-9). In more detail, g1 and g2 are binding at the NF-κB binding site, g3 and g8 are targeting the SP1 (specificity protein 1) binding site, g4 targets the TATA box, g5 and g6 are binding the TAR element and g7 as well as g9 are targeting the U5 (unique 5´) region of the LTRs. Four of our gRNAs are targeting the *gag* open reading frame. The gRNA gag binds the 18 nucleotides in front of the *gag* open reading frame and the two first nucleotides of the *gag* start codon. The target site of gRNA p17 spans the first 16 nucleotides of *gag* and the last nucleotide in front of the open reading frame. The gRNAs p24_1 and p24_2 are binding at the *p24* gene and int3, int4 and int5 are binding the *integrase* gene.
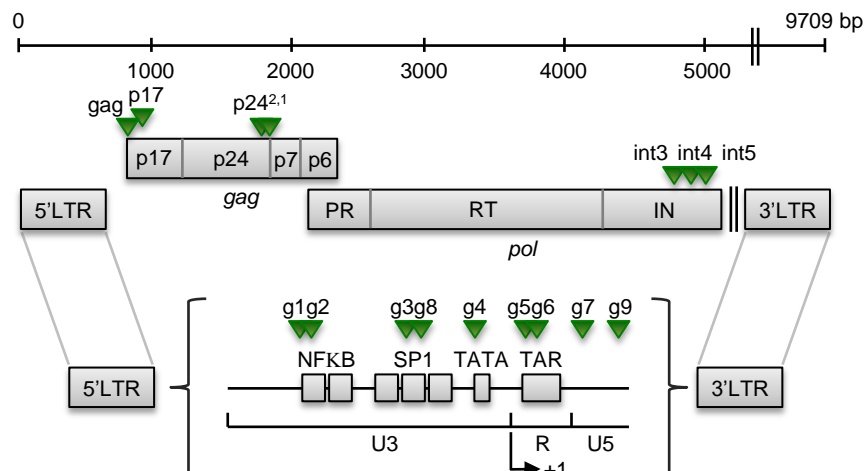
Figure 3.1: Target sites of the gRNAs used in this work. Schematic depiction of the HIV-1 NL4-3 genome and the target sites of gRNAs used in this work. LTRs and *gag* and *pol* open reading frames are depicted as rectangles. All other genes are not shown as indicated with the double slash. The scale on top indicates the size of the HIV-1 NL4-3 genome in bp. Binding sites of gRNAs are shown as arrowheads. The lower image shows the LTR sub-regions U3 (unique 3´), R (redundant) , U5 (unique5´) and important functional sites of the LTRs like the binding sites of nuclear factor kappa-light-chain-enhancer of activated B cells (NF-κB) or specificity protein 1 (SP1), the TATA box, the trans-activation response (TAR) element and the transcription start site (+1). IN, integrase; LTR, long terminal repeat; PR, proteinase; RT, reverse transcriptase.

All gRNAs have a length of 20 nt except for p17 and p24_1 which are 17 nt in length as gRNAs shorter than 20 nt were reported to show decreased mutagenesis at off-target sites [111]. The sequences of all gRNAs are listed in the supplementary table 5.1.

The design of the LTR-targeting gRNAs was performed by Prof. Dr. Dirk Grimm and Dr. Kathleen Börner. Therefore, the 5´LTR and 3´LTR sequences of the HIV-1 strains NL4-3 and HXB2 were aligned and screened for potential target sites (figure 3.2) using the ZiFiT online tool (http://zifit.partners.org/ZiFiT/Disclaimer.aspx) [197, 198]. These two HIV-1 strains were chosen for the gRNA design because our CRISPR/Cas9 system should be tested initially in HeLaP4-NLtr cells harboring an HIV-1 NL4-3 provirus and in J-Lat T cells harboring an HIV-1 HXB2 provirus.

Figure 3.2: Design of LTR-targeting gRNAs. Alignment of the 5´LTR and 3´LTR DNA sequences from the HIV-1 strains NL4-3 and HXB2. The U3 region is underlined blue, the R region is underlined orange and the U5 region is underlined green. GRNA target sites are marked with red brackets, the two guanines or cytosines of the PAM sequences are marked with green brackets. Nucleotides that are identical between the sequences are shown in yellow, transitions are highlighted in blue and transversions in green. Arrows on the right side indicate the direction of the gRNA target DNA strand.

All LTR-targeting gRNAs except for g3 exhibit 100 % conservation at both LTRs from both HIV-1 isolates. The gRNA g3 is 100 % identical with the NL4-3 3´LTR and both HXB2 LTRs but differs in three bases at the NL4-3 5´LTR.

The gRNAs targeting *gag* and *pol* were designed to bind at highly conserved target sites previously identified by ter Brake et al. [199]. Briefly, they aligned the HIV-1 strain LAI with 170 HIV-1 genomic sequences from all subtypes listed in the Los Alamos National Laboratory database and thereby identified 19 highly conserved regions in the LAI genome that are 100 % identical with at least 75 % of the aligned sequences. The gRNAs p17 and p24_1 were designed by Dr. Kathleen Börner, whereas the gRNAs gag, p24_2 and int3-5 were designed by myself.

60

To compare the conservation of all our gRNAs, together with Nils Kurzawa the gRNA sequences were blasted against the genomic sequences from isolates belonging to the HIV-1 subtypes A, B, C, F and G using the HIV Blast tool from Los Alamos National Laboratory (https://www.hiv.lanl.gov/content/sequence/BASIC_BLAST/basic_blast.html) (figure 3.3).
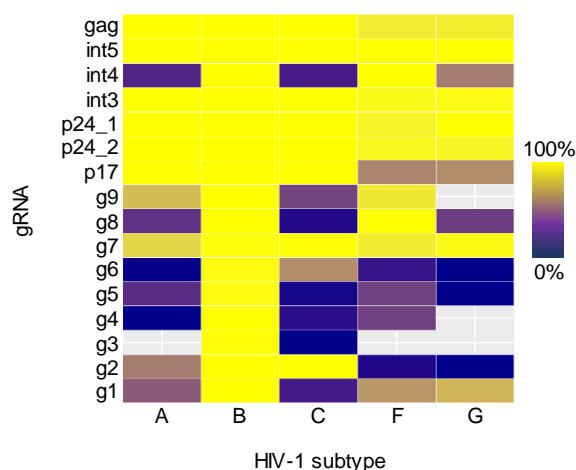

Figure 3.3: Conservation of gRNA target sites. Heatmap showing the conservation of gRNA target sites among different HIV-1 subtypes. GRNA sequences were aligned with HIV-1 genomic sequences from the Los Alamos National laboratory using the HIV Blast tool (https://www.hiv.lanl.gov/content/sequence/BASIC_BLAST/basic_blast.html). Colors represent levels of conservation: 1 (yellow) corresponds to 100 % of the sequences found by the tool showing 100 % identity with the gRNA sequence, while 0 (blue) indicates that none of the sequences found by the HIV blast tool show 100 % identity. Grey areas imply that the tool failed to perform a proper alignment.

A gRNA was defined as 100 % conserved when all of the sequences found by the tool were completely identical with the gRNA sequence, whereas 0 % conservation means that none of the found sequences were completely identical to the gRNA sequence. Almost all LTR-targeting gRNAs showed the highest conservation for isolates from subtype B, as they were designed to target the subtype B strains NL4-3 and HXB2. In contrast, g7 showed a broad conservation among all of the analyzed subtypes. The *gag*- and *pol*-targeting gRNAs, that were designed using previously described highly conserved target sites showed a broad conservation among the different subtypes except for int4 that is weakly conserved in isolates from subtype C and A.

To get an impression of the number of possible off-target sites in the human genome, an off-target prediction was performed with different online tools (table 3.1).

Table 3.1: Off-target prediction with different online tools. The table shows the number of predicted off-targets in the human genome (GRCh38/hg38) using the online tools "Cosmid" (https://crispr.bme.gatech.edu/), "CCTop" (http://crispr.cos.uni-heidelberg.de/index.html), "CRISPR Design" (http://crispr.mit.edu/) and "Cas-OFFinder" (http://www.rgenome.net/cas-offinder/ or CRISPR Design). Numbers in brackets indicate exonic off-target sites. Query parameters with Cosmid were 3 mismatches (mm) and no indels, 2 mm and 2 deletions, 2 mm and 2 insertions. Analysis with CCTop was done with 11 nt core length, 5 mm allowed in total, 2 mm allowed in core. CRISPR Design allows maximal 4mm. The query parameters with Cas-OFFinder were either 4 mm allowed (first number) or 5 mm allowed (second number). As CRISPR Design allows only analysis of gRNA sequences not shorter than 20 nt, no off-targets could be determined for p17 and p24_1. N.d., not determined.

gRNA	Cosmid	CCTop	CRISPR Design	Cas-OFFinder
g1	197	743 (51)	196	172, 1595
g2	86	649 (45)	173	108, 1272
g3	273	829 (41)	491	356, 3167
g4	659	3088 (394)	501	874, 6169
g5	48	628 (63)	132	105, 1078
g6	59	308 (22)	147	114, 984
g7	36	458 (30)	90	78, 853
g8	25	381 (48)	70	48, 615
g9	133	677 (28)	283	170, 1726
gag	622	3350 (152)	501	764, 1764
p17	1298	2605 (316)	n. d.	2786, 27622
p24_1	6492	13780 (909)	n. d.	7504, 52341
p24_2	222	817 (52)	417	306, 2395
int3	131	759 (82)	278	238, 2202
int4	201	890 (81)	350	234, 1844
int5	212	1093 (43)	342	324, 2986

The number of predicted off-targets was very variable between the different online tools as every tool uses different query parameters. For example, Cosmid allows three mismatches in the complete gRNA sequence, two mismatches in the gRNA sequence with one bp deleted and two mismatches with one bp inserted. The CCTop tool allows a maximum of five mismatches as it was shown that more than four mismatches most likely disrupt Cas9 cleavage [90, 200]. Two of these mismatches are allowed to be located in the 8 to 11 bp adjacent to the PAM sequence as

more mismatches at this site were previously shown to disrupt Cas9 cleavage [90, 95, 200]. The CRISPR Design tool allows four mismatches in total. The analysis with the Cas-OFFinder was performed either with 4 or 5 mismatches allowed in the gRNA sequence. The number of predicted off-targets ranged from 25 off-targets of g8 predicted by the Cosmid tool to 52341 off-targets of p24_1 predicted with Cas-OFFinder. Independent from the tool used least off-targets were found for the gRNAs g5, g6, g7 and g8 and most off-targets were found for p24_1. CCTop additionally gives information about the number of exonic off-targets. Maximally 13 % of the off-targets predicted with this tool were located in exons.

3.2 Application of the HIV-1-targeting CRISPR/Cas9 system in HeLaP4 cells

3.2.1 Validation of single gRNAs

The initial validation of the gRNAs was done using HeLaP4-NLtr reporter cells provided by Dr. Jens Bohne. These cells stably express the CD4 and CXCR4 receptors and carry a NL4-3 HIV-1 genome with a frameshift mutation in *env*, mutations in the start codons of *nef* and *tat* and a *gfp* sequence at the *nef* open reading frame. The gRNAs were cloned into a self-complementary AAV vector that expresses a single gRNA from the U6 promoter and carries a RSV (respiratory syncytial virus) promoter driven *gfp* reporter gene [201]. HeLaP4-NLtr reporter cells were either transfected with these vectors and a vector expressing Cas9 under the control of a short 224 bp CMV (cytomegalovirus) promoter (shCMV) or transduced with AAV crude lysates packaging these vectors. The full length CMV promoter cannot be used for Cas9-expression with AAV vectors as the promoter itself is already 612 bp in size and the whole construct including the ITRs would have a size of around 5.3 kb, which is too big for proper packaging into AAV capsids [169–171]. For the transduction of HeLaP4-NLtr reporter cells the synthetic serotype AAV9-A2 was used. This AAV9-based variant carries a peptide insertion in an exposed capsid region and was shown to transduce HeLaP4 cells by 100 % (Börner *et al.*, manuscript in preparation). Editing at the gRNA target sites was analyzed with T7 endonuclease assay. The T7 endonuclease assay for the LTR-targeting gRNAs was performed by Dr. Kathleen Börner. Therefore, different primer combinations were chosen to detect cleavage either at the 5´LTR, the 3´LTR or both LTRs (figure 3.4).

A

gRNA	T7 assay fragments (bp)		
	5′LTR	3′LTR	5′ & 3′LTR
g1	711, 67	458, 332	458, 67
g2	684, 94	431, 359	431, 94
g3	555, 223	488, 302	302, 223
g4	411, 367	632, 158	367, 158
g5	446, 332	711, 79	446, 79
g6	466, 311	732, 58	467, 58
g7	544, 234	n.d.	n.d.
g8	498, 280	510, 280	265, 260
g9	590, 188	n.d.	n.d.

B
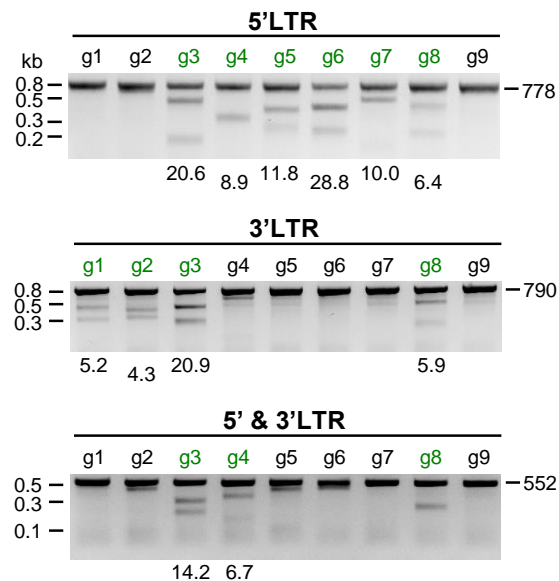
Figure 3.4: Validation of LTR-targeting gRNAs in HeLaP4-NLtr cells. (**A**) Predicted size of T7 endonuclease cleavage products for assays detecting editing at 5′LTR, at the 3′LTR or at both LTRs. (**B**) T7 endonuclease assays with LTR-targeting gRNAs. HeLaP4-NLtr cells were transfected with a gRNA expression plasmid and a Cas9 expression plasmid. T7 endonuclease assays were performed with primers amplifying the 5′LTR, the 3′LTR or both LTRs. Names of gRNAs with detectable cleavage are highlighted in green. Cleavage efficiencies in percent were calculated with ImageJ and are shown below the gel images.

For all gRNAs editing was detectable either at the 5′LTR or 3′LTR except for g9. As the sequences of both LTRs are identical at the target sites of all gRNAs except for g3 (chapter 3.1, figure 3.2), a gRNA that mediates editing at one LTR should also be functional at the other LTR. Hence, it is very likely that the editing at one LTR was not detectable with the assay because the T7 endonuclease cleavage in these cases results in one very big fragment, that cannot be easily separated from the input band, and one very small fragment, that is either too light for detection, because ethidium bromide migrates upwards, or cannot be separated from the primer dimer band. The same holds probably true for the cases where editing was detectable at one of the two LTRs but not in the assay detecting editing at both LTRs. For g3 and g8 T7 endonuclease cleavage products were detectable with all three assays.

The T7 assay for all *gag*- or *pol*-targeting gRNAs was performed by me. For all of these gRNAs the expected T7 assay cleavage products were detectable (figures 3.5, 3.6). As the T7 assays were performed to initially validate the functionality of the gRNAs, they were not repeated several times. Furthermore, the experiments were performed with crude AAV productions that were not titrated. Hence, it cannot be concluded from the cleavage efficiencies of these assays that certain gRNAs are more effective than others.
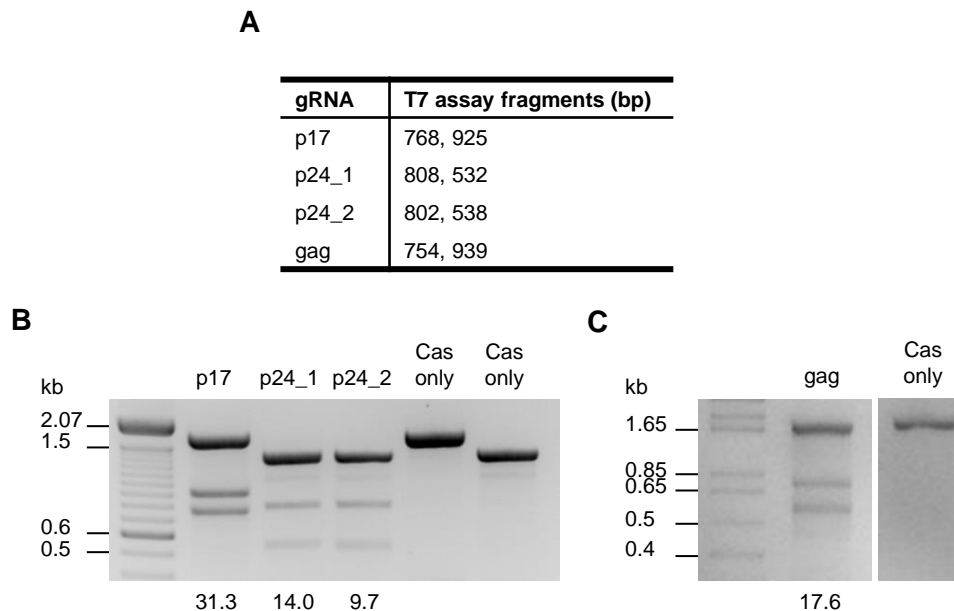
A

| gRNA	T7 assay fragments (bp)
p17	768, 925
p24_1	808, 532
p24_2	802, 538
gag	754, 939

B **C**

Figure 3.5: Validation of gRNAs targeting *gag*. (**A**) Predicted T7 endonuclease cleavage fragments in bp for the different *gag*-targeting gRNAs. (**B**) T7 endonuclease assays with *gag*-targeting gRNAs. HeLaP4-NLtr cells were transduced with AAV9-A2 crude lysates encoding the different gRNAs driven from U6 promoter and a Cas9 expressing vector or with a Cas9 expressing vector alone. Numbers below the gel images indicate cleavage efficiencies in percent calculated with ImageJ.

A **B**

gRNA	T7 assay fragments (bp)
int3	938, 753
int4	1088, 603
int5	1178, 513
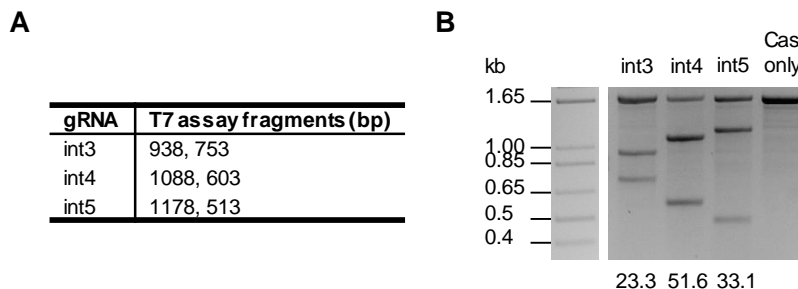
Figure 3.6: Validation of gRNAs targeting *pol*. (**A**) Predicted T7 endonuclease cleavage fragments in bp for the different *pol*-targeting gRNAs. (**B**) T7 endonuclease assay with *pol*-targeting gRNAs. HeLaP4-NLtr cells were transduced with AAV9-A2 crude lysates encoding the different gRNAs driven from U6 promoter and a Cas9 expressing vector or with a Cas9 expressing vector alone. Numbers below the gel images indicate cleavage efficiencies in percent calculated with ImageJ.

3.2.2 Comparison of different vector designs

For the expression of a single gRNA three different AAV vector designs were established in collaboration with the group of Prof. Dr. Grimm (figure 3.7). In the "standard" design a single gRNA is expressed under control of the Pol III promoter U6. In the "F+E" (flip and extension) design, which is based on a study of Chen et al. [202] a single gRNA is expressed under control of the

U6 promoter as well. However, in contrast to the "standard" design an A-U base flip in the gRNA scaffold was introduced to destroy a potential Pol III termination site. Furthermore, the scaffold is extended by five base pairs. It was shown by Chen et al. that this design leads to an increased assembly of gRNA and a cleavage deficient GFP-labeled Cas (dCas) resulting in better signal to background ratios in microscopy-based experiments. In the "all-in-one" design one gRNA and the Cas9 are expressed from one construct, where gRNA expression is controlled by the H1 promoter and Cas9 expression by the shCMV promoter [201]. The advantage of this design is that the cells only need to be transduced with one virus, whereas with the other designs the cells need to be co-transduced with a Cas9 encoding AAV limiting the efficiency of the system especially in poorly transducable cells as editing will only occur in cells double transduced with both AAVs.
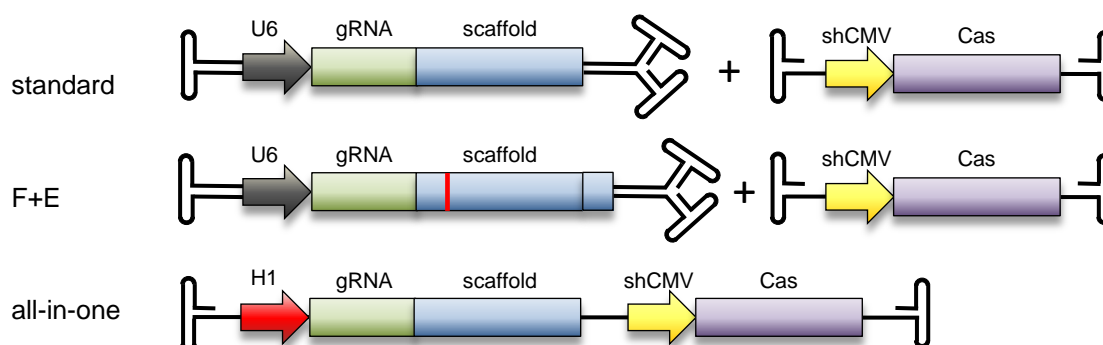

Figure 3.7: AAV vector designs for gRNA and Cas9 expression. Schematic depiction of the three tested AAV vector designs. AAV ITRs are depicted as loop structures. In the standard design one gRNA is expressed from the Pol III promoter U6. In the "F+E" (flip and extension) design an A-U base flip in the gRNA scaffold (indicated by the red line) was introduced to destroy a potential Pol III termination site and the scaffold was extended by five base pairs. Both vectors are self-complementary. As the Cas9 is not expressed from the two vectors, cells need to be treated with a second Cas9 encoding vector. In the "all-in-one" design one gRNA and the Cas9 are expressed from the same single stranded AAV vector construct, where gRNA expression is controlled by the H1 promoter and Cas9 expression by a short variant of the CMV promoter.

To compare the editing efficiencies reached with the different vectors, the LTR-targeting gRNAs g3, g5, g6 and g7 were cloned into the three different vectors. These constructs were then packaged into AAV9-A2 and crude lysates were produced. In parallel, a vector expressing Cas9 from the shCMV promoter was packaged into AAV9-A2. HeLaP4-NLtr reporter cells were transduced with the three different vector designs and cells transduced with the F+E and standard vectors were co-transduced with the shCMV-Cas vector. After 48 hours the cells were transduced a second time and another 48 hours later genomic DNA was isolated to perform a T7 assay (figure 3.8). The experiment was performed with three independent crude lysate productions.
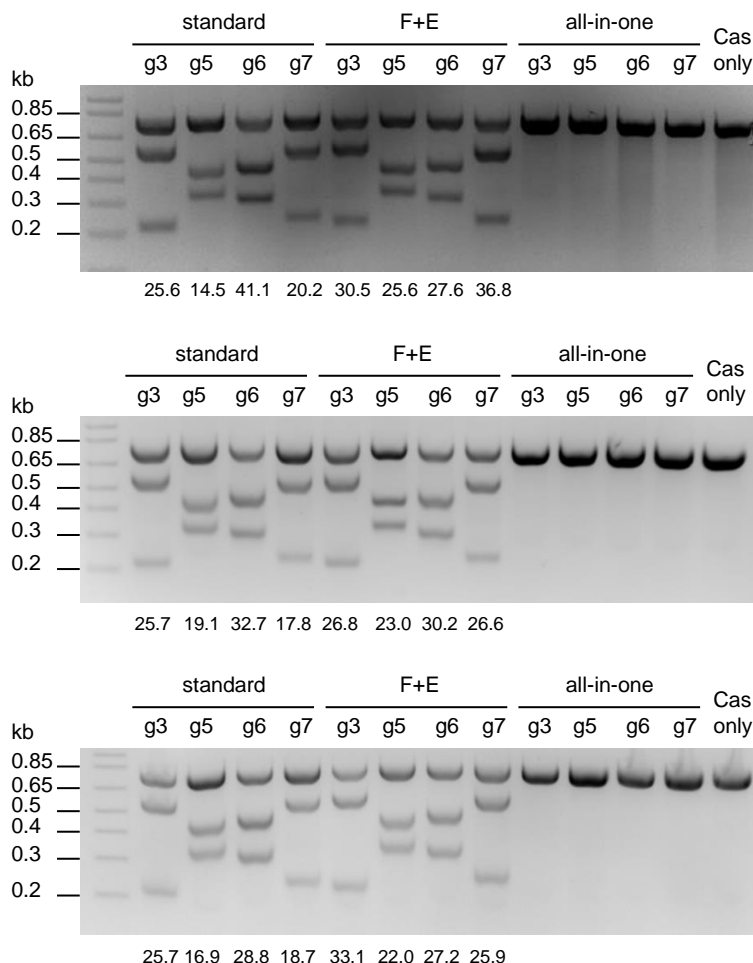
Figure 3.8: Comparison of editing with LTR-targeting gRNAs in HeLaP4-NLtr cells using different AAV vector designs. T7 endonuclease assay with genomic DNA of HeLaP4-NLtr cells treated with Cas9 and different LTR-targeting gRNAs expressed from three different vector designs. The cells were transduced twice either with AAV9-A2 encoding a shCMV promoter driven Cas9 and AAV9-A2 encoding single gRNAs expressed from the standard or F+E design vectors or with AAV9-A2 encoding the "all-in-one" vector. Two days after the second transduction, genomic DNA was isolated from the cells and T7 endonuclease assay was performed. The experiment was performed three times, each time with a different crude lysate production. Numbers below the gel images indicate the editing efficiencies in percent calculated with ImageJ.

Editing efficiencies with the F+E and the standard vector design were comparable for all gRNAs. With the all-in-one design no cleavage was detected. Although, the F+E design did not perform better in the T7 assay than the standard design, it was chosen for all further experiments, as it could be beneficial for later microscopy-based experiments due to the previously described better signal-to-background ratios described by Chen *et al.*.

3.2.3 Effect of CRISPR/Cas9-mediated cleavage at the HIV-1 5´LTR on its promoter function

After having shown that different target sites of the HIV-1 provirus can be edited with CRISPR/Cas9, the functional consequence of such mutations should be analyzed. As the consequence of mutations in protein encoding regions is relatively easy to predict, we focused on the influence of mutations in the LTR on its promoter function. Therefore, HeLaP4-NLtr cells were either transduced with crude AAV9-A2 lysates encoding Cas9 expressed from the shCMV promoter and a g5 or a g6 encoding vector, or with the Cas9 encoding vector in combination with both gRNA expressing vectors to check if targeting the g5 and g6 target sites would more efficiently reduce promoter function than targeting only one target site. The 5´LTR sequences from the CRISPR-treated cells and from untreated cells were PCR-amplified and cloned into a modified psiCheck2 plasmid (chapter 2.4.7) to drive the expression of Renilla luciferase. HEK293T cells were transfected with the cloned constructs and a Tat-expression plasmid to enable the detection of effects on promoter function caused by mutations in the TAR element. 72 hours after transfection, a dual luciferase assay was performed and values of Renilla luciferase were normalized with values of firefly luciferase expressed from the same plasmid (figure 3.9A). A reduction of up to 80 % in Renilla luciferase expression in comparison to the expression with the wildtype LTR promoter sequence was detected. In total, 11 out of the 13 analyzed clones showed a reduction in Renilla luciferase expression, whereas two clones (g5 #9, g5g6 #4) showed expression at wildtype level. Sequencing revealed mutations at the gRNA target sites in all clones (figure 3.9B). G5 and g6 are binding in the TAR element, which forms a RNA hairpin with a bulge and an apical loop which are bound by Tat and other cellular factors, thereby enhancing the LTR promoter function [203, 204]. To analyze if the reduction in promoter function was caused by an impaired folding of the TAR element, we modelled the RNA folding of the TAR sequences from the 13 clones and compared them to the folding of the wildtype TAR element (table 3.2). The RNA folding was predicted using the mfold web server (http://unafold.rna.albany.edu/?q=mfold/RNA-Folding-Form). Indeed, all clones with reduced LTR promoter function showed a destroyed folding of the TAR element, whereas the mutations in the two clones with LTR promoter function comparable to the wildtype (g5 #9, g5g6 #4) did not impair the TAR RNA folding. These results demonstrate that the mutations introduced with the gRNAs g5 and g6 can reduce LTR promoter function by destroying proper folding of the TAR element.
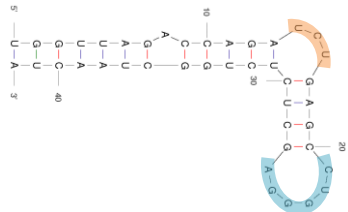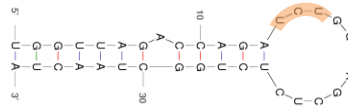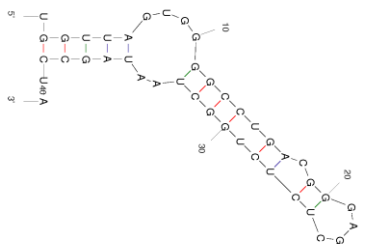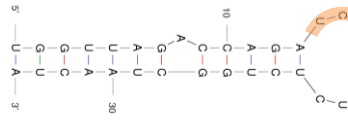
A
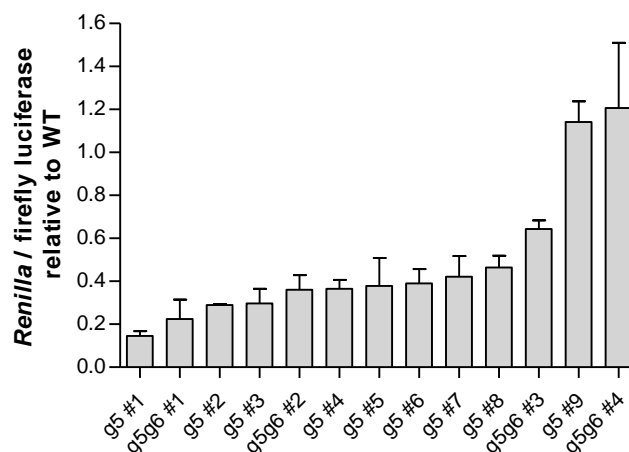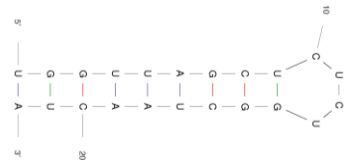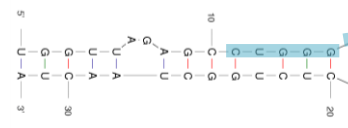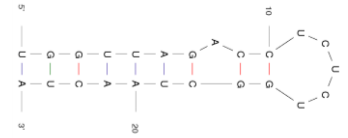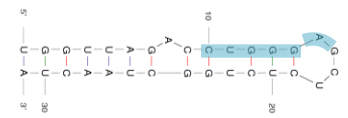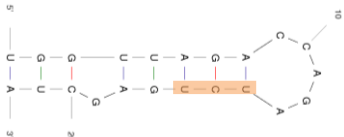
B

```
                        g5                                   g6
WT        TGGTTAGACCAGATCTG------AGCCTGGGAGCTCTCTGGCTAA----CTAGGGAACCC
g5 #1     TGGTTAGACCAGATCTG-----------GGAGCTCTCTGGCTAA----CTAGGGAACCC (-6)
g5g6 #1   TGGTTAG-TGGGGCCTGAC---------GGGAGCTCTCTGGCTAATAGCCTAGGGAACCC (+/-0)
g5 #2     TGGTTAGACCAGATCTG-------------AGCTCTCTGGCTAA----CTAGGGAACCC (-8)
g5 #3     TGGTTAG-------------------------CTCTCTGGCTAA----CTAGGGAACCC (-20)
g5g6 #2   TGGTTAG---------------AGCCTGGGAGCTCTCTGGCTAA----CTAGGGAACCC (-10)
g5 #4     TGGTTAGAC----------------------CTCTCTGGCTAA----CTAGGGAACCC (-18)
g5 #5     TGGTTAGAC----------------CTGGGAGCTCTCTGGCTAA----CTAGGGAACCC (-11)
g5 #6     TGGTTAGACCAGATCTG---------CTGGGAGCTCTCTGGCTAA----CTAGGGAACCC (-3)
g5 #7     TGGTTAGACCAGATCTGAG----------------------------CTAGGGAACCC (-18)
g5 #8     TGGTTAGACCAGATCTGATCAGAAGCCTGGGAGCTCTCTGGCTAA----CTAGGGAACCC (+6)
g5g6 #3   TGGTTAGACCAGATCTG-------------------------AA----CTATGGAACCC (-20)
g5 #9     TGGTTAGACCAGATCTGA-----AGCCTGGGAGCTCTCTGGCTAA----CTAGGGAACCC (+1)
g5g6 #4   TGGTTAGACCAGATCTG------AGCCTGGGAGCTCTCTGGCTT----------AACCC (-7)
```
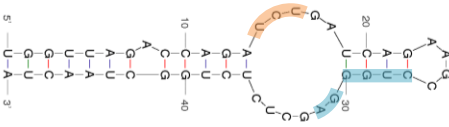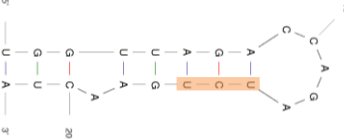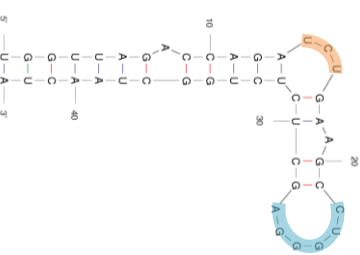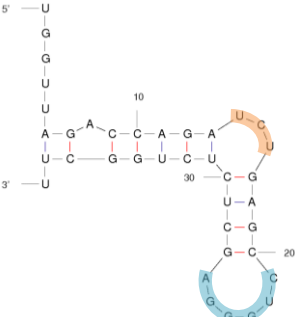
Figure 3.9: CRISPR/Cas9-mediated reduction of LTR promoter function in HeLaP4-NLtr cells. (**A**) Luciferase expression from g5/g6 modified LTR sequences. HeLaP4-NLtr cells were transduced twice with AAV9-A2 encoding g5 or g6 and Cas9. After isolation of genomic DNA, the LTRs were PCR-amplified and cloned into a modified psiCheck-2 in front of the Renilla luciferase cDNA. HEK293T cells were transfected with the resulting plasmids and a HIV Tat-expression plasmid, to enable detection of effects caused by mutations in the TAR element. Signals from Renilla luciferase were normalized to those from Firefly luciferase that is co-expressed from psiCheck-2. Data were further normalized to the values detected with the wild-type LTR that was subcloned from a HeLaP4-NLtr control which was not transduced with AAVs. Shown are means from two biological and two technical replicates with standard deviation. (**B**) TAR sequences of all analyzed clones and the wildtype (WT). Binding sites of gRNAs 5 and 6 are shown in green or red in the wildtype sequence. The TAR loop and bulge sequence is shown in bold letters. Point mutations are depicted in blue, insertions are underlined. Numbers on the right side indicate the total difference of base pairs compared to the wildtype sequence for each clone.

Table 3.2: Modelled TAR RNA structures of CRISPR-edited LTR sequences. The right column shows the TAR RNA structures of the clones analyzed with luciferase assay (figure 3.9). The structures were modelled with the mfold webserver (http://unafold.rna.albany.edu/?q=mfold/RNA-Folding-Form). The TAR loop structure is highlighted in blue, the TAR bulge structure is marked in red. The promoter activity analyzed with luciferase assay is shown in the middle column.

Clone	Promoter activity	TAR RNA structure
WT	100 %	
g5 #1	14.5 %	
g5g6 #1	22.5 %	
g5 #2	28.9 %	
g5 #3	29.7 %	
g5g6 #2	36.1 %	
g5 #4	36.6 %	
g5 #5	37.8 %	
g5 #6	39.0 %	

Clone	Promoter activity	TAR RNA structure
g5 #7	42.2 %	
g5 #8	46.4 %	
g5g6 #3	64.3 %	
g5 #9	114.3 %	
g5g6 #4	120.6 %	

3.2.4 Design and initial validation of gRNA multiplexing constructs

To enable the simultaneous editing of different sites in the HIV-1 genome and thereby increase the chance to functionally inactivate the HIV-1 provirus, we cloned our gRNAs into multiplexing constructs. These self-complementary AAV vectors allow the expression of three gRNAs from the promoters U6, H1 and 7SK (figure 3.10A). In total, 11 multiplexing constructs were generated (figure 3.10B). The constructs MP1-MP4 were cloned by Dr. Kathleen Börner and Florian Schmidt, whereas MP5-MP11 were generated by myself.

The constructs MP1-MP3 were established first and MP4-MP11 were designed later. In these later established constructs, the gRNA gag was used instead of the gRNA p17, as we found that this gRNA is not functional in J-Lat cells (chapter 3.3.2). Furthermore, some of these constructs were designed to express the same gRNAs from different promoters (MP9 and MP10; MP5 and MP11; MP6 and MP8) to analyze if some gRNAs are expressed better from a specific promoter.
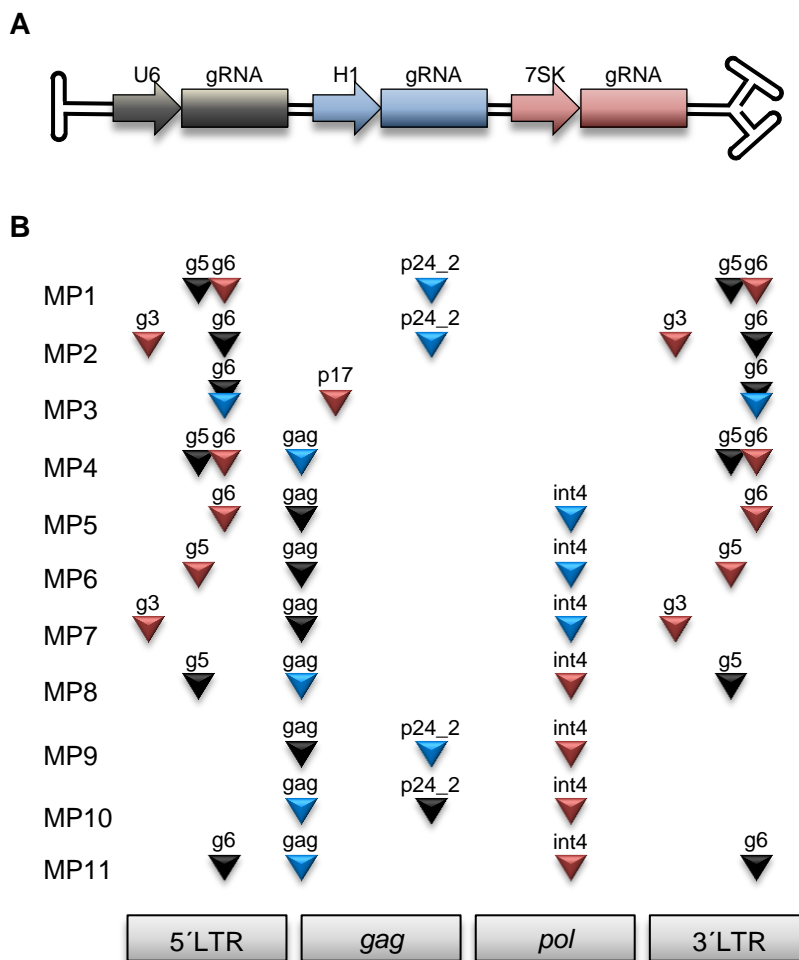
Figure 3.10: gRNA multiplexing constructs. (**A**) Schematic depiction of the gRNA multiplexing construct. The ITRs are depicted as loop structures. The self-complementary construct expresses three gRNAs from the U6, H1 and 7SK promoter. (**B**) Scheme that shows the target sites of the different gRNAs encoded from the multiplexing constructs MP1-MP11. The HIV-1 LTRs and the *gag* and *pol* open reading frames are depicted as rectangles. For simplicity all other genes are not shown. Binding sites of the gRNAs are depicted as arrowheads. Colors of the arrowheads indicate from which promoter gRNA expression is driven (Black: U6, Blue: H1, Red: 7SK). Gag, group-specific antigen; LTR, long terminal repeat; pol, polymerase.

To initially test the functionality of the different multiplexing constructs, iodixanol purified AAV9-A2 encoding MP1-MP11 or an EFS (elongation factor 1α short) promoter driven Cas9 was produced. As we found that the EFS promoter works better than the shCMV promoter for expres-

sion of Cas9 in J-Lat cells (chapter 3.3.1) and that editing efficiencies using EFS-Cas9 and shCMV-Cas9 are comparable in HeLaP4-NLtr cells (supplementary figure 5.1), the EFS-Cas9 construct was used for all further experiments with HeLaP4 cells. HeLaP4-NLtr cells were transduced with 1.2×10^7 vg/cell of the gRNA multiplexing vectors and with 1.1×10^6 vg/cell of the Cas9 encoding vector. 48 hours after the first transduction, the cells were transduced a second time and another 48 hours later, genomic DNA was isolated from the cells to perform a T7 endonuclease assay. As the multiplexing constructs encode gRNAs targeting different regions in the HIV-1 genome that cannot be covered by one PCR, several T7 endonuclease assays were performed to detect editing at the different target sites. The target sites of the LTR- and the *p17*-binding gRNAs could be covered by one PCR resulting in a 1693 bp large product (figure 3.11A). Editing at these sites was therefore analyzed with one T7 assay (figure 3.11B).

With this assay editing at all gRNA target sites at the LTR and *gag p17* was detected. Only in some cases one of the two T7 cleavage products could not be detected. For example, the small 220 bp cleavage product resulting from cleavage at the g3 target site after treatment with MP2 or MP7 and Cas9 was detectable, whereas the larger 1473 bp product was not detected, either because it could not be resolved from the 1689 bp input band or because it was additionally edited at the target sites of the gRNAs g6 or gag that are also expressed from MP2 and MP7. Furthermore, the 768 bp band resulting from cleavage at the p17 target site after treatment with MP3 was not detected and the 754 bp cleavage product caused by editing at the gag target site was in general also very light when LTR-targeting gRNAs are expressed from the same construct. Hence, both cleavage products were most probably additionally cut by another gRNA and therefore not or only weakly detectable. In addition to the T7 endonuclease cleavage products other bands were detected after treatment with Cas9 and MP2, MP3, MP4, MP5, MP7, MP8 and MP11. Due to the size of these bands we hypothesized that they display shorter versions of the provirus caused by excision of fragments between the target sites of the different gRNAs expressed from the particular multiplexing constructs. To proof this theory and to show that the bands are not caused by T7 endonuclease mediated cleavage, a PCR was performed with the same DNA samples but without a following T7 assay (figure 3.11C). Indeed, the same bands were still visible demonstrating that the gRNA multiplexing constructs not only allow simultaneous editing at different target sites but also excision of whole fragments between these sites.
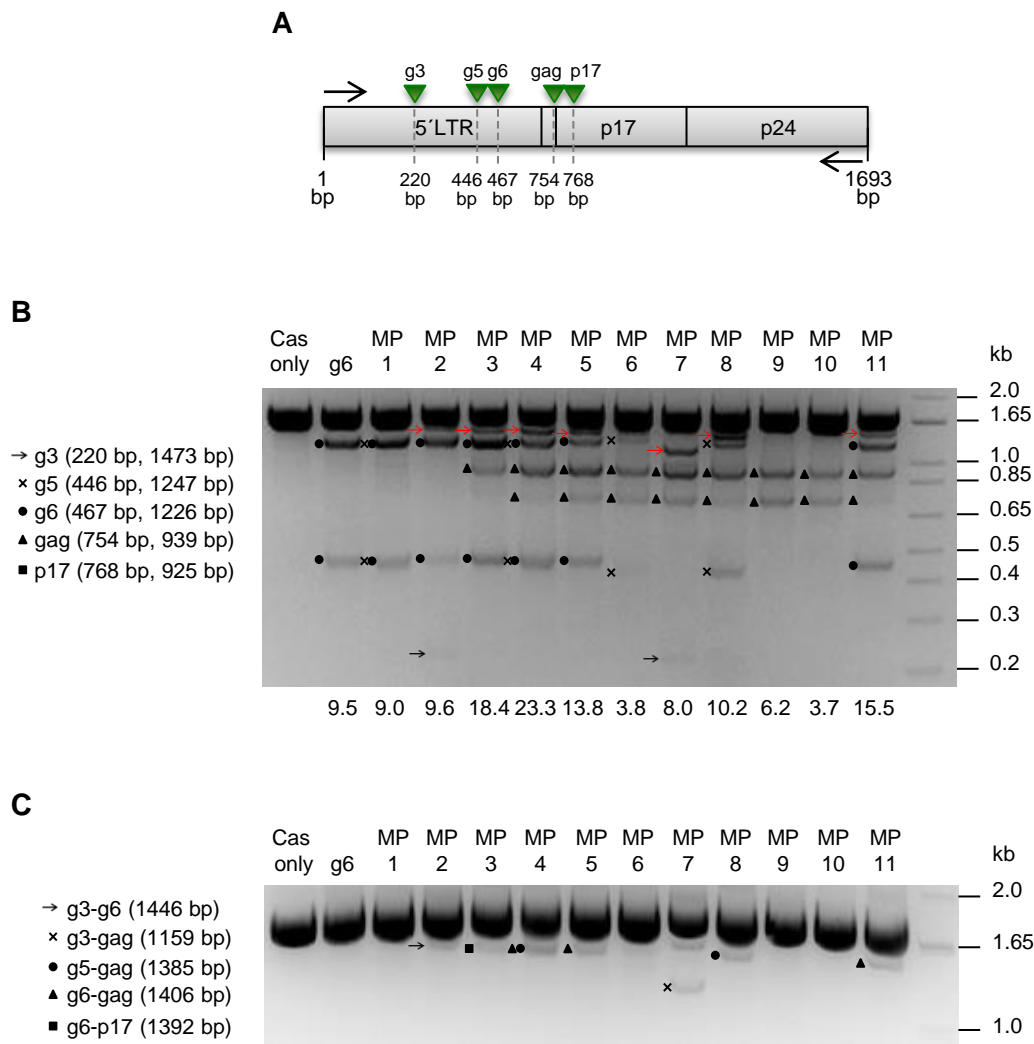
Figure 3.11: Editing at the 5´LTR and *gag p17* with gRNA multiplexing constructs in HelaP4-NLtr cells. HeLaP4-NLtr cells were transduced with AAV9-A2 vectors packaging the multiplexing constructs MP1-MP11 or the single g6 and an EFS promoter driven Cas9. Two days later, the cells were transduced a second time. After another two days the cells were lysed and genomic DNA was isolated to perform PCR and T7 assays. (**A**) Schematic depiction of the PCR amplified proviral part for the detection of editing at the 5´LTR and *p17*. GRNA binding sites are depicted as green arrowheads. The primers are depicted as arrows. Numbers below the scheme indicate the size of the PCR product in bp and the position of the cutting sites. (**B**) T7 endonuclease assay showing editing at the 5´LTR and *gag p17*. T7 endonuclease cleavage products from individual gRNAs are marked with different symbols that are explained by the legend on the left side of the gel image which also indicates the size of the T7 endonuclease fragments after cleavage at the different gRNA target sites. Numbers below the gel images indicate editing efficiencies in percent calculated with ImageJ. Additional bands which are no T7 endonuclease cleavage products are marked with red arrows. (**C**) PCR amplification of the 5´LTR- and *gag*-spanning target site. Shorter PCR products resulting from excision of DNA between two gRNA binding sites are marked with symbols. The legend on the left site states the names of these two gRNAs and the size of the shorter PCR products.

At the *gag p24* target site only very weak cleavage products could be detected with DNA from HeLaP4-NLtr cells treated with Cas9 and MP9 or MP10 (figure 3.12A). Treatment with MP1 and MP2 did not result in detectable cleavage. At the *pol* target site treatment with all int4 expressing

multiplexing constructs resulted in detectable T7 endonuclease cleavage bands whereupon the bands from MP8, MP9, MP10 and MP11 treated samples were too weak for quantification (figure 3.12B).

As this experiment was done to verify that the multiplexing constructs are functional, it was only performed one time and thereby the results do not allow conclusion about which constructs are more efficient in editing or which promoters are best for the expression of certain gRNAs. To answer these questions, the same T7 assays were performed three times with J-Lat T cells treated with the gRNA multiplexing constructs (chapter 3.3.3).
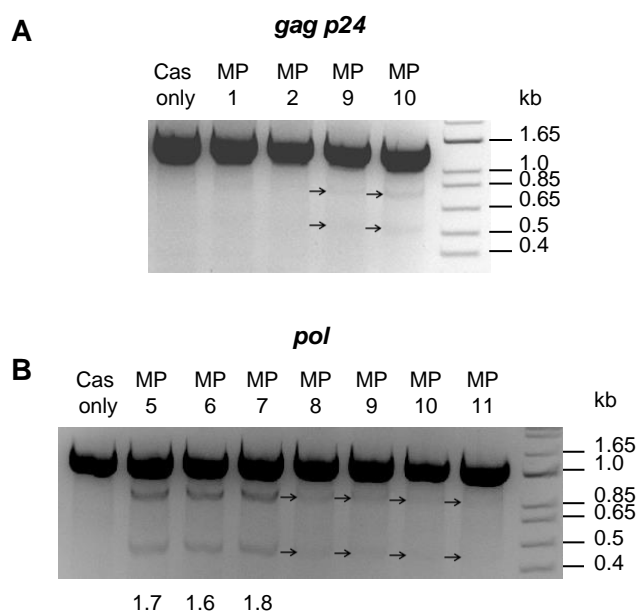
Figure 3.12: CRISPR/Cas9-mediated editing at *gag p24* and *pol* in HelaP4-NLtr cells with gRNA multiplexing constructs. HeLaP4-NLtr cells were transduced with AAV9-A2 vectors packaging the multiplexing constructs MP1-MP11 or the single g6 and an EFS promoter driven Cas9. Two days later, the cells were transduced a second time. After another two days the cells were lysed and genomic DNA was isolated to perform PCR and T7 assays. (**A**) T7 assay at the *gag p24* target site. Arrows highlight weakly detected cleavage bands. (**B**) T7 assay at the *pol* target site. Numbers under the gel picture indicate the cleavage efficiencies in percent calculated with ImageJ.

3.2.5 Protective effect against HIV-1 infection

After having shown editing at the LTR, *gag* and *pol* as well as the excision of fragments between gRNA target sites with gRNA multiplexing constructs, we aimed to analyze if HeLaP4 cells can be protected against HIV-1 infection after pretreatment with the multiplexing constructs (figure 3.13A). Additionally, we wanted to investigate if the multiplexing constructs would be more effective than a single gRNA. Therefore, we also treated cells with a vector expressing only g6, one

of our most effective gRNAs, from the U6 promoter. All gRNA expressing constructs as well as an EFS promoter driven Cas9 construct were packaged into AAV9-A2, the viruses were purified by iodixanol gradient centrifugation and titrated with qPCR. HeLaP4 cells were transduced with 1.2×10^7 vg/cell of the gRNA multiplexing vectors and with 1.1×10^6 vg/cell of the Cas9 encoding vector. Three days after first transduction, cells were transduced a second time and infected with 48 ng p24 of HIV-1 NL4-3. After 36 hours, the cells were fixed, stained with an anti-p24 antibody and Hoechst, and imaged (figure 3.13B). Automated image segmentation [205] was performed to determine the percentage of p24-positive cells (figure 3.13C).

Pretreatment with all multiplexing constructs and with the g6-encoding construct resulted in a significant reduction in the percentage of HIV-1-infected cells. The strongest reduction of around 80 % was reached with the constructs MP3 and MP11 which both express a U6 promoter driven g6 in combination with a *gag p17*-targeting gRNA (p17 or gag). To analyze if this reduction in HIV-1 infection would still be detectable in a second round of infection due to a decreased amount or infectivity of viral particles produced after CRISPR treatment, C8166 cells were infected with a dilution series of the HeLaP4 supernatants at the day of fixation. Seven days after infection, syncytia indicative for HIV-1 infection were counted and the number of infectious units per ml was calculated (figure 3.13D). All supernatants from cells treated with gRNA- and Cas9-encoding vectors still showed a significant reduction in infectious units per ml in comparison to cells only treated with the Cas9-expressing vector. With supernatants from MP3, MP4 and MP11 treated HeLaP4 cells a 100-fold reduction of infectious units/ml was detected, whereas treatment with the single gRNA6 reduced infectious units/ml only 10-fold.
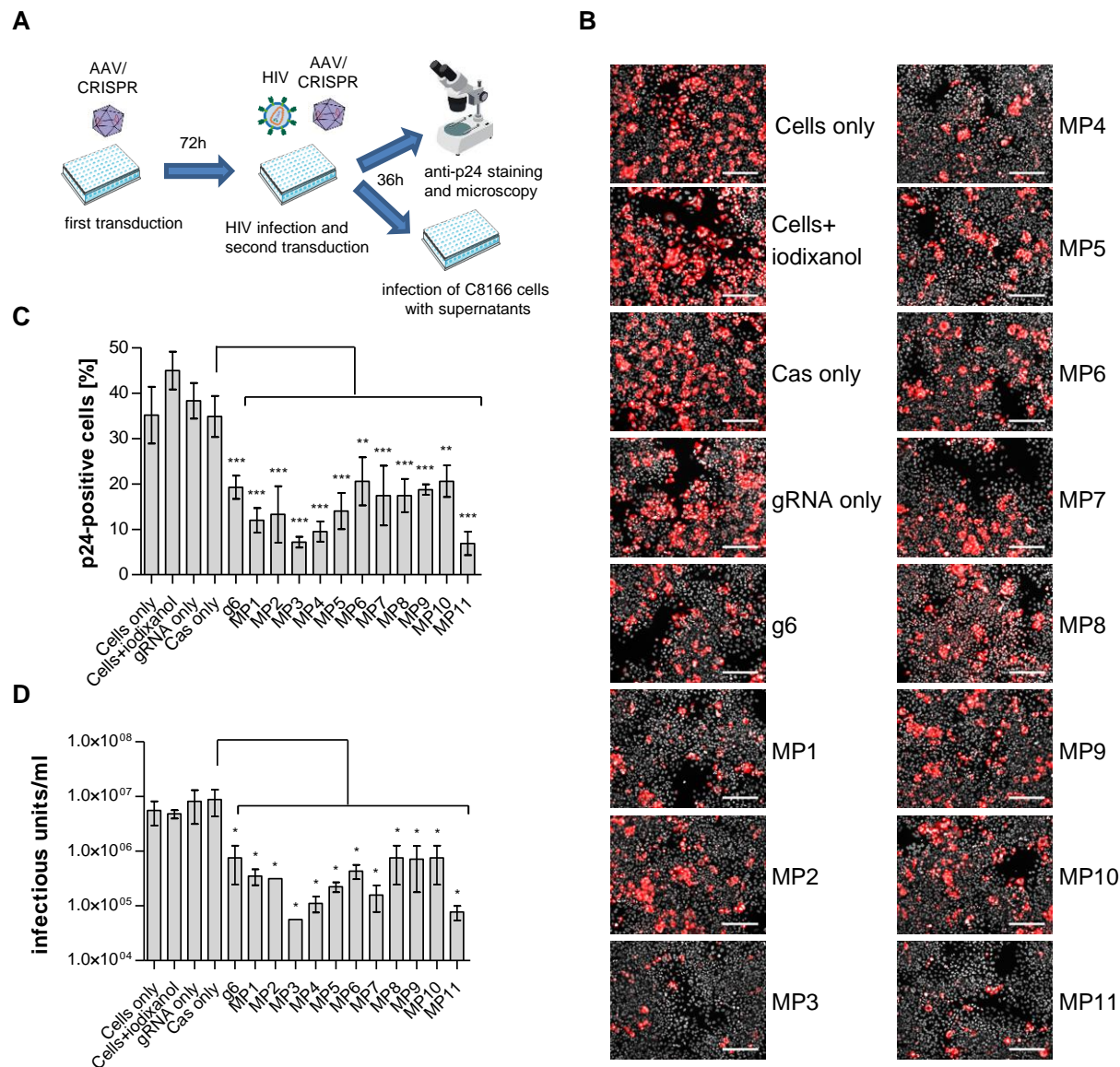
Figure 3.13: Protective effect against HIV-1 infection in HeLaP4 cells and reduction of infectious particles produced. (**A**) Schematic depiction of the experimental procedure. HeLaP4 cells were transduced with different gRNA multiplexing AAV vectors or single gRNA6 and a Cas9 expressing AAV vector. After 72 hours, they were infected with HIV-1 NL4-3 and transduced again. Another 36 hours later, the cells were fixed and stained with Hoechst and a p24-binding antibody to visualize HIV-infected cells. At the same day C8166 cells were infected with the supernatants from the HeLaP4 cells and 7 days post infection syncytia formation indicative for HIV infection was analyzed and infectious units/ml were calculated. (**B**) Overlays of the nucleic stains (grey) with p24 expression (red) as marker of viral infection. Automated image segmentation was performed to classify infected and non-infected cells. Scale bar = 200 μm. (**C**) Percentage of p24-positive HeLaP4 cells. Shown are means of three biological replicates with SD. Differences between CRISPR-treated cells and Cas only control were determined by Dunnett's post-hoc test after one-way ANOVA. ** $p<0.01$; *** $p<0.001$. (**D**) Amount of infectious units/ml in the supernatant of AAV-transduced and HIV-1-infected HeLaP4 cells. Shown are means of three biological replicates with SEM. Differences between CRISPR-treated cells and Cas only control were determined by Dunnett's post-hoc test after one-way ANOVA. * $p<0.05$.

3.3 Application of the HIV-1-targeting CRISPR/Cas9 system in J-Lat T cells

After successfully establishing the HIV-1-targeting CRISPR/Cas9 system in HeLaP4-NLtr cells, it should be applied to J-Lat T cells. This Jurkat-based cell line contains a latent HIV-1 provirus and was established by Jordan et al. [188]. They infected Jurkat cells with VSV-G pseudotyped viral particles containing a HIV-R7/E⁻/GFP genome (figure 3.14). This HXB2-based molecular clone carries a frameshift mutation in *env* and a *gfp* open reading frame in place of the *nef* gene [206]. 4 Days after infection, the population of GFP-negative cells containing uninfected and latently infected cells was selected. This population was then treated with TNFα (tumor necrosis factor alpha) to activate the proviral transcription. The GFP-positive cells were selected and cell lines were generated from individual clones, that carry the HIV-1 provirus at different sites in their genome.
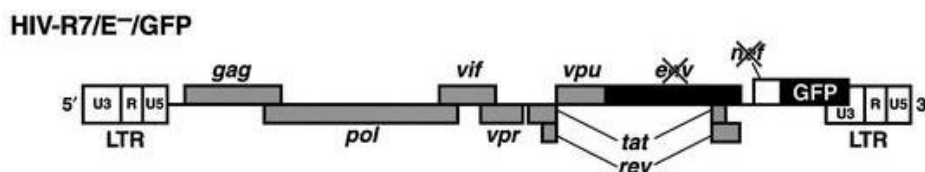
Figure 3.14: Genome of the molecular HIV-1 clone HIV-R7/E⁻/GFP integrated in J-Lat cells. Schematic depiction of the HIV-R//E⁻/GFP genome. The HIV-1 molecular clone carries a frameshift mutation in *env* and a *gfp* open reading frame instead of *nef*. Taken from [188].

Treatment of J-Lat cells with latency reversing agents like TNFα or TPA (12-O-Tetradecanoylphorbol-13-acetate) leads to the transcriptional activation of the latent provirus and thereby to the expression of the integrated GFP. Hence, this cell line allowed us to analyze if targeting a latent HIV-1 genome with our CRISPR/Cas9 system leads to functional inactivation of the provirus by imaging the cells or measuring the amount of viral particles released (chapter 3.3.3). Furthermore, as the exact integration site of the provirus in the different J-Lat clones is known, we could analyze by PCR with primers flanking the provirus, if our CRISPR/Cas9 system facilitates the excision of the provirus with LTR-targeting gRNAs (chapter 3.3.4).

3.3.1 Optimization of CRISPR/Cas9 mediated proviral editing

For the transduction of J-Lat cells with our CRISPR constructs the serotype AAV9-A2 was used since it was shown by Dr. Kathleen Börner that this peptide insertion variant is able to transduce Jurkat cells by 100 % (Börner et al., manuscript in preparation). To compare the functionality of our CRISPR system in HeLaP4-NLtr and J-Lat cells, the cells were transduced in parallel with crude AAV9-A2 vectors packaging g5 or g6 and a shCMV promoter driven Cas9 (figure 3.15). The gRNA-encoding vectors were either diluted 1:10 or used undiluted for transduction. Where-as editing at the g5 and g6 target sites was detectable in HeLaP4-NLtr cells with T7 assay, no editing was detected in J-Lat cells (clone 15.4).
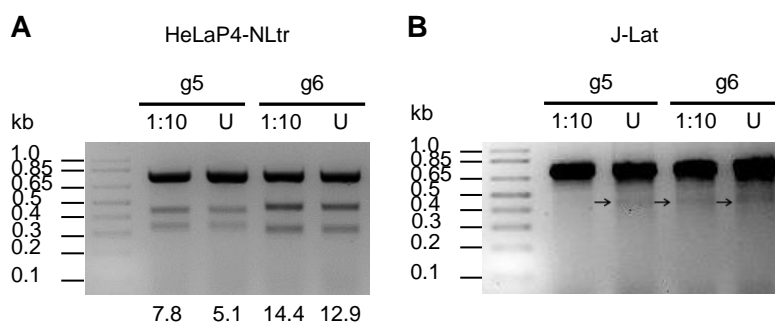

Figure 3.15: Editing at the HIV 5´LTR in J-Lat T cells and HeLaP4-NLtr cells using a shCMV promoter driven Cas9 vector. HeLaP4-NLtr and J-Lat cells (clone 15.4) were transduced with undiluted (U) or 1:10 diluted crude AAV9-A2 vectors encoding g6 or g5 and with a vector encoding a shCMV promoter driven Cas9. Genomic DNA was isolated from the transduced cells and T7 assays were performed. (**A**) T7 endonuclease assay with genomic DNA from the CRISPR-treated HeLaP4 cells. (**B**) T7 endonuclease assay with genomic DNA from the CRISPR-treated J-Lat cells. Numbers below the gel picture indicate cleavage efficiencies in percent calculated with ImageJ. Arrows mark weakly detectable cleavage bands.

As the 1:10 dilution of the gRNA vector did not decrease the cleavage efficiency drastically, we concluded that the Cas9 vector is the limiting factor of the system and that the shCMV promoter that drives the Cas9 expression might not work properly in J-Lat cells. To analyze this, Dr. Kathleen Börner and Florian Schmidt tested different other promoters in combination with the bovine growth hormone (bGH) polyadenylation signal or a minimal 60 bp polyadenylation signal (min-polyA) for Cas9 expression in J-Lat cells. Therefore, J-Lat cells (clone 15.4) were transduced with crude AAV9-A2 vectors packaging g6 and vectors expressing Cas9 from the EFS, the PGK (phosphoglycerate kinase), the TK (thymidine kinase), the full length CMV, the Syn (synapsin) or the SV40 (simian virus 40) promoter. Transduction of the cells with the EFS-Cas9 vector containing the min-polyA site or the bGH-polyA site and transduction with the TK-Cas9 vector containing the min-polyA site resulted in detectable T7 endonuclease cleavage (figure 3.16). The

combination of EFS promoter and min-polyA site was used for all further experiments with J-Lat T cells in this work as it resulted in the strongest cleavage of about 6 %, whereas the cleavage products detected with the other two vectors were too weak for quantification.
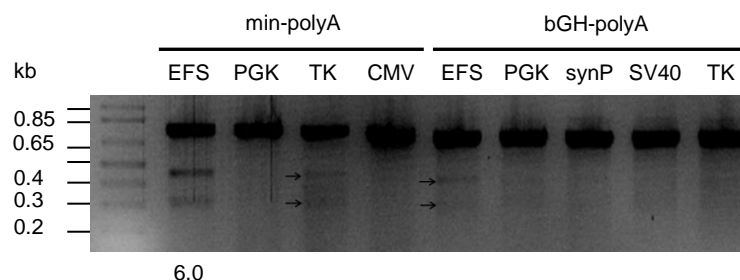
Figure 3.16: Editing at the 5´LTR in J-Lat cells using Cas9 expressing AAV vectors with different promoters and polyA sites. J-Lat cells (clone 15.4) were transduced with crude AAV9-A2 vectors encoding g6 or Cas9 expressed from the elongation factor 1α short (EFS), the Phosphoglycerate kinase (PGK), thymidine kinase (TK), the full length CMV, the synapsin (Syn) or the Simian virus 40 (SV40) promoters in combination with a short 60 bp polyA site or the bovine growth hormone (bGH) polyA site. Genomic DNA was isolated from the cells and T7 assay was performed. Arrows mark weakly detectable cleavage bands. Numbers below the gel picture indicate cleavage efficiencies in percent calculated with ImageJ.

3.3.2 Validation of single gRNA cleavage in J-Lat cells

The single LTR-targeting gRNAs were not all evaluated in J-Lat cells. Instead, g3, g5 and g6 were cloned into gRNA multiplexing constructs and thereby shown to be functional in J-Lat cells (chapter 3.3.3).

The single gRNAs targeting *gag* or *pol*, that were previously shown to be functional in HeLaP4-NLtr cells, were also tested in J-Lat cells (clone 9.2). Therefore, the cells were transduced with crude AAV9-A2 vectors expressing the single gRNAs from the U6 promoter and an EFS promoter driven Cas9 vector. Two days after the first transduction, the cells were transduced again and three days later they were lysed to extract the genomic DNA and perform a T7 endonuclease assay. The result for the *gag*-targeting gRNAs is shown in figure 3.17.

A

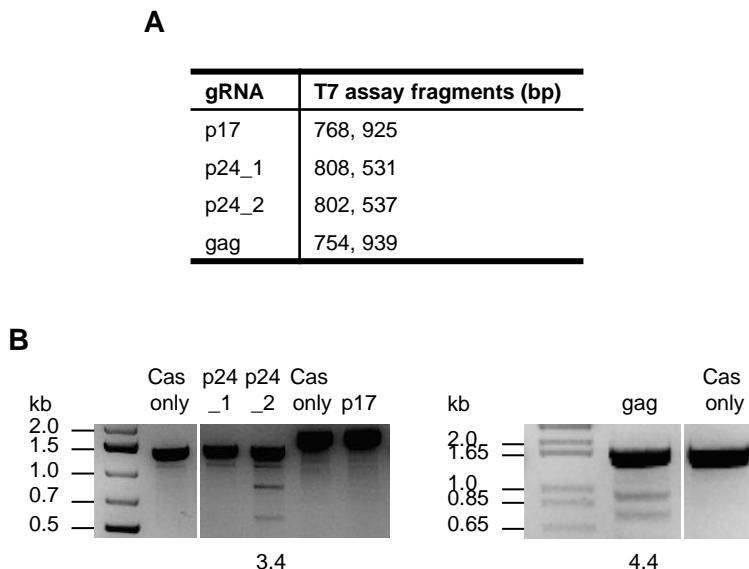| gRNA	T7 assay fragments (bp)
p17	768, 925
p24_1	808, 531
p24_2	802, 537
gag	754, 939

B

Figure 3.17: Validation of *gag*-targeting gRNAs in J-Lat cells. (**A**) Predicted T7 endonuclease cleavage fragments in bp for the different *gag*-targeting gRNAs. (**B**) T7 endonuclease assays with *gag*-targeting gRNAs. J-Lat cells (clone 9.2) were transduced with AAV9-A2 crude lysates encoding the different gRNAs expressed from U6 promoter and a Cas9-expressing vector or with a Cas9-expressing vector alone. Numbers below the gel images indicate cleavage efficiencies in percent calculated with ImageJ.

Treatment with the gRNAs p24_1 and p17 did not result in any T7 endonuclease cleavage products. This was already seen in previous T7 assays (data not shown). The reason that these gRNAs do not work in J-Lat cells is most likely that their PAM sequence in the HXB2 isolate is "NAG" instead of "NGG". It has been previously reported that this PAM sequence is also recognized by SpCas9 but less efficiently than "NGG" [106]. Hence, two new gRNAs with "NGG" PAM sequences in NL4-3 and HXB2 were designed. The gRNA gag binds at the same conserved region as p17 and p24_2 binds at the same conserved region as p24_1. Indeed, the new designed gRNAs showed the expected cleavage pattern in the T7 endonuclease assay (figure 3.17).

For the *pol*-targeting gRNAs only treatment with int3 and int4 resulted in quantifiable T7 endonuclease cleavage (figure 3.18). With genomic DNA from int5-treated cells only the upper cleavage band was detectable. However, as the assay was only performed once, it cannot be concluded that int5 is not working efficiently in J-Lat T cells.
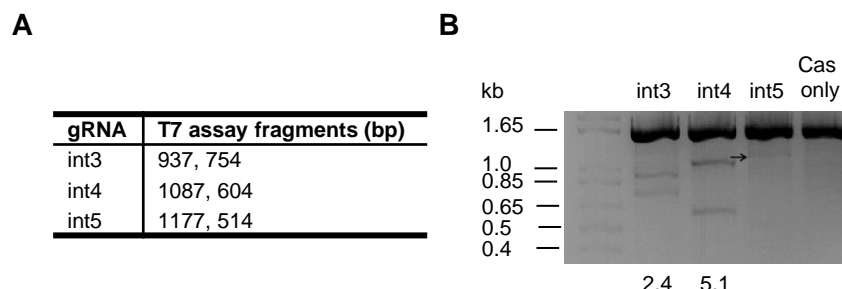
A

gRNA	T7 assay fragments (bp)
int3	937, 754
int4	1087, 604
int5	1177, 514

B

Figure 3.18: Validation of *pol*-targeting gRNAs in J-Lat cells. (**A**) Predicted T7 endonuclease cleavage fragments in bp for the different *pol*-targeting gRNAs. (**B**) T7 endonuclease assays with *pol*-targeting gRNAs. J-Lat cells (clone 9.2) were transduced with AAV9-A2 crude lysates encoding the different gRNAs expressed from U6 promoter and a Cas9-expressing vector or with a Cas9-expressing vector alone. Arrows mark weakly detectable cleavage bands. Numbers below the gel images indicate the cleavage efficiencies in percent calculated with ImageJ.

3.3.3 Analysis of editing and functional inactivation of the HIV-1 provirus in J-Lat cells using gRNA multiplexing constructs

To validate editing at the LTR, *gag* and *pol* with the gRNA multiplexing constructs in J-Lat cells and analyze, if treatment leads to a functional inactivation of the provirus, J-Lat cells (clone 9.2) were transduced with 1.2×10^6 vg per cell of purified AAV9-A2 vectors encoding MP1-MP11 or g6 and with 1.1×10^5 vg per cell of a EFS promoter driven Cas9 expression vector (figure 3.19). After 54 hours, the cells were split and transduced a second time. 21 hours later, HIV-1 proviral transcription was activated with TPA and TNFα for 5 hours. After another 40 hours, a part of the cells was lysed to extract the genomic DNA and perform T7 assays. Another part was imaged to quantify the percentage of GFP-positive cells as a marker for proviral expression. In addition, the supernatant of the cells was collected to analyze the amount of reverse transcriptase with SG-PERT as a marker for the amount of viral particles released. The experiment was performed three times.
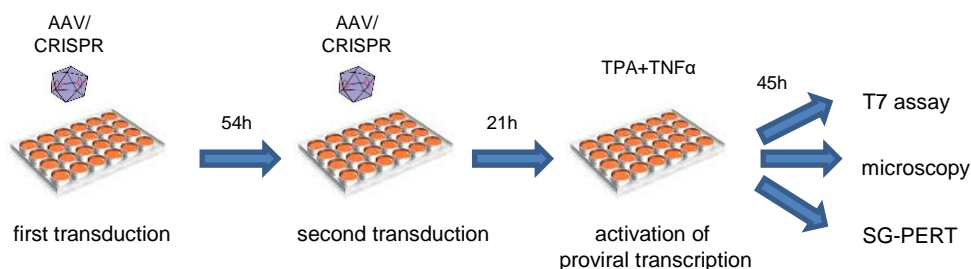
Figure 3.19: Experimental procedure for the analysis of editing and functional inactivation of the HIV-1 provirus in J-Lat cells using gRNA multiplexing AAV vectors. J-Lat cells (clone 9.2) were transduced with AAV9-A2 encoding different gRNA multiplexing constructs or single gRNA g6 and with AAV9-A2 encoding Cas9. After 54h, the cells were transduced a second time. 21h later, the proviral transcription was activated with TPA and TNFα. After another 45h, genomic DNA was isolated to perform a T7 assay, supernatant was collected to perform SG-PERT and the cells were imaged to analyze GFP-expression.

At the target site spanning the 5´LTR and *gag* the expected T7 endonuclease cleavage products for all gRNAs except for p17 encoded by MP3 were detected (figure 3.20). As described previously (chapter 3.3.2), p17 is probably not functional in J-Lat cells because the PAM is "NAG" instead of "NGG" in the isolate HXB2. Hence, p17 was replaced by the gRNA gag in the later cloned constructs MP4-MP11. Some constructs (MP9 and MP10, MP5 and MP11, MP6 and MP8) were designed to express the same gRNAs from different promoters to analyze if some gRNAs are more efficiently expressed from a certain promoter. Treatment of the cells with MP9 expressing gag from the U6 promoter and MP10 expressing gag from 7SK promoter resulted in comparable cleavage efficiencies. The combination of gag expressed from the promoter U6 and g6 expressed from the H1 promoter in MP5 resulted in comparable cleavage efficiencies as the treatment of the cells with MP11 expressing g6 from the U6 promoter and gag from the 7SK promoter. In two of the three experiments treatment of the cells with MP6 expressing g5 from the 7SK promoter did not result in detectable cleavage at the g5 target site. In the other experiment cleavage was only detectable very weakly. In contrast, expression of g5 from the U6 promoter in MP8 resulted in detectable cleavage at the g5 target site in all three experiments. Overall the highest cleavage efficiencies at the 5´LTR- and *p17*-spanning target site were reached with MP1, MP3, MP4, MP5 and MP11, which either express g6 in combination with gag or g3 or which express two copies of g6.
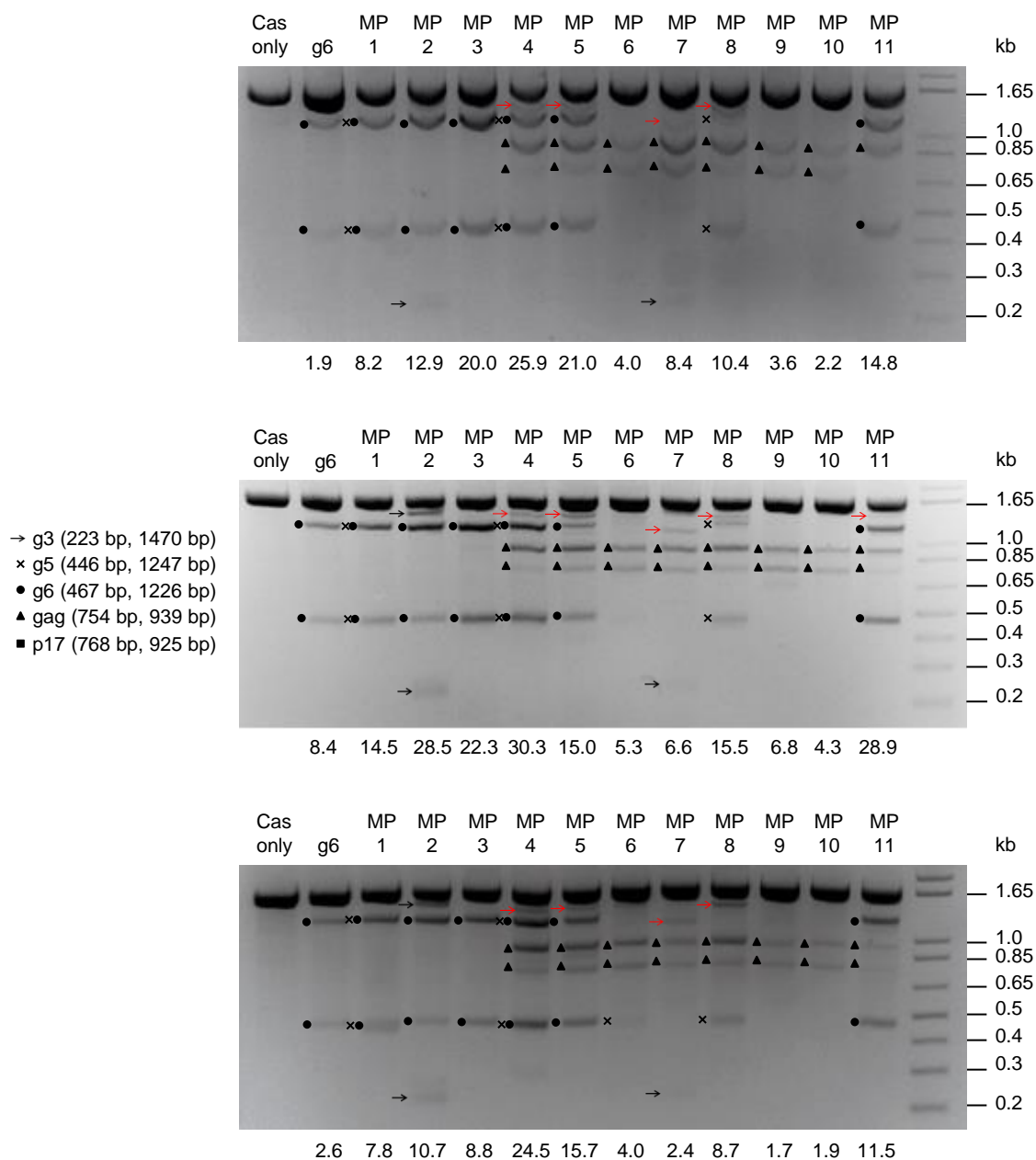
Figure 3.20: CRISPR/Cas9-mediated editing at the 5´LTR and *gag p17* with gRNA multiplexing constructs and single gRNA6. Shown are results from T7 endonuclease assays performed after two consecutive transductions of J-Lat clone 9.2 with purified AAV9-A2 vectors expressing either Cas9 or different triple-gRNA combinations/single gRNA6. T7 endonuclease cleavage products from individual gRNAs are marked with different symbols that are explained by the legend on the left side of the gel image which additionally indicates the size of the T7 endonuclease fragments. Numbers below the gel images indicate editing efficiencies in percent calculated with ImageJ. Additional bands which are no T7 endonuclease cleavage products are marked with red arrows.

At the *pol* target site quantifiable T7 endonuclease mediated cleavage was only detectable after treatment with MP5-7 (figure 3.21), which express the gRNA int4 from the H1 promoter. In contrast, treatment of the cells with MP8-11, which express int4 from the 7SK promoter, resulted either in very weak cleavage bands or no cleavage at all.

84

Figure 3.21: CRISPR/Cas9-mediated editing at *pol* with gRNA multiplexing constructs. Shown are results from T7 endonuclease assays performed after two consecutive transductions of J-Lat clone 9.2 with purified AAV9-A2 vectors expressing either Cas9 or different gRNA multiplexing constructs. Arrows mark weakly detectable cleavage bands. Numbers below the gel pictures indicate cleavage efficiencies in percent calculated with ImageJ.

At the *p24* target site cleavage was only detectable with the constructs MP9 and MP10 in one of the three experiments (figure 3.22). However the cleavage was too weak for quantification. Treatment with MP1 and MP2 did not result in detectable editing in any of the three experiments.
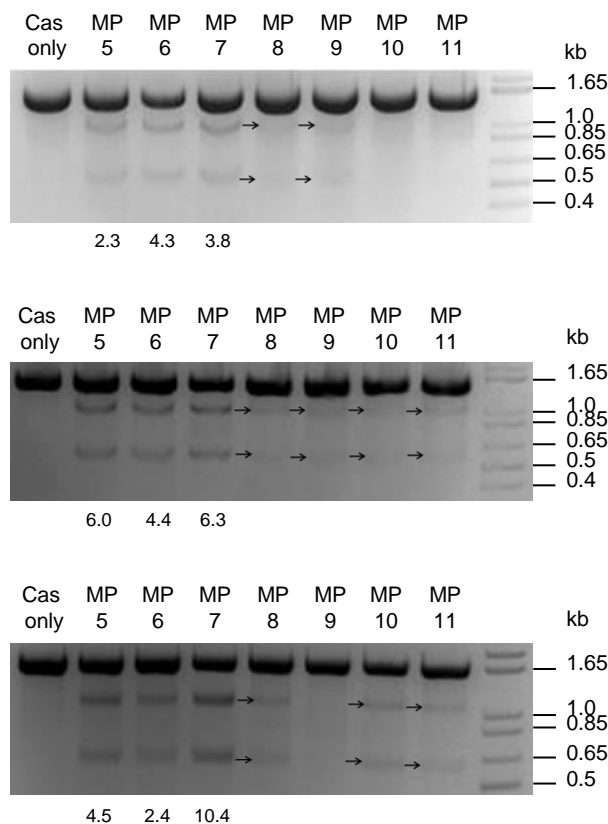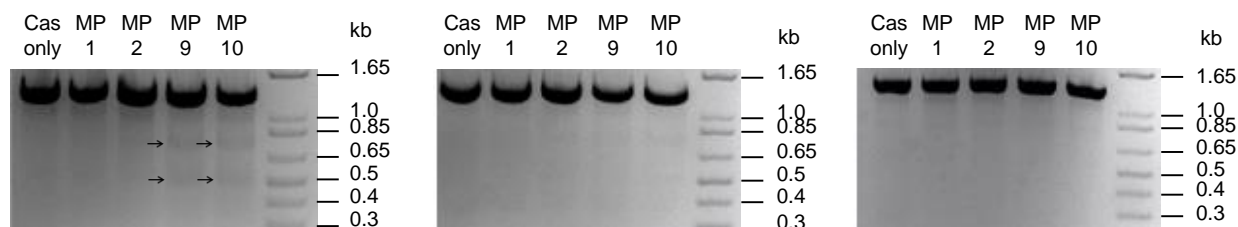

Figure 3.22: CRISPR/Cas9-mediated editing at *gag p24* with gRNA multiplexing constructs. Shown are results from T7 endonuclease assays performed after two consecutive transductions of J-Lat clone 9.2 with purified AAV9-A2 vectors expressing either Cas9 or different gRNA multiplexing constructs. Arrows mark weakly detectable cleavage bands.

As previously seen with HeLaP4-NLtr cells (chapter 3.2.4), treatment of J-Lat cells with our gRNA multiplexing vectors also resulted in additional bands detected with T7 assay at the 5´LTR/*p17*-spanning target site (figure 3.20). Hence, as previously done with samples from CRISPR-treated HeLaP4-NLtr cells, we performed a PCR without following T7 assay with the DNA samples of the CRISPR-treated J-Lat cells from all three experiments to proof that these bands are no T7 endonuclease cleavage products but display shorter variants of the provirus after excision of DNA sequences between different gRNA target sites (figure 3.23). Indeed, shorter PCR products were detected after treatment with MP4, MP5, MP7 and MP8 with DNA from all three experiments. Treatment with MP11 resulted in a shorter PCR product only in one of the experiments.

Figure 3.23: Excision of proviral fragments between the 5´LTR and *p17*. PCR amplification of the 5´LTR/p17-spanning target site. Shorter PCR products resulting from excision of DNA between different gRNA target sites are marked with symbols that are explained by the legend on the left site of the gel images.

To analyze if the transduction of the J-Lat cells with our CRISPR-AAV vectors decreases proviral expression, the cells were imaged to detect the expression of the *gfp* that is integrated in the proviral se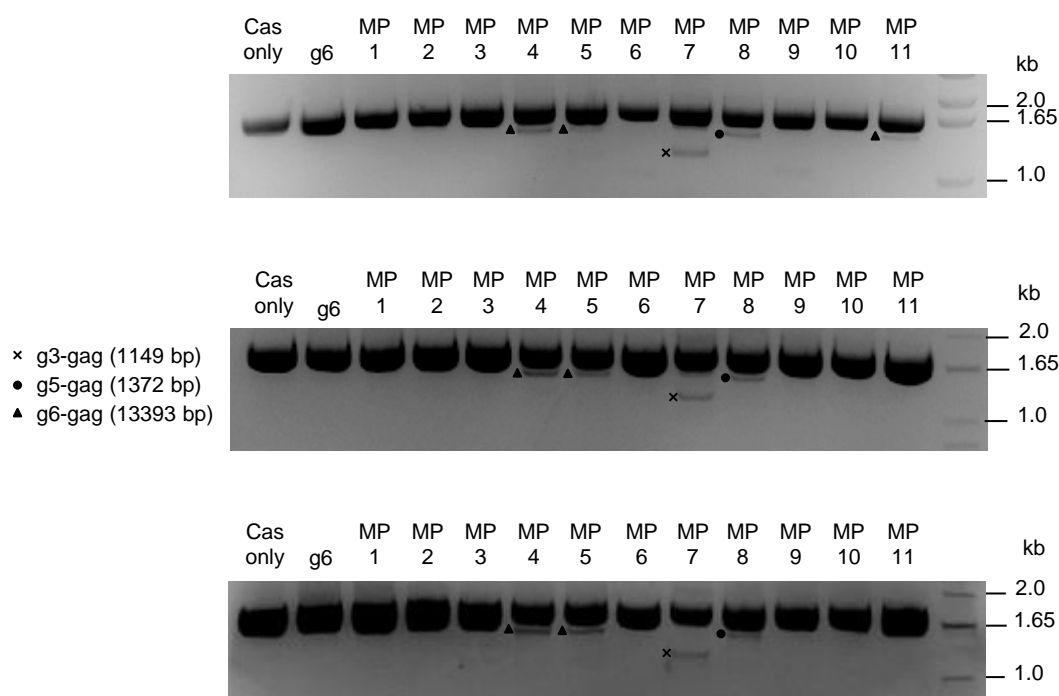quence in J-Lat cells (figure 3.14). The cells transduced with the single g6 could not be analyzed because this vector expresses GFP as well. As the *gfp* sequence in J-Lat cells is integrated in the *nef* open reading frame, only the effect of LTR mutations can be detected with this readout. Indeed, treatment with MP9 and MP10, which do not encode a LTR-targeting gRNA, did not result in a significant reduction of GFP-expression compared to cells only transduced with the Cas9-encoding vector (figure 3.24A). Also treatment with MP7 did not result in a significantly reduced number of GFP-positive cells. All other constricts mediated a significant reduction of proviral transcription and the highest reduction of about 73 % to 75 % was reached with the constructs MP4 and MP11.

To additionally analyze the effect on the release of viral particles, SG-PERT was performed with medium from the CRISPR-treated and untreated J-Lat cells (figure 3.24B). Treatment with all multiplexing constructs and with the single gRNA g6 resulted in a significant reduction of detectable RT. Furthermore, transduction with all gRNA vectors that mediate editing at two or three proviral sites in J-Lat cells resulted in a stronger reduction of viral release than transduction with g6 and the construct MP3, that only mediates editing at the g6 target site in J-Lat cells as the gRNA p17 is not functional in these cells. The lowest amount of RT compared to the Cas only control was detected in the supernatant of cells transduced with MP4 and MP8. The amount of RT was reduced by 72 % after treatment with MP8 and by 74 % after treatment with MP4. Collectively, constructs encoding a LTR-targeting gRNA in combination with the gRNA gag (MP4-8, MP11) were most effective in reducing viral release. To exclude, that the reduction of the viral release detected in this experiment is caused by toxic effects of the AAVs on the cells, a viability test was performed with transduced and untransduced cells (supplementary figure 5.2) and no reduction in viability of transduced cells was seen in comparison with untransduced cells.
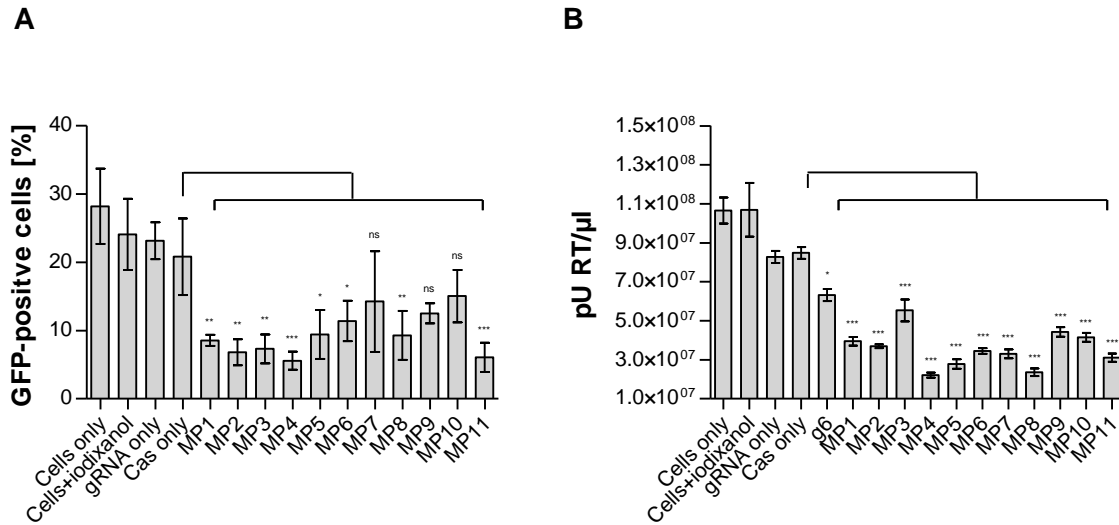
A

B

Figure 3.24: Functional inactivation of the HIV-1 provirus in J-Lat cells. J-Lat 9.2 cells were seeded and co-transduced with purified AAV9-A2 vectors encoding different gRNA multiplexing constructs or gRNA6 alone and with a Cas9-expressing AAV. As control, cells were transduced only with a Cas9/gRNA-encoding vector alone or treated with iodixanol. After 48 hours, the cells were split and transduced a second time. Another 20 hours later, HIV-1 proviral DNA transcription was activated by adding TPA/TNFα for 5 hours, before the cells were washed and incubated for 42 hours until analysis. (**A**) Percentages of GFP-positive J-Lat cells after activation of proviral expression with TPA/TNFα. Shown are means of three biological replicates with standard deviation. Differences between CRISPR-treated cells and Cas only control were determined using Dunnett's post-hoc test after one-way ANOVA. * $p<0.05$; ** $p<0.01$; *** $p<0.001$. (**B**) Results from SG-PERT assay which measures the activity of encapsidated viral reverse transcriptase (RT) in HIV-1 particles and thus permits HIV progeny quantification. Shown is the mean from three biological replicates with SD. Differences between CRISPR-treated cells and Cas only control were determined by Dunnett's post-hoc test after one-way ANOVA. * $p<0.05$; *** $p<0.001$.

3.3.4 Proviral excision in J-Lat cells

After having found that treatment with our multiplexing vectors not only enables editing at different sites of the provirus but also leads to the excision of fragments between the 5´LTR and *gag*, we wanted to analyze if our CRISPR system also facilitates the excision of the whole proviral sequence between the LTRs. Therefore, I performed a PCR with genomic DNA from J-Lat cells (clone 9.2) prepared by Dr. Kathleen Börner. The cells were transduced with AAV9-A2 vectors encoding MP1-3 and an EFS promoter driven Cas9. 54 hours later, the cells were transduced a second time. 21 hours after the second transduction, the proviral transcription was activated 5 hours with TPA and TNFα. After another 40 hours, the genomic DNA was extracted from the cells. To amplify of the proviral sequence by PCR, the primers P2 and P3 described by Lenasi et al. [207] were used. These primers are flanking the proviral sequence integrated into the *pp5* (serine/threonine phosphatase 5) gene in the J-Lat clone 9.2 (figure 3.25A).
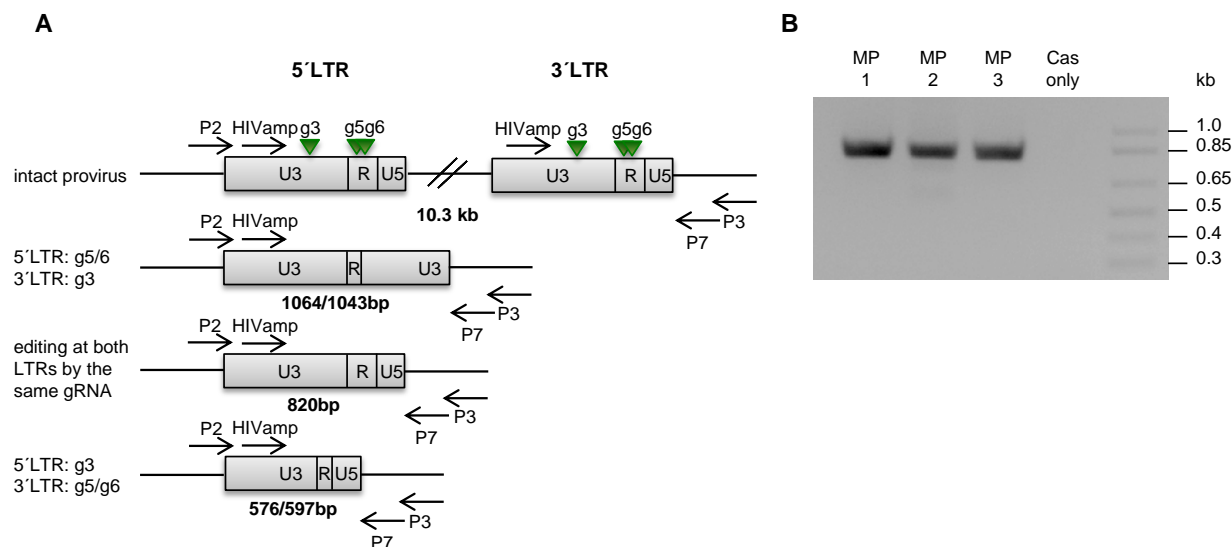
Figure 3.25: Excision of the proviral sequence between the LTRs in J-Lat cells using gRNA multiplexing vectors. (**A**) Schematic depiction of proviral DNA before and after cleavage by Cas9 using different LTR-targeting gRNAs. Primers used for PCR amplification (P2, P3) and sequencing primers (HIVamp, P7) are depicted as arrows. Expected band sizes are shown below each picture. The left number indicates the band size in case of g5 cleavage and the right number indicates the size in case of g6 cleavage. (**B**) Gel picture after PCR with gDNA from either untreated J-Lat clone 9.2 or cells treated with AAV9-A2 encoding Cas9 and MP1, MP2 or MP3.

Our standard DNA polymerase and the PCR conditions used (chapter 2.4.8) do not allow amplification of the complete proviral sequence with a length of around 10 kb. Hence, the PCR will only amplify short versions of the provirus resulting from excision of DNA between the LTRs. As MP1-3 express three different LTR-targeting gRNAs (g3, g5, g6), the PCR products can have variable sizes depending on the gRNA target site at which the DNA double-strand break at the 5´LTR and the 3´LTR was made (figure 3.25A). If the break at both LTRs is mediated at the same target site, this will result in a 820 bp PCR product. If the break in the 5´LTR is performed at the g3 target site and the 3´LTR is cut at the g5 or g6 target site, this will result in either a 576 bp or 597 bp PCR product. If the 5´LTR is cut at the g5 or g6 target site and the 3´LTR is cut at the g3 target site, this results in a 1064 bp or a 1043 bp PCR product. PCR amplification of the provirus in J-Lat clone 9.2 treated with MP1-3 resulted in a 820 bp PCR product (figure 3.25B) indicating that both LTRs were cut at the same gRNA target site. The same PCR with DNA from cells transduced only with a Cas-expressing AAV did not result in a PCR product.

To analyze at which gRNA target site the LTRs were cut, the PCR products were sequenced at the 5´LTR (figure 3.26) and the 3´LTR (figure 3.27) using the primers HIVamp and P7 (figure 3.25A). The sequencing reads for the PCR products from cells treated with MP1 and MP3 were destroyed at the g6 target site at the 5´LTR and at the 3´LTR. The read of the PCR product from

MP2-treated cells showed mutations from the g3 target site on but still continued to the g6 target site from where on it was completely destroyed, which indicates that the sequences were mutated at the g3 target site but that cleavage occurred at the g6 target site. At the 3´LTR the read was also destroyed at the g6 target site. Collectively, the results show that our CRISPR system enables the excision of the proviral sequences between the g6 target sites of the 5´LTR and the 3´LTR.
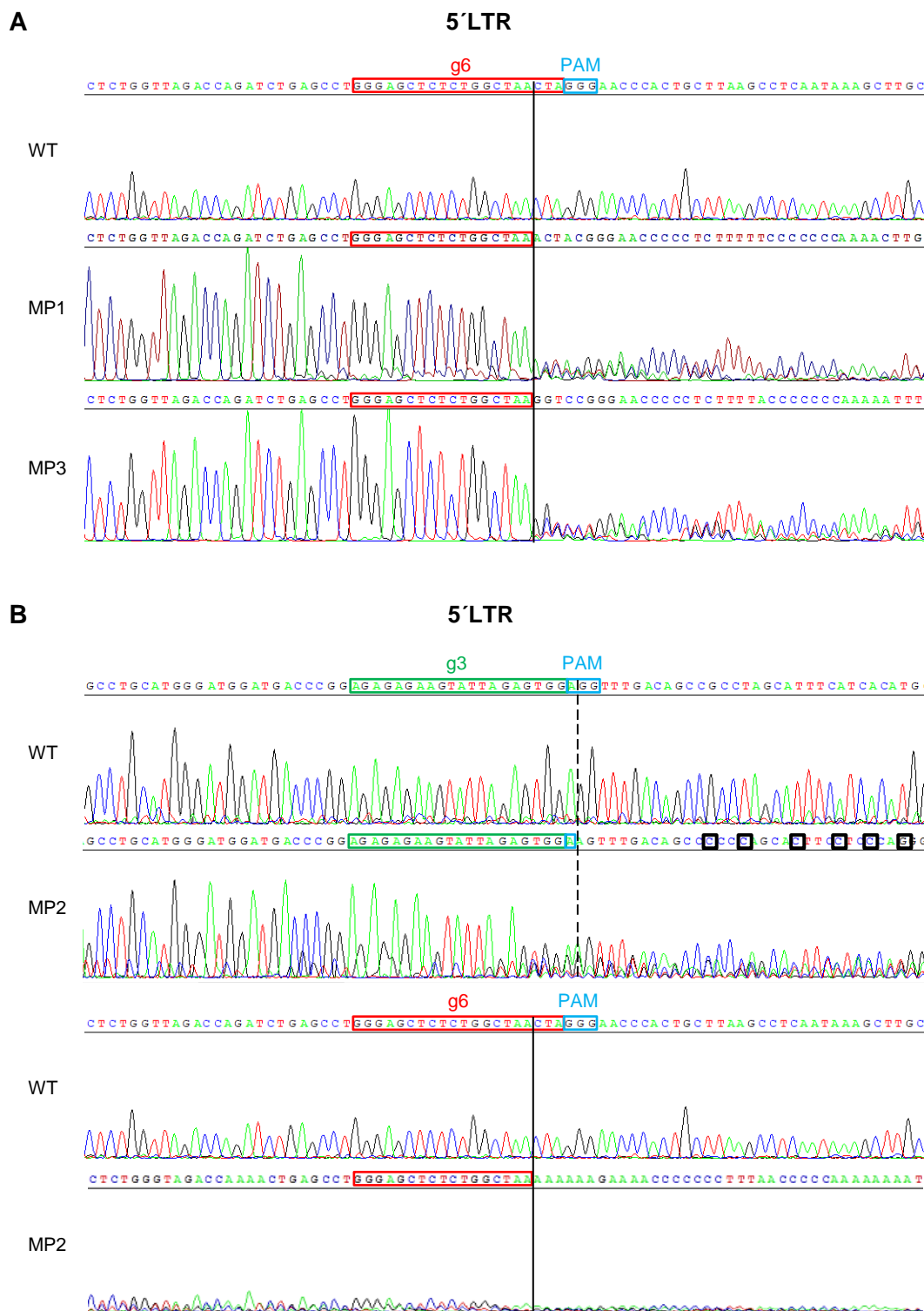
Figure 3.26: 5´LTR sequences of proviral DNA amplified with the primers P2 and P3. Chromatogram of SANG-ER sequencing using the primer HIVamp and DNA extracted from the gel shown in figure 3.25. For comparison the sequencing read of the wildtype (WT) sequence is also depicted. (**A**) Sequencing reads of PCR products from cells treated with the gRNA multiplexing constructs MP1 and MP3. (**B**) Sequencing reads of the PCR product from cells treated with the gRNA multiplexing construct MP2. Black lines mark sites from where the read is destroyed. The dashed black line marks a site from where the read shows mutations (black boxes). Red boxes highlight the g6 target site, the green box depicts the g3 target site and the blue boxes mark the PAM sequences.
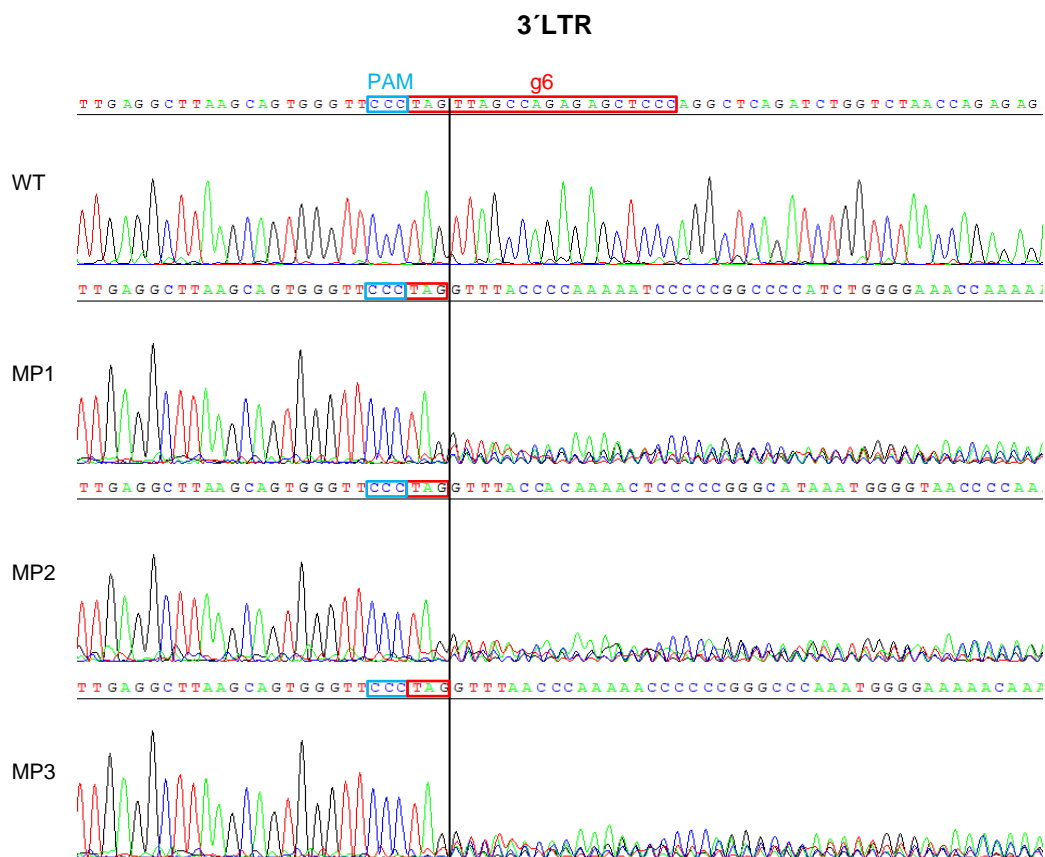
3´LTR

Figure 3.27: 3´LTR sequences of proviral DNA amplified with the primers P2 and P3. Chromatogram of SANG-ER sequencing using the primer P7 and DNA extracted from the gel shown in figure 3.25. For comparison the sequencing read of the wildtype (WT) sequence is also depicted. Black lines mark sites from where the read is destroyed. The dashed black line marks a site from where the read shows mutations (black boxes). Red boxes highlight the g6 target site, the green box depicts the g3 target site and the blue boxes mark the PAM sequences.

3.4 Application of the HIV-1-targeting CRISPR/Cas9 system in primary human CD4$^+$ T cells

3.4.1 Comparison of different AAV serotypes for transduction of primary CD4$^+$ T cells

To enable the application of our CRISPR system in primary human CD4$^+$ T cells, different AAV serotypes were compared for their transduction efficiencies of these cells. Therefore, a CMV promoter driven YFP construct was packaged by Dr. Kathleen Börner into AAV2, AAV5, AAV6 and AAV9-A2 capsids. To initiate proliferation and enable HIV-1 infection, T cells need to be activated. Hence, two methods for activation of the T cells were compared in this experiment to analyze if they would make a difference in the transduction efficiencies of the tested AAVs. One method uses so-called Dynabeads, which are iron oxid beads covalently coupled to anti-CD3 and anti-CD28 antibodies. These beads mimic the *in vivo* stimulation of T cells by two signals that are mediated by binding of the antigen/MHC (major histocompatibility complex) complex on an antigen-presenting cell (APC) to the T cell receptor/CD3 complex and by binding of the transmembrane proteins CD80 and CD86 on the APC to CD28 on T cells [208]. The other method uses phytohemagglutinin (PHA), a mitogenic lectin which binds the T cell receptor [209]. In addition to the Dynabeads and PHA, the T cell growth factor interleukin-2 (IL-2) was added to the cells.

T cells from buffy coats of two donors were isolated and activated with the previously mentioned methods for three days. Then they were transduced with 2.7 x 10^4 vg per cell of the different AAVs. Three days after transduction, the cells were analyzed by flow cytometry (figure 3.28). Independent from the activation method used, cells from both donors were transduced best with AAV2 and AAV6, whereas AAV5 and AAV9-A2 transduced the cells only very poorly. The activation with Dynabeads and IL-2 resulted in higher transduction efficiencies for cells from both donors. For example, after activation with Dynabeads 51 % of the cells from donor A and 33 % of the cells from donor B were transduced with AAV6. In contrast, after activation with PHA only 9.7 % of the cells from donor A and 6.9 % of the cells from donor B were transduced with AAV6. Hence, the activation method using Dynabeads was chosen for all further experiments. As Dr. Kathleen Börner observed that AAV6 is also very efficiently transducing macrophages (data not shown), this serotype was chosen for all further experiments enabling sharing of the AAV productions for the application in macrophages and primary CD4$^+$ T cells.

A

B

C
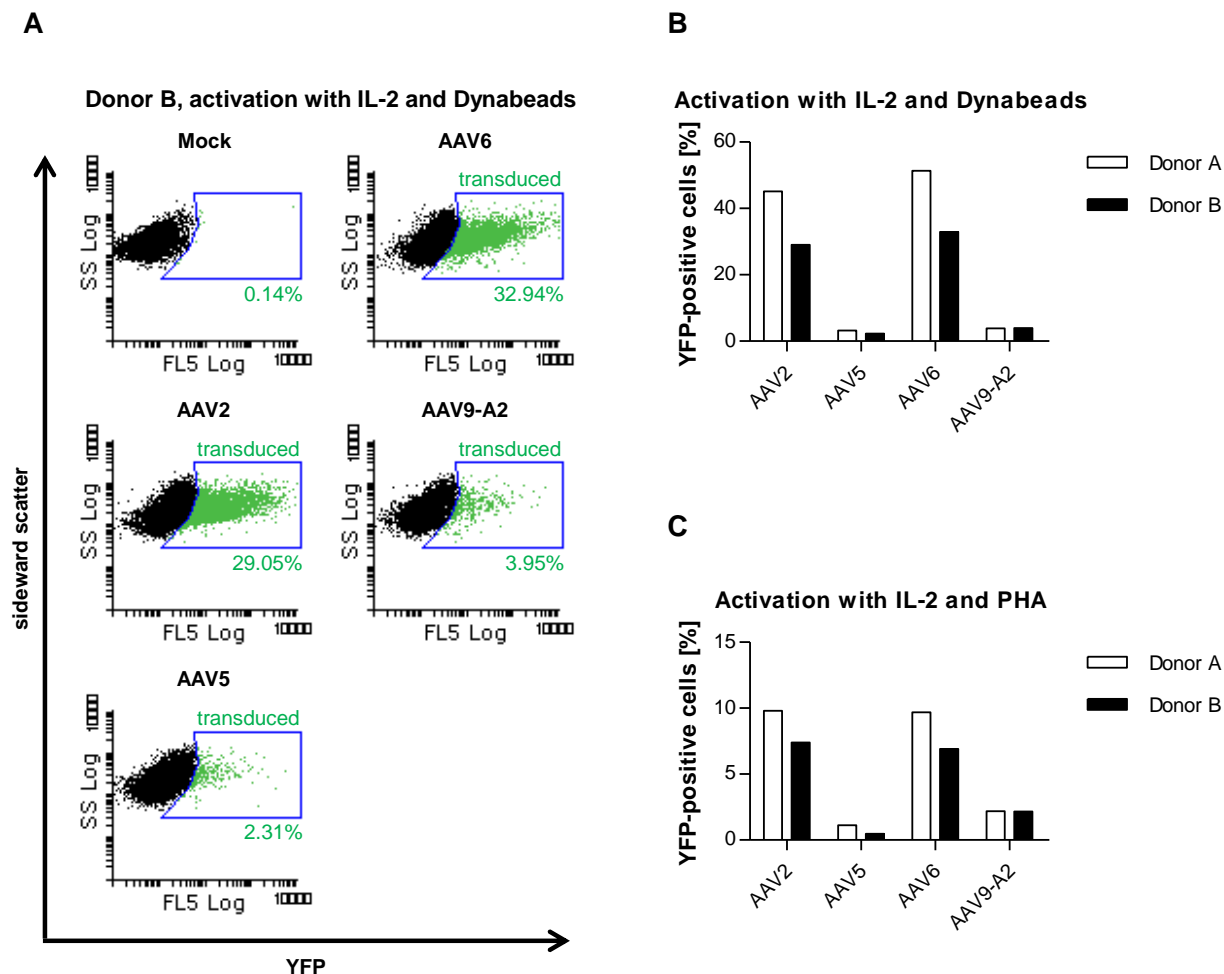
Figure 3.28: Transduction efficiencies of different AAV serotypes in primary CD4$^+$ T cells. Human primary CD4$^+$ T cells were activated either with Dynabeads and IL-2 or with PHA and IL-2 for three days and then transduced with different AAV serotypes encoding a CMV promoter driven YFP. 72 hours after transduction, the cells were analyzed by flow cytometry. (**A**) Exemplary dot plot of the flow cytometry analysis of transduced and untransduced cells from Donor B activated with Dynabeads ad IL-2. (**B**) Percentage of YFP-positive cells from donor A and B activated with Dynabeads and IL-2. N=1 (**C**) Percentage of YFP-positive cells from donor A and B activated with IL-2 and PHA. N=1

3.4.2 Comparison of different promoters for transgene expression in CD4$^+$ T cells

After having identified AAV6 as a serotype efficiently transducing primary human CD4$^+$ T cells, we wanted to compare different promoters for efficient transgene expression in these cells. For that purpose, YFP reporter constructs containing either the CMV, the EFS or the SFFV (spleen focus-forming virus) promoter were packaged into AAV6 capsids. CD4$^+$ T cells from three donors were activated three days and subsequently transduced with 5 x 10^4, 1 x 10^5, 2 x 10^5 and 4 x 10^5 vg per cell of AAV6 encoding the different reporter constructs. Three days after transduction the cells were fixed and analyzed by flow cytometry (figure 3.29).
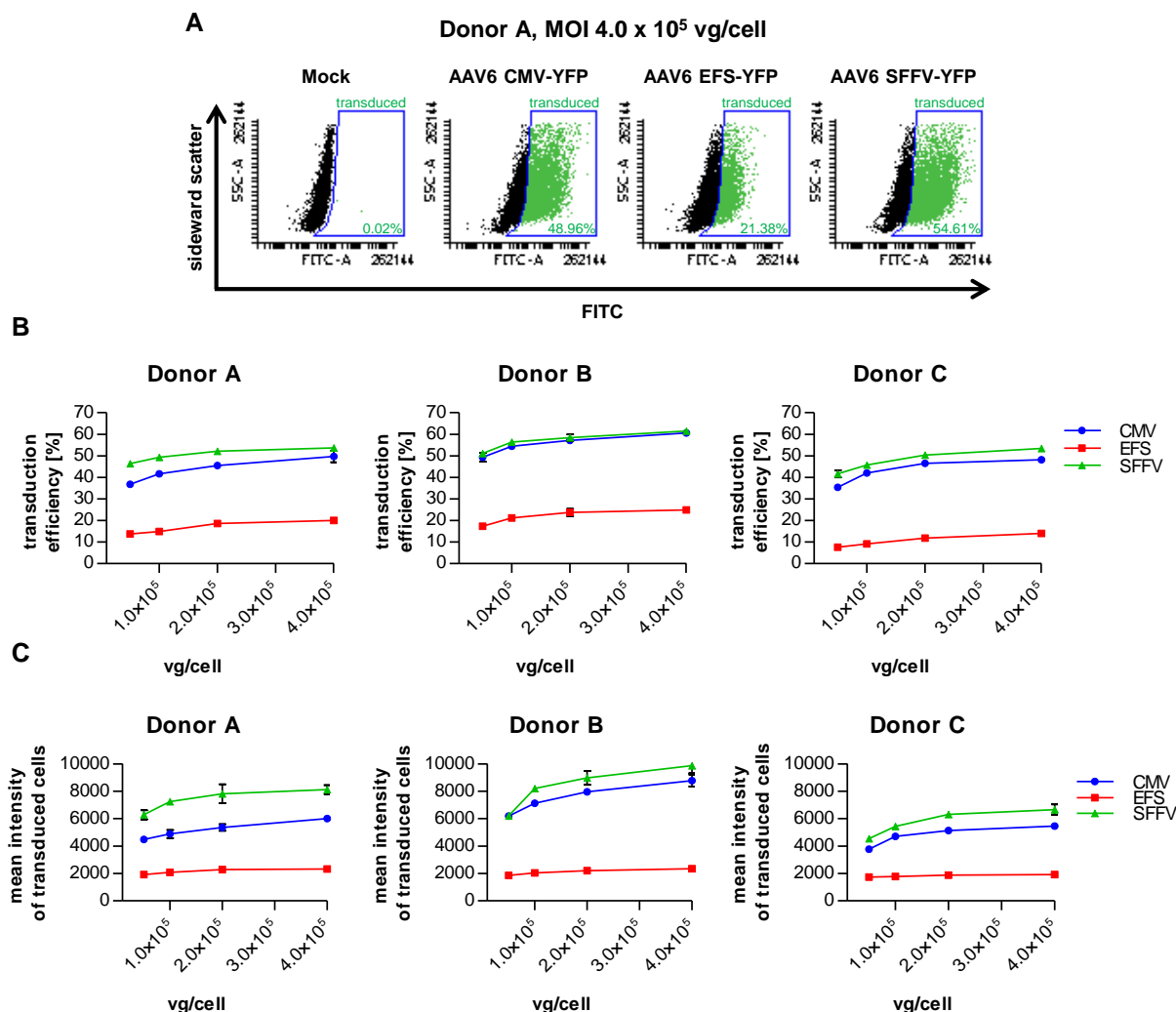
Figure 3.29: Comparison of different promoters for transgene expression in primary human CD4$^+$ T cells. Primary CD4$^+$ T cells from three donors were activated three days and subsequently transduced with 5 x 10^4, 1 x 10^5, 2 x 10^5 or 4 x 10^5 viral genomes per cell of AAV6 particles packaging either a CMV, an EFS or a SFFV promoter driven YFP. Three days after transduction, the cells were fixed and analyzed with flow cytometry. (**A**) Exemplary FACS dot plot of cells from donor A transduced at a MOI of 4 x 10^5 vg/cell. To set the gates for YFP-positive cells untransduced cells (mock) were analyzed in parallel. YFP-positive events are shown in green. The percentage of YFP-positive cells is depicted in the gate. (**B**) Mean transduction efficiencies and standard deviation for all three donors. N=3 (**C**) Mean intensity and standard deviation of YFP-positive cells for all three donors. N=3.

Two parameters were analyzed. The percentage of YFP-positive cells, which is determined by the AAV capsid and thereby should be the same for all reporter constructs used, and the intensity of YFP-positive cells, which is determined by the promoter. The highest mean intensity of YFP-positive cells from all donors was reached with the SFFV promoter whereas the weakest mean intensity was seen with cells transduced with the EFS promoter driven YFP construct. The mean intensity of EFS-YFP transduced cells was about 3- to 4-fold lower than that of the cells transduced with the SFFV-YFP constructs. The mean intensity of CMV-YFP transduced cells

was either the same as the mean intensity of the cells transduced with SFFV-YFP or weaker by a factor of 1.1 to 1.5.

The transduction efficiency, that is determined by the capsid and therefore should be the same for all three YFP constructs at the same MOI, was much lower with the EFS driven YFP construct. Whereas for example with the CMV and SFFV driven YFP constructs a maximal transduction efficiency of about 60 % was reached with cells from donor B at the highest MOI, only 25 % of the same cells were transduced at the same MOI with the EFS-YFP construct. Even if the transduction efficiencies of the cells transduced with the CMV and SFFV promoter driven YFP construct were very similar, they were significantly different with cells from donor C at all MOIs and with cells from donor A at the MOIs 5×10^4, 1×10^5 and 2×10^5. The intensities reached with the EFS promoter driven YFP constructs were in general very low as previously mentioned. The intensities of cells from donor A and C transduced with the CMV-YFP reporter were also low compared to the intensities of cells from donor B. Therefore, in these cases the flow cytometer was probably not sensitive enough to detect all transduced cells.

3.4.3 Test of CRISPR-mediated protection against HIV-1 infection

To initially test if our CRISPR system works in primary human CD4$^+$ T cells, we decided to analyze if the cells can be protected from an HIV infection, as already shown for HeLaP4 cells (chapter 3.2.5), by pretreating them with gRNA multiplexing constructs and a Cas9 encoding construct (figure 3.30).
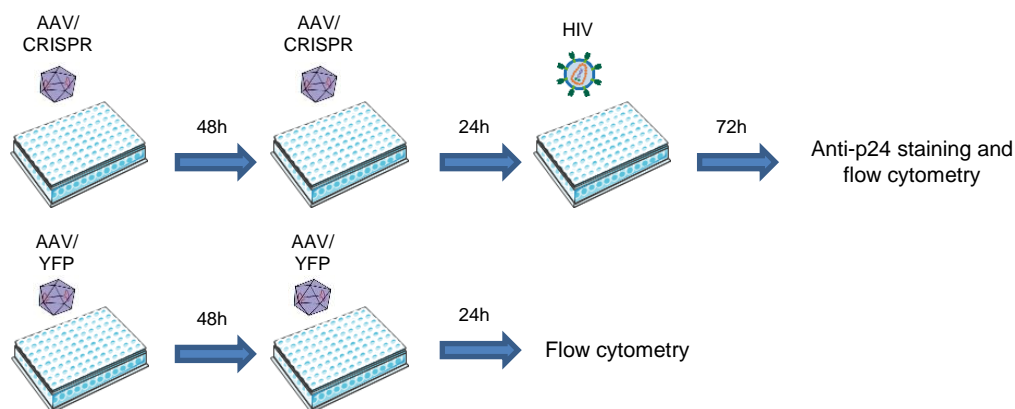
Figure 3.30: Experimental procedure for the analysis of protection against HIV-1 infection with primary human CD4+ T cells using gRNA multiplexing AAV vectors. Activated human primary CD4+ T cells were transduced with AAV6 vectors encoding Cas9 and with AAV6 vectors encoding gRNA multiplexing constructs or with vectors encoding a YFP reporter construct. 48h after the first transduction, the cells were transduced a second time. 24h later, the cells transduced with the YFP reporter were fixed and the transduction efficiency was analyzed by flow cytometry. At the same day the cells treated with the CRISPR vectors were infected with HIV-1 NL4-3. 72h after infection, the cells were fixed, stained with a FITC-labeled anti-p24 antibody and the percentage of HIV infected cells was anlyzed by flow cytometry.

As MP3, MP4 and MP11 turned out to be the most effective constructs in the experiments with HeLa and J-Lat cells (chapters 3.2.5 and 3.3.3), they were chosen for the experiments with primary human CD4+ T cells. As we saw that the CMV promoter (full length) is functional in primary CD4+ T cells (chapter 3.4.2), we first used the shCMV promoter driven Cas9 construct, that was already used in HeLa cells. Primary human CD4+ T cells from one donor were activated three days and subsequently transduced with 2×10^5 vg per cell of AAV6 encoding MP3, MP4, MP11 and with 2.8×10^6 vg per cell of AAV6 encoding the shCMV promoter driven Cas9. To analyze the transduction efficiency at the day of HIV-1 infection, cells were also transduced with 2×10^5 vg per cell of AAV6 encoding a SFFV promoter driven YFP. Two days after the first transduction, the cells were transduced a second time and one additional day later, the cells were infected with 3.7×10^{-5} ng p24 per cell of HIV-1 NL4-3. At the same day the YFP transduced cells were fixed and analyzed by flow cytometry (figure 3.31A,B). The CRISPR-treated cells were fixed and analyzed by flow cytometry three days after HIV infection (figure 3.31C,D). The transduction with the YFP reporter construct resulted in approximatly 50 % transduced cells at the day of HIV infection. Hence, also around 50 % of the cells treated with the CRISPR AAV vectors should be transduced with the gRNA multiplexing constructs and even more cells should be transduced with the Cas9 encoding vector as cells were transduced at an higher MOI with this construct. However, the pretreatment of the cells with the gRNA multiplexing constructs and the shCMV-Cas9 vector did not result in a reduction of HIV infection in comparison to cells only transduced with the Cas9 vector.
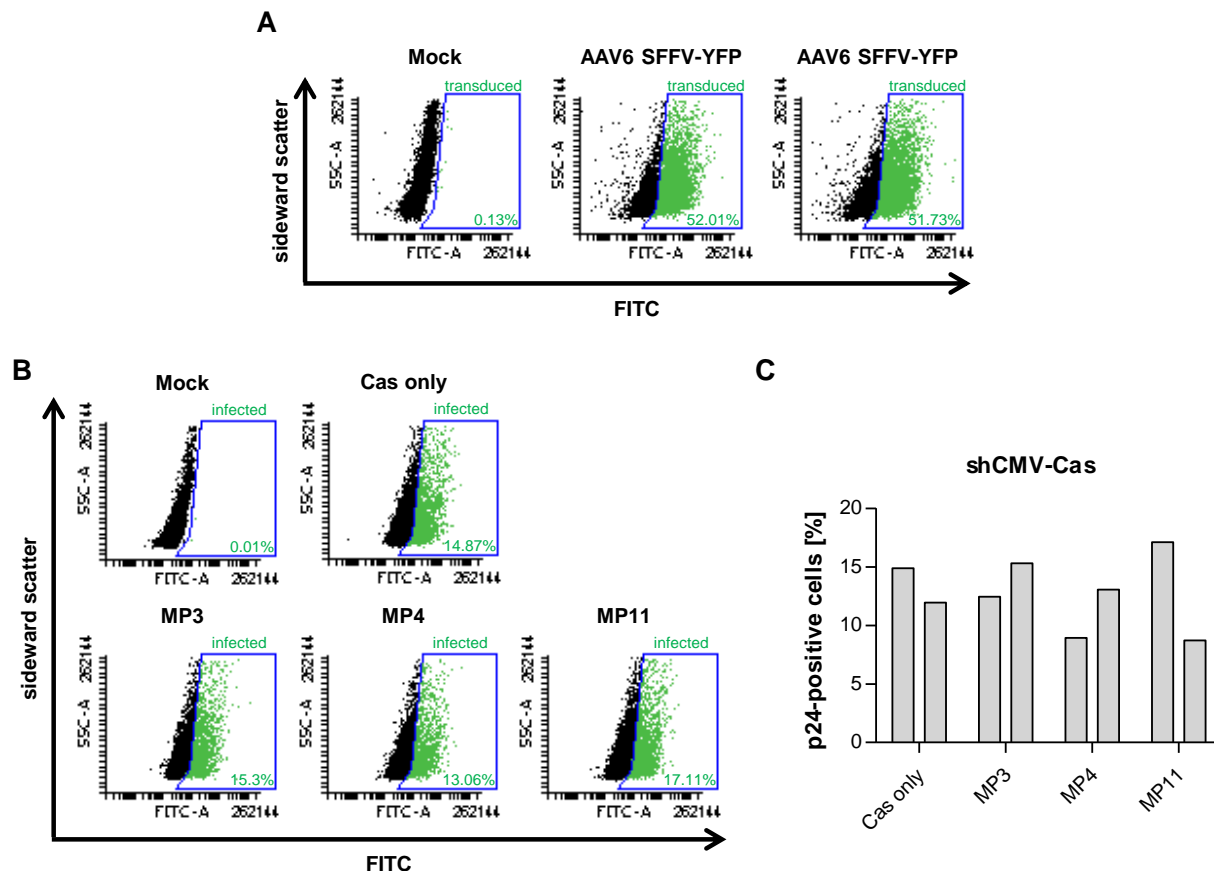
A

B

C

Figure 3.31: Analysis of protection against HIV infection using multiplexing gRNA vectors and shCMV-Cas. CD4$^+$ T cells from one donor were activated three days and then transduced with AAV6 encoding different gRNA multiplexing vectors (MP3, MP4, MP11) and a shCMV-Cas9-encoding vector or with AAV6 encoding a SFFV-YFP reporter. As control, cells were only transduced with the Cas9 encoding AAV6. Two days later, the cells were transduced a second time. One day after the second transduction, the cells transduced with the YFP encoding vector were fixed and analyzed by flow cytometry to determine the transduction efficiency. The CRISPR-treated cells were infected with HIV-1 NL4-3. Three days post infection, the cells were fixed, stained with a FITC-labeled anti-p24 antibody and analyzed with flow cytometry to determine the percentage of HIV-infected cells. (**A**) FACS dot plot showing YFP-positive events from untransduced cells (mock) or from cells transduced with the YFP-reporter. YFP-positive events are depicted in green and the percentage of YFP-positive cells is shown in the gate. (**B**) Exemplary FACS dot plot showing p24-positive events from uninfected cells (mock) or from one replicate of cells either transduced with the Cas9-expressing vector and a gRNA multiplexing vector or with the Cas9-expressing vector alone. P24-positive events are depicted in green and the percentage of p24-positive cells is shown in the gate. (**C**) Percentage of p24-positve cells for both replicates each.

To check if the promoter used for Cas9 expression was the reason for the failure of the experiment, similar as seen with J-Lat cells (chapter 3.3.1), we next tested other promoters for the expression of Cas9. Since the SFFV promoter is very efficient in primary human CD4$^+$ T cells (chapter 3.4.2), I cloned a SFFV-Cas9 construct. With a size of 5.1 kb this construct is 300 bp larger than the wildtype AAV genome and thus, it cannot be guaranteed that the construct is efficiently packaged into the AAV capsid. Therefore, we decided to test the EFS-Cas construct in parallel. Even if this promoter was shown not to be very efficient in human primary CD4$^+$ T cells

in comparison to the CMV and SFFV promoter (chapter 3.3.1), the construct was already shown to be functional in HeLaP4 and J-Lat cells.

CD4$^+$ T cells from one donor were transduced twice with 1 x 10^5 vg per cell of AAV6 packaging either MP3, MP4, MP11 or a SFFV-YFP reporter and with 2 x 10^5 vg per cell of AAV6 packaging the EFS-Cas9 or SFFV-Cas9 construct.

Figure 3.32: Analysis of protection against HIV infection using multiplexing gRNA vectors and SFFV-Cas. CD4$^+$ T cells from one donor were activated three days and then transduced with AAV6 encoding different gRNA multiplexing vectors (MP3, MP4, MP11) and a SFFV-Cas9-encoding vector or with AAV6 encoding a SFFV-YFP reporter. As control, cells were only transduced with the Cas9-encoding AAV6. Two days later, the cells were transduced a second time. One day after the second transduction, the cells transduced with the YFP-encoding vector were fixed and analyzed by flow cytometry to determine the transduction efficiency. The CRISPR-treated cells were infected with HIV-1 NL4-3. Three days post infection, the cells were fixed, stained with a FITC-labeled anti-p24 antibody and analyzed with flow cytometry to determine the percentage of HIV-infected cells. (**A**) Exemplary FACS dot plot showing YFP-positive events from untransduced cells (mock) or from one of the replicates of cells transduced with the YFP-reporter. YFP-positive events are depicted in green and the percentage of YFP-positive cells is shown in the gate. (**B**) Mean transduction efficiency with standard deviation. N=3 (**C**) Exemplary FACS dot plot showing p24-positive events from uninfected cells (mock) or from one replicate of cells either transduced with the Cas9-expressing vector and a gRNA multiplexing vector or with the Cas9-expressing vector alone. P24-positive events are depicted in green and the percentage of p24-positive cells is shown in the gate. (**D**) Mean percentage of p24-positve cells with standard deviation. N=3. Differences between CRISPR-treated cells and Cas only control were determined by Dunnett's post-hoc test after one-way ANOVA. * p<0.05; ns, not significant.

One day after the second transduction, the cells treated with the CRISPR vectors were infected with 1.2×10^{-5} ng p24 per cell of HIV-1 NL4-3 and the cells treated with the YFP reporter were fixed and analyzed by flow cytometry (figure 3.32A,B). The CRISPR-treated cells were fixed and analyzed three days after HIV-1 infection (figure 3.32C,D).

The transduction efficiency at the day of HIV-1 infection was approximately 30 %. Pretreatment with MP3 and SFFV-Cas9 did not result in a significant reduction in the percentage of HIV-1-positive cells. In contrast, preatreatment with SFFV-Cas9 and MP4 reduced the percentage of HIV-infected cells around 55 % and transduction with SFFV-Cas and MP11 resulted in a reduction of HIV infected cells of about 70 %. With the EFS-Cas construct a significant reduction in HIV infection was not seen in combination with MP3 and MP4 (figure 3.33). However, transduction with EFS-Cas and MP11 resulted in a significant reduction of HIV-1 infection of about 77 %.
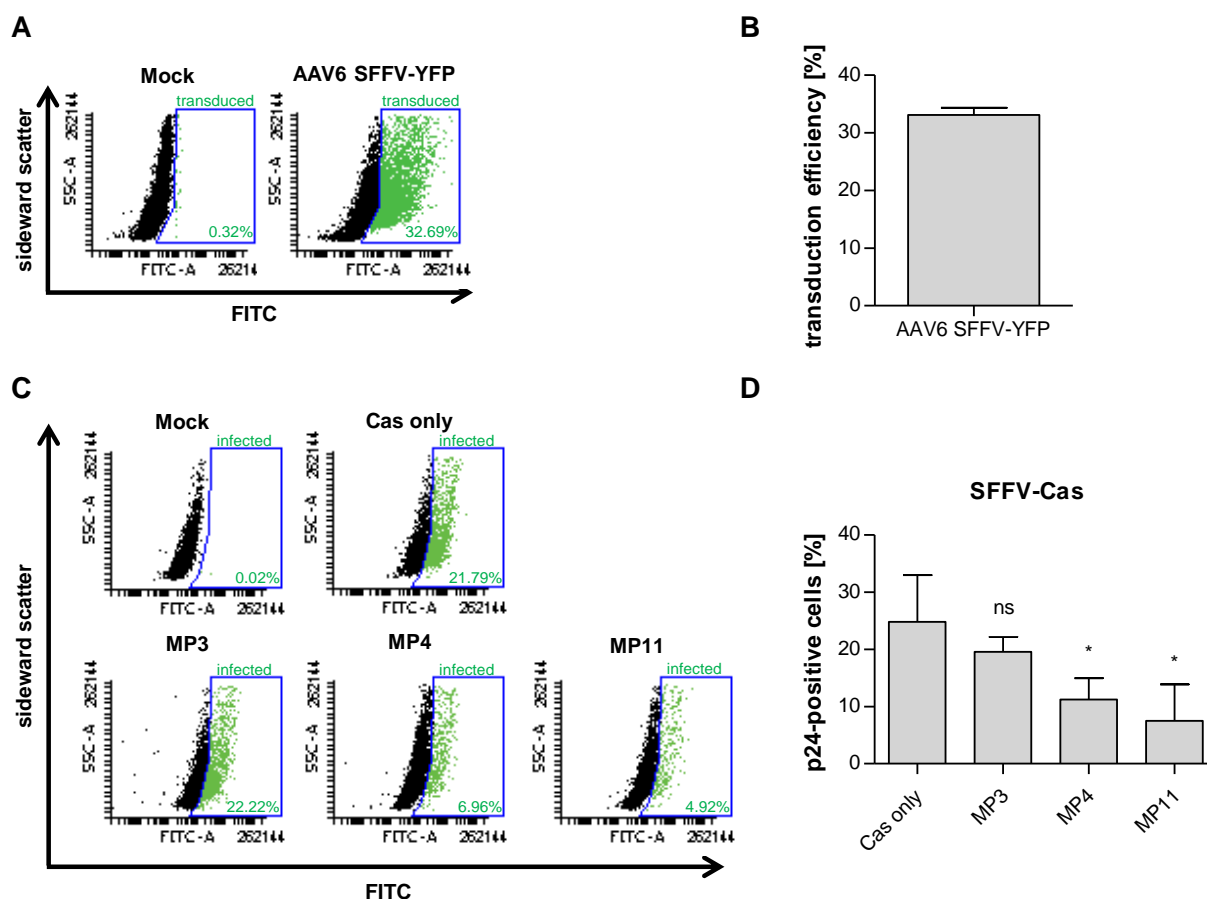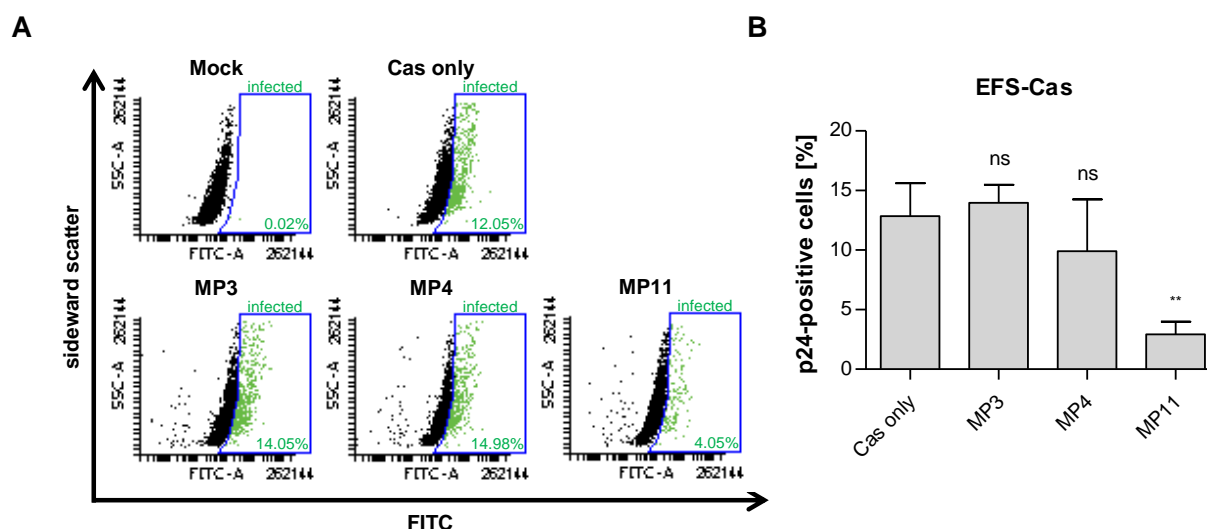

Figure 3.33: Analysis of protection against HIV infection using multiplexing gRNA vectors and EFS-Cas. CD4^{+} T cells from one donor were activated three days and then transduced with AAV6 encoding different gRNA multiplexing vectors (MP3, MP4, MP11) and a EFS-Cas9-encoding vector or with AAV6 encoding a SFFV-YFP reporter. As control, cells were only transduced with the Cas9-encoding AAV6. Two days later, the cells were transduced a second time. One day after the second transduction, the cells transduced with the YFP-encoding vector were fixed and analyzed by flow cytometry to determine the transduction efficiency, which is shown in figure 3.32. The CRISPR-treated cells were infected with HIV-1 NL4-3. Three days post infection, the cells were fixed, stained with a FITC-labeled anti-p24 antibody and analyzed with flow cytometry to determine the percentage of HIV-infected cells. (**A**) Exemplary FACS dot plot showing p24-positive events from uninfected cells (mock) or from one replicate of cells either transduced with the Cas9-expressing vector and a gRNA multiplexing vector or with the Cas9-expressing vector alone. P24-positive events are depicted in green and the percentage of p24-positive cells is shown in the gate. (**B**) Mean percentage of p24-positve cells with standard deviation. N=3. Differences between CRISPR-treated cells and Cas only control were determined by Dunnett's post-hoc test after one-way ANOVA. ** $p < 0.01$; ns, not significant.

As this experiment was performed only with cells from one donor, we wanted to check if the result was reproducible with cells from other donors. Since with the SFFV-Cas construct a reduction of HIV infection was seen in combination with two out of the three multiplexing constructs and with the EFS-Cas construct a significant reduction of HIV infection was only seen with MP11, the SFFV-Cas construct was chosen for the next experiment.

Therefore, CD4$^+$ T cells from three donors were activated three days and transduced with 1 x 10^5 vg per cell of AAV6 encoding MP3, MP4, MP11 or SFFV-YFP and 2 x 10^5 vg per cell of AAV6 packaging the SFFV-Cas9 construct. Two days later, the cells were transduced a second time. One day after the second transduction, the cells treated with the CRISPR vectors were infected with 6.1 x 10^{-6} ng p24 per cell of HIV-1 NL4-3 and the cells treated with the YFP reporter were fixed and analyzed by flow cytometry. The CRISPR-treated cells were fixed and stained three days after HIV-1 infection.

The transduction efficiency was approximately 30 % for cells from donor A, 60 % for cells from donor B and 50 % for cells from donor C (figure 3.34A,B). Unfortunately, no significant reduction in HIV-1 infection was detectable with cells from all three donors, no matter which of the three gRNA multiplexing constructs was used (figure 3.34C).

In addition to the percentage of p24-positve cells we checked if the mean fluorescence intensity of p24-positive cells is reduced after pretreatment with our gRNA multiplexing constructs (supplementary figures 5.3, 5.4, 5.5). Unfortunately, this was not the case in all of the experiments shown in this chapter.
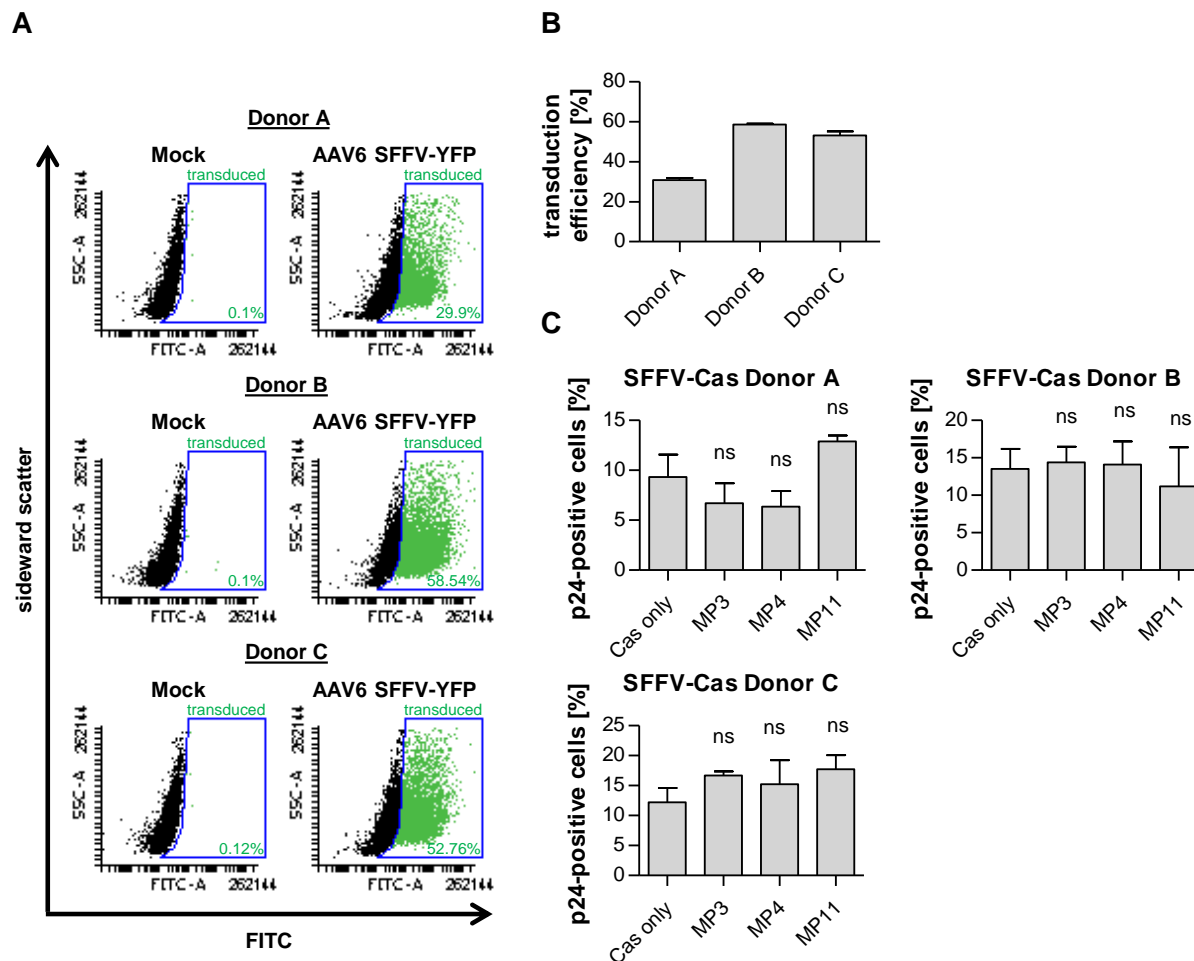
Figure 3.34: Analysis of protection against HIV infection with cells from three donors using multiplexing gRNA vectors and SFFV-Cas. CD4^{+} T cells from three donors were activated three days and then transduced with AAV6 encoding different gRNA multiplexing vectors (MP3, MP4, MP11) and a SFFV-Cas9-encoding vector or with AAV6 encoding a SFFV-YFP reporter. As control, cells were only transduced with the Cas9-encoding AAV6. Two days later, the cells were transduced a second time. One day after the second transduction, the cells transduced with the YFP-encoding vector were fixed and analyzed by flow cytometry to determine the transduction efficiency. The CRISPR-treated cells were infected with HIV-1 NL4-3. Three days post infection, the cells were fixed, stained with a FITC-labeled anti-p24 antibody and analyzed with flow cytometry to determine the percentage of HIV-infected cells. (**A**) Exemplary FACS dot plot showing YFP-positive events from untransduced cells (mock) or from one of the replicates of cells transduced with the YFP-reporter. YFP-positive events are depicted in green and the percentage of YFP-positive cells is shown in the gate. (**B**) Mean transduction efficiency with standard deviation. N=4 (**C**) Mean percentage of p24-positve cells with standard deviation. N=4. Differences between CRISPR-treated cells and Cas only control were determined by Dunnett's post-hoc test after one-way ANOVA. ns, not significant.

3.4.4 Analysis of Cas9 expression from different promoters

As the protective effect against HIV-1 infection in primary CD4^{+} T cells after pretreatment with our CRISPR AAV vectors was only seen with one donor and could not be reproduced, we wanted to analyze if Cas9 is maybe only weakly expressed or not expressed at all. Therefore, CD4^{+} T cells from three different promoters were transduced with 2 x 10^5 vg per cell of AAV6 vectors encoding Cas9 either expressed from the EFS, the shCMV and the SFFV promoters. Two days later, the cells were transduced a second time and one day later, when the cells were infected with HIV-1 in the previous experiments (chapter 3.4.3, figure 3.30), mRNA was isolated from the cells to analyze the Cas9 expression level at the day of HIV infection. In parallel we analyzed the Cas9 expression in HeLaP4 cells, since we could previously show protection of these cells against HIV-1 infection with our CRISPR constructs (chapter 3.2.5). Therefore, HeLaP4 cells were transduced with 1.1 x 10^6 vg per cell of AAV9-A2 encoding EFS-Cas9 and mRNA was isolated three days later, which corresponds to the day of HIV infection in the previously described experimental outline (chapter 3.2.3, figure 3.13A). After RNA isolation, the samples were digested with DNAse to get rid of AAV DNA. Then, mRNA was reversely transcribed into cDNA and the expression of Cas9 and the housekeeping gene *RPP30* (ribonuclease P protein subunit p30) was measured with digital droplet PCR (ddPCR) using fluorescently labeled probes binding the two genes. To determine the background values caused by genomic DNA or AAV DNA in the samples a minus RT control was included in the analysis. Therefore, all RNA samples were pooled and measured without reverse transcription.

Tables 3.3 and 3.4 show the copies of Cas9 mRNA and RPP30 mRNA per µl detected in primary human CD4^{+} T cells and in HeLaP4 cells with ddPCR. The copy numbers of Cas9 mRNA detected in primary human CD4^{+} T cells were either not significantly different from the minus RT control or only slightly higher. The maximum value was 1.9 copies of Cas9 per µl. In contrast, in HeLaP4 cells more than 1000 copies per µl of Cas9 mRNA were detected and the Cas9 mRNA values were more than 20 times higher than the minus RT values. Collectively, this result shows that indeed Cas9 is not expressed efficiently with our vectors in human primary CD4^{+} T cells.

Table 3.3: Cas9 and RPP30 expression in primary human CD4$^+$ T cells. The table shows the mRNA copy numbers per µl of the housekeeping gene RPP30 or of Cas9. Each condition was analyzed with three biological replicates. Bold numbers indicate that the Cas9 values were significantly higher than that of the minus RT control, which was determined with Student`s t-test ($p < 0.05$).

	Donor A		Donor B		Donor C	
	RPP30	Cas9	RPP30	Cas9	RPP30	Cas9
shCMV	11.1	0.16	25.3	0.58	14.3	0.15
	16.7	0.28	23.3	0.73	7.9	0.57
	22.7	0.75	21.9	0.54	0.07	0.27
SFFV	17.9	1.1	26.1	**1.9**	14.4	**1.7**
	13.5	1.1	14.2	**0.86**	10.9	**1**
	3.2	0.63	26.3	**1.8**	7	**1**
EFS	5	0.36	14.9	**1.2**	23.9	**1.5**
	20.4	1.2	10.6	**1.2**	16.5	**1.2**
	9.4	0.46	22.8	**0.89**	13.3	**1.8**
minus RT	0	0.27				
	0	0.71				
	0	0.22				

Table 3.4: Cas9 and RPP30 expression in HeLaP4 cells. The table shows the mRNA copy numbers per µl of the housekeeping gene RPP30 or of Cas9. Each condition was analyzed with three biological replicates.

	RPP30	Cas9
EFS	7840	1242
	6840	1366
	8180	1660
minus RT	0	52
	0	64
	0	66

4. Discussion

4.1 Establishment of the HIV-1-targeting CRISPR/Cas9 system

4.1.1 GRNA design and gRNA multiplexing strategy

Targeting highly conserved regions is of special interest as these sequences should be of either structurally or functionally importance and mutating those should have a big impact on viral replication. In addition, Roychoudhury et al. [210] showed that selecting highly conserved target regions among different HIV-1 subtypes is important for clinical application as it enables targeting of most global and within-host variants. Furthermore, it was shown that editing conserved proviral regions delays the emergence of viruses resistant to CRISPR/Cas9 [211, 212], which occur through CRISPR/Cas9 induced mutations, that do not impair viral replication and prevent further gRNA binding.

For the establishment of our CRISPR/Cas9 system we designed gRNAs targeting the LTRs, *gag* and *pol*. For the design of the LTR-binding gRNAs the 3´ and 5´LTRs of the subtype B HIV-1 strains NL4-3 and HXB2 were aligned and regions that were identical among those sequences were chosen as gRNA target sites. The gRNAs targeting protein-encoding regions were chosen to target highly conserved regions identified by ter brake et al. [199], who aligned the genomic sequences of the LAI HIV-1 strain with 170 HIV-1 genomic sequences from all HIV-1 subtypes listed in the Los Alamos National Laboratory database. To compare the conservation of all our gRNAs we blasted the gRNA sequences against the genomes of HIV-1 strains belonging to the subtypes A, B, C, F and G available in the Los Alamos National Laboratory database. Indeed, the gRNAs targeting the highly conserved regions described by ter brake et al. showed a high conservation among the different subtypes. Only the gRNA int4 is weakly conserved in isolates from subtype A and C. Among the LTR-binding gRNAs only g7 showed a broad conservation whereas the other LTR-targeting gRNAs were highly conserved in isolates from subtype B and weakly conserved in the other isolates. These results suggest that our LTR-targeting gRNAs are well suited for the work with subtype B HIV-1 strains, but for later experiments with patient cells it might be necessary to design new gRNAs binding at highly conserved sites of the LTRs to enable targeting of different global and within-host HIV-1 variants and to prevent the emergence of resistances against CRISPR/Cas9.

To analyze the potential of CRISPR/Cas9 to functionally inactivate HIV-1 in cell lines and prima-ry CD4$^+$ T cells, we used vectors expressing three gRNAs. This gRNA multiplexing strategy im-proves the antiviral activity of the system. On the one hand it allows simultaneous editing of dif-ferent sites of the proviral genome as we showed with T7 assay in HeLaP4 cells and J-Lat cells. On the other hand we and others [213, 214] found that it allows the excision of proviral DNA be-tween different gRNA target sites. Hence, it was not surprising that several of our multiplexing constructs were more efficient than the single gRNA g6 in protecting HeLaP4 cells against HIV-1 infection or in functional inactivation of the latent HIV provirus integrated in J-Lat cells. This find-ing is supported by several other studies that compared editing of HIV with single and multiple gRNAs in actively HIV-1 producing cell lines and in latently HIV-1-infected cell lines [213, 215–217]. Another advantage of the gRNA multiplexing strategy, that was not analyzed in this work, but was shown by two recent studies is, that it prevents the emergence of CRISPR-resistant vi-ruses [217, 218]. These studies showed that the combination of only two gRNAs can already block the breakthrough of resistant viruses. As we combine three different gRNAs in the most multiplexing constructs, our CRISPR system should be very effective in blocking the develop-ment of CRISPR-resistant viruses.

Another important point that needs to be addressed for the development of a CRISPR/Cas9-based cure for HIV-1 infections is the cleavage of sites in the host genome that are similar to the gRNA target site in the HIV-1 proviral genome. Several studies have analyzed such off-target effects of CRISPR/Cas9 so far, but there does not seem to exist a simple rule that can be ap-plied to gRNA design to prevent off-targeting. However it seems that mismatches near to the PAM sequence are less well tolerated than mismatches in the PAM distal region of the gRNA [83, 90, 109]. To get an impression of the number of possible off-targets of our gRNAs we per-formed an in silico off-target prediction with different online tools. These tools predict off-targets based on sequence similarity with the gRNA sequence. As the tools allow different numbers of mismatches and some tools also restrict the position of the mismatches in the sequence, the number of predicted off-targets was very variable between the different online tools. For exam-ple, the Cosmid tool that allows only three mismatches found for most gRNAs the least off-targets, whereas the most off-targets were found by Cas-OFFinder when 5 mismatches were allowed. As these online tools only consider sequence similarity and do not account for other factors that influence gRNA binding like for example accessibility of the off-target site through chromatin structure [100, 219], a sequencing-based analysis like GUIDE-Seq [103] would be necessary to make a more realistic statement about the number of existing off-targets of our gRNAs.

4.1.2 Delivery of the CRISPR components with AAV vectors

All studies applying CRISPR/Cas9 to target HIV-1 in cell lines used either transfection to deliver Cas9 and gRNAs into the cells or used lentiviral vectors to create cell lines stably expressing Cas9 and gRNAs. In contrast, we chose AAV vectors to deliver the Cas9 and gRNA encoding constructs into the target cells. The use of AAV vectors for delivery of an HIV-1-targeting CRISPR/Cas9 system has currently been described by two studies of one group who applied the vectors to mice and rats [77, 78]. We decided to use AAV vectors from the beginning of the establishment of the system. This allowed us to first test our system in easy to handle HeLaP4 cells and adapt the system stepwise regarding to the choice of regulatory elements for Cas9 expression in human T cells.

Several preclinical and clinical studies have shown that AAV vectors are safe and mediate long-term expression. Furthermore as they only very rarely integrate into the host genome [179–181] there is no risk of insertional mutagenesis as with lentiviral vectors. As currently 13 naturally occurring AAV serotypes with different tropisms have been identified [147] and different capsid engineering techniques have been developed to change their tropisms [135], AAV vectors allow to target many different cell types. This offered us the opportunity to apply our CRISPR system to HeLa cells, to J-Lat T cells and finally to primary human CD4$^+$ T cells.

When we compared different vector designs for single gRNA expression in HeLaP4-NLtr cells, the all-in-one design, which should allow the expression of Cas9 and one gRNA from one construct, did not result in detectable editing with T7 assay. Possible reasons for this could be that either the H1 promoter does not efficiently express g6, the second-strand synthesis is limited in these cells or the construct with a size of around 5.1 kb is too big for efficient packaging. As the other vector designs for single gRNA expression, that were co-transduced with a single-stranded Cas9 AAV vector, mediated editing at the g6 target site, the second-strand synthesis is not limited in HeLaP4-NLtr cells. Furthermore, it can be excluded that the H1 promoter is not functional in these cells as in later experiments with multiplexing constructs the gRNAs int4 and gag could be expressed from the promoter. Therefore, it is most likely that the construct was not efficiently packaged into AAV capsids, which is further supported by studies that showed the packaging efficiency of sequences larger than 5 kb is reduced and that such sequences have truncated 5´ ends [169, 171]. The packaging limit of around 5 kb is a major limitation of AAV vectors. As the SpCas9 coding sequence has already a size of around 4 kb, the choice of promoters is limited to small promoters. In this work, for example we used the shCMV promoter with a size of 224 bp or the EFS promoter with a size of 257 bp for Cas9 expression from AAV vectors in cell lines. Though, these promoters did not allow Cas9 expression in primary human CD4$^+$ T cells. Lentivi-

ral vectors, that can package sequences with a size of 9 to 10 kb, would allow the use of larger promoters. However, as our constructs encode gRNAs targeting the HIV-1 LTRs there is the risk that the gRNAs would also target the vector from which they are expressed and thereby would inactivate their own expression in the long run. An elegant solution that allows the expression of Cas9 from AAV vectors using larger promoters, is the so-called "SplitCas9" approach [220]. Here, the N-terminus and the C-terminus of Cas9 are expressed from two different constructs which reassemble to a functional Cas9 in the cell. Hence, there is around 2 kb more space for regulatory elements and also for gRNAs on each vector. As the field of gene therapy approaches using Cas9 is rising and AAV vectors are popular vectors for gene therapeutic applications, it is very probable that soon more strategies will be developed that simplify Cas9 expression from AAV vectors.

4.2 Application of the HIV-1-targeting CRISPR/Cas9 system in cell lines

4.2.1 CRISPR/Cas9 mediates the protection of HeLaP4 cells against HIV-1 infection

Treatment of HeLaP4 cells with Cas9 and our gRNA multiplexing constructs or single g6 and subsequent infection with HIV-1 NL4-3, resulted in a reduction of the population of HIV-1-infected cells of up to 80 %. Hence, pretreatment with our CRISPR-AAV vectors facilitated protection of cells against HIV-1 infection. Such a protective effect has already been described by others [211–213, 216–218, 221–227]. Most of these studies used SupT1 cells that stably express Cas9 and gRNAs, but one study also showed the protection of physiologically more relevant cells like primary human CD4$^+$ T cells or macrophages against HIV-1 infection [216]. Even if this feature is not absolutely necessary for targeting the latent HIV-1 reservoir, in a scenario where CRISPR/Cas9 would be used in combination with a shock and kill approach in patients under ART it could support the prevention of new infections mediated by ART.

The protective effect that we and others observed is probably not only mediated by modification of the integrated proviral DNA but also by targeting of the pre-integrated viral DNA. Liao et al. [216] found for example, that CISPR/Cas9 mediated inhibition of GFP expression from a non-integrative lentiviral reporter construct to a similar extent as inhibition of GFP expression from an integrating lentiviral construct. Furthermore, Mefferd et al. [212] found that in the presence of the integrase inhibitor Raltegravir CRISPR-mediated editing of HIV-1 DNA occurred at a similar effi-

ciency as in the absence of Raltegravir and that CRISPR/Cas9 treatment results in a 3- to 4-fold decrease of integrated proviral DNA.

Some of the studies, which show that CRISPR/Cas9 can protect cells against HIV-1 infection, used combinations of several gRNAs and found that this was more effective than just using a single gRNA [217, 218]. We also addressed this point by comparing the protective effect mediated by treatment with our most potent gRNA g6 to the effect mediated by treatment with different multiplexing constructs. Indeed, the combination of several gRNAs was at least as efficient as treatment with g6 alone or more effective. One reason why multiplexing is more effective than treatment with a single gRNA is, that it allows editing at several sites of the HIV-1 genome. As not all CRISPR-induced mutations will have an effect on viral replication, targeting different proviral sites simultaneously increases the chance to introduce mutations that are deleterious to the virus. Indeed, we could prove with T7 assay that our multiplexing constructs mediate simultaneous editing at the LTR at *gag p24*, *gag p17* and *pol*. Another reason why gRNA multiplexing increases the antiviral power of the system is that it facilitates the excision of fragments between the gRNA target sites. PCR amplification of a proviral region spanning the 5´LTR and gag p17 in HeLaP4-NLtr cells treated with our multiplexing constructs revealed shorter extra bands. Even if they were not sequenced, the sizes of the bands lead to the conclusion that they resulted from excision of proviral DNA between different gRNA target sites. For example we detected bands with truncations of around 250 or 300 bp which corresponds to excision of DNA between g3 and g6 target sites, between g5 or g6 and gag target sites and between g6 and p17 target sites. Furthermore, we detected bands with deletions of around 530 bp which corresponds to excision of DNA between g3 and gag target sites. The excision of fragments between the target sites of the LTR-targeting gRNAs g3, g5 or g6 and the *gag p17*-targeting gRNAs p17 and gag should completely inhibit the synthesis of new viral particles as many functional elements are located at this region like for example the primer binding site, the packaging signal, the TAR element or the major splice donor site. Also the excision of the proviral sequence within the LTR between the g3 and g6 target sites should inhibit the production of new virus as it deletes the TATA box and the TAR element.

In general we found that constructs with a U6 promoter driven g6 in combination with a *gag p17*-targeting gRNA (MP3 and MP11) were most efficient in protecting cells against HIV-1 infection. As the T7 assays that show editing with the multiplexing cells in HeLaP4-NLtr cells were only performed once, they do not allow any conclusion about ideal promoter usage for gRNA expression. Hence, it can only be speculated that the U6 promoter is more effective in HeLa cells than the 7SK promoter that drives g6 expression in the constructs MP1, MP4 and MP5. This hypoth-

esis is supported by a study that showed that the U6 promoter was more effective than the 7SK promoter in driving the expression of a short RNA in HEK293T cells and in driving the expression of a luciferase reporter gene in the cervix carcinoma cells C33A [228]. The combination of g6 and a *gag p17*-targeting gRNA might be especially effective because excision between those sites removes many functionally important elements as previously mentioned. Very effective as well was the combination of the gRNAs g5, g6 and gag expressed from the construct MP4. As g5 and g6 both target the TAR element and we and others [212] found that CRISPR/Cas9-mediated editing of the TAR element decreases LTR promoter function, the combination of both gRNAs in one construct might increase the chance to introduce promoter inhibiting mutations at this site. Furthermore, we detected excision of proviral DNA between the g5/g6 and the gag target site which probably also contributed to the strong reduction of p24 positive cells mediated by treatment with Cas9 and MP4.

In addition to analyzing p24 expression from CRISPR/Cas9-pretreated HeLaP4 cells, we measured the amount of infectious viruses in the supernatant of the cells. This was done by infection of C8166 cells with the supernatant of the HeLaP4 cells and by counting syncytia indicative for HIV-1 infection 7 days post infection. As we used the same volume of supernatants from all samples for infection and did not adjust the amount of virus between the different samples, supernatants from cells that showed a the strongest reduction in the amount of p24 positive cells should also contain the lowest amount of infectious virus unless certain gRNAs would cause mutations that do not affect p24 expression but viral infectivity. As the overall trend of the readout was the same as in the microscopy readout for p24 detection, this did not seem to be the case or maybe only to a small extent. Since the readout was performed 7 days post infection, which corresponds to several rounds of HIV replication, CRISPR resistant virus variants or variants with mutations that enhance viral replication as described by several other groups [212, 217, 223–225, 227, 229] could have emerged. This was not seen in our experiment and supernatants from all CRISPR/Cas9-treated cells showed a significantly reduced amount of infectious units compared to untreated cells. However, most of the aforementioned studies passaged the virus several times and followed viral replication over periods of 20 days or more. Breakthrough of resistant viruses was usually detected after 8 days or later. Hence, a similar analysis of viral replication over a longer period of time would be necessary to exclude the emergence of resistant HIV-1 variants against our CRISPR constructs.

4.2.2 Targeting of the HIV-1 latent provirus in J-Lat cells results in a reduction of proviral expression and of the amount of released viral particles

To analyze if our CRISPR/Cas9 system facilitates the functional inactivation of latent HIV-1, we applied our CRISPR-AAV vectors to J-Lat T cells. These cells harbor a transcriptionally silent HIV-1 provirus with a GFP expression cassette in the *nef* open reading frame [230]. We transduced the cells twice with AAV vectors expressing Cas9 and our multiplexing constructs or the single gRNA g6. Subsequently, proviral expression was activated with TPA and TNFα. We analyzed the effect on proviral transcription by measuring the amount of GFP-positive cells, the effect on release of viral particles by performing an SG-PERT and editing at the different target sites with T7 assay.

Treatment with all multiplexing constructs except for MP7, MP9 and MP10 resulted in a significant reduction in the number of GFP-positive cells. As the construct expressing g6 alone also encodes GFP it could not be analyzed in this readout. As the GFP expression cassette is placed in the *nef* open reading frame, which has an own start codon and is placed at the 3´end of the proviral genome, mutations introduced into *gag* or *pol* should not have an influence on GFP expression. Hence, only mutations in the 5´LTR that reduce transcription or the excision of proviral DNA between the LTR and *gag* or *pol* will lead to a reduction of GFP expression, which explains why the constructs MP9 and MP10, that do not contain a LTR-targeting gRNA, did not reduce the number of GFP-positive cells significantly. All other multiplexing constructs were comparably efficient in reducing proviral transcription.

In addition to measuring the amount of GFP-positive cells the amount of reverse transcriptase in the supernatant of the cells, indicative for the amount of viral particles released, was measured. The single gRNA6 as well as all multiplexing constructs significantly reduced the amount of viral particles released. Furthermore, treatment with all multiplexing constructs except for MP3 resulted in a significantly stronger reduction of viral particles as treatment with the single gRNA g6. This is in agreement with two other studies that show that treatment of J-Lat cells with combinations of two or three gRNAs were at least as efficient or even more efficient as a single gRNA in reducing the amount of released virus [213, 215]. Interestingly, MP3, which only mediates editing at the g6 target site in the LTR as shown with T7 assay, was very efficient in reducing proviral transcription but was not as effective as the other constructs in reducing the amount of viral particles released. Furthermore, MP9 and MP10, which did not significantly reduce proviral transcription, mediated significant reduction viral release. This indicates that in addition to reduction of proviral transcription other mechanisms play an important role in the reduction of viral release.

As cleavage at the p24 target site was only very weakly detectable with T7 assay in one of the three experiments and as mutations at the int4 target site should have no influence on the release of viral particles, probably mutations at the gag target site make a major contribution to the effect on viral release seen with MP9 and MP10. As the gRNA gag binds at the beginning of the *gag* open reading frame, mutations introduced at this site have the potential to either destroy the myristoylation site of *gag* or the start codon and thereby have a high chance to completely inhibit viral release. In general, we found that constructs that encode a LTR-targeting gRNA in combination with the gRNA gag were very effective in reducing the amount of viral particles released. This could be either because of the addition of both effects mediated by mutations introduced to the LTR and *gag* or because of the excision of proviral fragments between the LTR and *gag*. These excision events were detected after treatment with MP4, MP5, MP7, MP8 and MP11 and were additionally already seen in HeLaP4-NLtr cells after treatment with our multiplexing constructs. As the excision of proviral DNA between 5´LTR and *gag* removes many functional sites, this should completely destroy the release of new viral particles. However, since for the excision of these fragments two DNA breaks need to be induced relatively simultaneously, these events might be not as efficient as the introduction of mutations at different target sites as also stated by others [231, 232]. This is also underlined by the observation that MP6 was quite effective in reducing viral release even if we did not detect excision between g5 and gag with PCR in all three experiments.

In addition to the introduction of mutations at different proviral sites and the excision of proviral fragments, the excision of the whole proviral genome between the LTRs, which has also been reported by other groups [216, 221, 222, 233], contributes to the antiviral effect of our CRISPR system. The excision of the proviral genome was detected in a separate experiment in which DNA from J-Lat cells treated with Cas9 and MP1-MP3 was amplified with primers flanking the provirus. Treatment with all three constructs resulted in detectable PCR products that display the residual proviral sequence after excision. Sequencing of the bands revealed that the excision of the proviral sequence after treatment with all three constructs was mediated by the gRNA g6. As discussed previously the introduction of mutations at different target sites is probably more frequently happening than the excision of DNA between two gRNA target sites. Therefore, gRNAs that are not as potent in inducing mutations as others will also be less potent in facilitating the excision of proviral DNA. Comparing the editing efficiencies at the LTR and gag spanning target site with the constructs MP5-7, which only differ in the LTR-targeting gRNA, shows that g6 is more efficient in editing than g3 or g5. This might explain why we did not observe excision of the proviral DNA with these gRNAs.

Some of the constructs (MP5 and MP11, MP6 and MP8, MP9 and MP10) were designed to express the same gRNA combinations but from different promoters to analyze if certain promoters are better for expression of certain gRNAs. Indeed we found that expression of g5 from the 7SK promoter with the construct MP6 did not result in efficient cleavage detected with T7 assay in comparison to the expression of g5 from the U6 promoter with the construct MP8. In addition editing with int4 expressed from 7SK promoter with the constructs MP8-MP11 was either not detectable or too weak for quantification. In contrast, expression of int4 with constructs MP5-MP7 from H1 resulted in quantifiable cleavage in all three experiments. This finding is supported by other studies which show that the 7SK promoter is weaker than the U6 promoter in various human cell lines [228, 234]. However, g6 cleavage products were detectable no matter if the gRNA was expressed from U6 promoter with the construct MP11 or from the 7SK promoter with the construct MP5. As gRNA6 is in general one of the most potent gRNAs that we designed, maybe weaker expression does not have a big effect on editing of this gRNA. The aforementioned observations with the gRNAs int4 and g5 expressed from the 7SK and U6 promoters were also seen with CRISPR-treated HeLaP4-NLtr cells. Hence, these results suggest that less potent gRNAs should be expressed from the U6 or H1 promoter and more potent gRNAs from the 7SK promoter.

4.3 Pretreatment of primary human CD4$^+$ T cells with AAVs encoding gRNA multiplexing constructs or Cas9 does not result in protection against HIV-1 infection

The aim of this work was develop a CRISPR/Cas9 system that targets the latent HIV-1 reservoir. Since CD4$^+$ T cells are the best described latent reservoir, we wanted to apply our system to human primary CD4$^+$ T cells after having proven its functionality in cell lines. To enable the application of our CRISPR/Cas9 system in primary human CD4$^+$ T cells we first of all compared different AAV serotypes for their transduction efficiencies of these cells and found that among these, AAV2 and AAV6 mediated the highest transduction efficiencies of around 40 to 50 %. As also other studies showed that AAV6 efficiently transduces human primary CD4$^+$ T cells or hematopoietic stem cells [175, 235, 236] and as Dr. Kathleen Börner found that this serotype also mediates efficient transduction of primary human macrophages, which possibly are also part of the latent HIV-1 reservoir [32, 237], we decided to choose this serotype for all further experiments.

In addition to transduction efficiency Cas9 expression is an important parameter for the successful application of the system. When editing with g5 and g6 in combination with a shCMV promoter driven Cas9 was compared between HeLaP4-NLtr cells and J-Lat cells, it was found that a 1:10 dilution of the gRNA encoding vector did not dramatically affect the cleavage efficiency which led us to the conclusion that Cas9 is the rate limiting factor of CRISPR/Cas9. Indeed, after changing the promoter that drives Cas9 expression, the system worked also in J-Lat cells. Because of these earlier findings we tested different promoters using a YFP reporter construct with the aim to choose the most efficient one for Cas9 expression. It was found that the highest mean intensity of transduced CD4$^+$ T cells from three donors was reached with the SFFV promoter directly followed by the CMV promoter which reached either the same mean intensities or intensities lower by a factor of 1.1 to 1.5. In contrast, the EFS promoter was clearly the weakest promoter with mean intensities that were 3- to 4-fold lower than that reached with the SFFV promoter. The SFFV promoter has a size of 404 bp and the SFFV driven Cas9 construct has a size of around 5.1 kb. As it was shown by others that sequences larger than 5 kb are packaged with truncations into AV capsids and are therefore not expressed efficiently [171], we decided to first test the shCMV promoter for Cas9 expression. This construct was functional in HeLaP4 cells and the full length CMV promoter performed well in primary CD4$^+$ T cells. Unfortunately, pretreatment with the shCMV driven Cas9 construct and the multiplexing constructs MP3, MP4 and MP11 did not result in a reduction of HIV-1 infection in comparison to cells only treated with the Cas9 encoding vector. Therefore, we next tested the SFFV promoter driven Cas9 construct and the EFS promoter driven construct. Even if the EFS promoter was the weakest one in the experiments with the YFP reporter construct, the promoter has only a size of 257 bp and the EFS-Cas9 construct has a size of approximately 5 kb including the ITRs and therefore should be packaged into AAV capsids without truncations [169–171]. Furthermore, the construct was shown to be functional in J-Lat cells and in HeLaP4 cells. Indeed, the pretreatment of cells from one donor with the two Cas9 constructs and MP11 resulted in a significant reduction in the number of p24-positive cells. In combination with the SFFV promoter driven Cas9 also MP4 treatment resulted in significant reduction of p24 positive cells. As this experiment was only performed with cells from one donor, we aimed to reproduce this result with cells from three more donors. For this next experiment the SFFV-Cas9 construct was chosen as it mediated protection of cells against HIV-1 infection in combination with MP4 and MP11. Unfortunately, the effect seen was not reproducible with all three donors even if the percentage of transduced cells was 50 % and 60 % for two donors and therefore higher than in the previous experiment where only around 30 % of the cells were transduced. As we still hypothesized that Cas9 expression is not efficient in the cells, Cas9 expression with all three constructs was analyzed using ddPCR and

compared with Cas9 expression from the EFS-Cas9 construct in HeLaP4 cells. Indeed, in primary human CD4+ T cells Cas9 was either not detectable at all or with a maximum of 1.9 copies per µl only slightly over background levels, whereas in HeLaP4 cells more than 10,000 copies per µl were detected. These results suggest that our system did not facilitate protection of primary human CD4+ T cells because of inefficient Cas9 expression. However as the expression of the gRNAs was not analyzed in this work, it cannot be excluded that these are weakly expressed as well.

There are different possible reasons for the weak Cas9 expression levels. One reason could be that the tested promoters were either too large for packaging into AAV capsids or not potent in primary human CD4+ T cells. The EFS-Cas9 and the shCMV-Cas9 constructs were functional in HeLaP4 and J-Lat cells. Therefore, these constructs can certainly be packaged. However, since we tested the full length CMV promoter for YFP expression, it is possible that the shorter shCMV promoter used for Cas9 expression is not as efficient in the primary CD4+ T cells as in HeLaP4 cells. As this promoter did also not mediate Cas9 expression in J-Lat cells the promoter might be in general not efficient in T cells. Furthermore, the EFS promoter as already shown with the YFP reporter construct is probably not efficient enough in these cells and the SFFV promoter which was very efficient for the expression of YFP might be too large together with the Cas9-encoding sequence. Since other promoters that have been reported to be efficient in human primary CD4+ T cells ,like the MSCV (murine stem cell virus) or the PGK promoters [238], have size of 500 bp or more, they can also not be used to express SpCas9 with AAV vectors. Therefore, one solution could be to design shorter variants of the SFFV promoter and analyze them for their efficiency to express Cas9. Another solution could be the use of split Cas9 [220]. This strategy would allow the use of larger promoters as both halves of Cas9 are expressed from two separate vectors.

In addition to the size or efficiency of the promoters tested for Cas9 expression it can also not be excluded that the second-strand synthesis of the AAV DNA is not efficient in these cells. It has been reported previously that AAV second-strand synthesis is a rate limiting step [166, 167]. One study even reported that transduction of primary cells using AAV is inefficient in comparison to cell lines and the block occurs after viral entry [239]. As the YFP reporter constructs used for the comparison of transduction efficiencies with different serotypes and used for the comparison of different promoters are self-complementary double-stranded vectors and the Cas9 constructs are conventional single-stranded vectors, it is possible that the low Cas9 expression levels are caused by inefficient second-strand synthesis in primary human CD4+ T cells. This could be tested by comparing transduction efficiencies over several days with a single-stranded and a

double-stranded YFP reporter construct. If second-strand synthesis is limited in human primary CD4$^+$ T cells, SpCas9 cannot be applied to those cells with AAV vectors, because the coding sequence is too large to express it from self-complementary vectors. An alternative would then be to use the smaller Cas9 enzyme from *staphylococcus aureus* (SaCas9) and express the N- and C-terminal halves on separate double-stranded AAV genomes. However, as SaCas9 uses a different PAM than SpCas9, new gRNAs would need to be designed in this case.

Even if Cas9 expression can be optimized, still the transduction efficiencies that we observed with AAV6 ranging from 30 % to 60 % might not be sufficient to achieve a strong reduction of HIV-1 infection. Since many different strategies are available for AAV capsid engineering, this problem might be overcome by identification of a synthetic capsid variant with enhanced trans-duction efficiency in human primary CD4$^+$ T cells. One interesting mutant that could be tested in future experiments is for example the AAV6 triple mutant Y705 + 731F + T492V that has been described by Ling et al. [240] and has been shown to transduce human hematopoietic stem cells more efficiently then wildtype AAV6.

4.4 Future perspectives

In this work we established an AAV-delivered CRISPR/Cas9 system that targets the HIV-1 ge-nome at up to three different sites and showed that it enables protection of HeLaP4 cells against HIV-1 infection and functional inactivation of the latent provirus in J-Lat T cells. Furthermore, we tested different gRNA combinations in parallel, which enabled us to identify particularly efficient ones that can be used in future experiments. In addition, the first test in primary human CD4$^+$ T cells enabled us to identify the current limitations of the system for an application in these cells.

Hence, the next step will be to optimize the system in regard to Cas9 expression and transduc-tion efficiency in human primary CD4$^+$ T cells. Also gRNA expression levels in these cells should be analyzed. The optimized system will then provide the basis for later *in vivo* applications in humanized mice. The three studies that have described *in vivo* targeting of the HIV-1 genome with CRISPR/Cas9 so far used experimental settings or mice models that do not recapitulate HIV-1 latency in a patient under ART. One study used a transgenic mouse model harboring HIV-1 proviral genomes in all tissues [77]. The second study used in addition to the aforemen-tioned transgenic mouse model mice that were acutely infected with an HIV-luciferase reporter virus. Even if they show reduction of the acute infection upon CRISPR-treatment, this does not permit conclusion about elimination of the latent reservoir [78]. The third study used mice en-

grafted either with *in vitro* HIV-1 infected human PBMCs or PBMCs from HIV-1 infected patients under ART [79]. Since the mice were not further kept under ART and viral loads were not analyzed at the day of CRISPR-treatment, a rebound of viral loads before treatment cannot be excluded and the reported reduction of viral levels in blood cells and the spleen do not allow conclusions about successful targeting of the latent reservoir. Even if these studies show the great potential of CRISPR/Cas9 to target HIV-1 *in vivo*, they still leave important questions unanswered. As the size of the HIV-1 latent reservoir has been described to be very small with approximately 1 of 10^6 resting CD4$^+$ T cells latently infected [241, 242], it needs to be clarified if CRISPR/Cas9 can be delivered to these few cells. Furthermore, as resting CD4$^+$ T cells display low levels of transcription factors and dNTPs [36–41], it is questionable if Cas9 and gRNAs will be expressed efficiently in these cells. Hence, further *in vivo* studies will be necessary to address these questions. Furthermore, as one major concern about application of CRISPR/Cas9 in humans is the safety of the system in regard to off-targeting effects, optimization of the system to prevent off-targeting will be absolutely necessary to come closer towards later clinical applications.
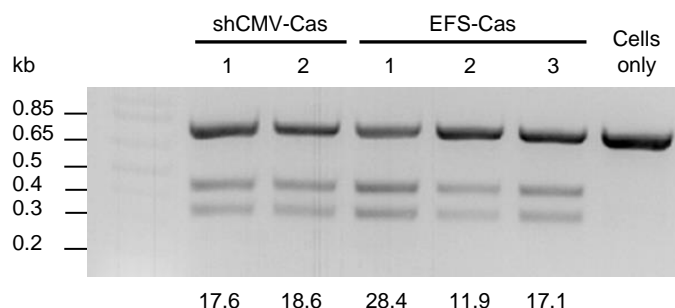
5. Supplement

Figure 5.1: Editing in HeLaP4-NLtr reporter cells using a shCMV- or EFS-Cas9 encoding AAV vector. HeLaP4-NLtr cells were transduced with AAV9-A2 crude lysates encoding g6 driven from U6 promoter and different productions of AAV9-A2 crude lysates encoding a shCMV- or EFS-promoter driven Cas9. Numbers below the gel images indicate the cleavage efficiencies in percent calculated with imageJ.
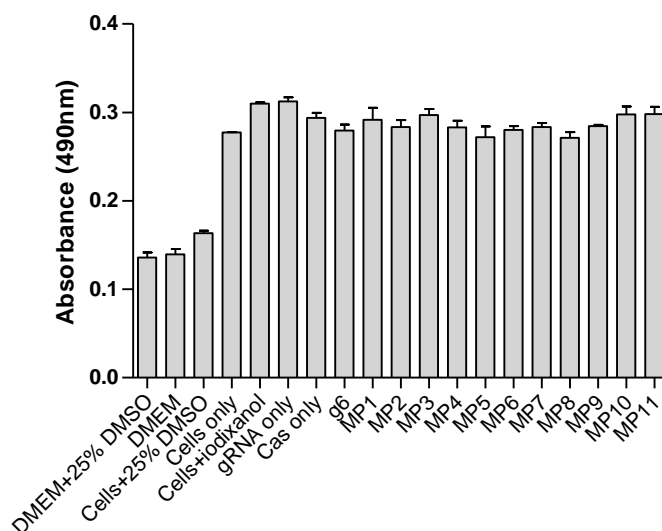

Figure 5.2: MTS assay with AAV transduced or untransduced J-Lat cells. J-Lat 9.2 cells were seeded and co-transduced with purified AAV9-A2 vectors encoding different triple-gRNA combinations or gRNA6 alone and with a Cas9-expressing AAV. As control, cells were either not treated with AAV or transduced only with a Cas9/gRNA-encoding vector alone or treated with iodixanol. After 48 hours, the cells were split and transduced a second time. 21 h later HIV proviral transcription was activated with TPA and TNFα for 5 h, cells were washed and then incubated for 24 h before the MTS assay was performed. The MTS reagent is reduced by living cells to a colored formazan product that can be quantified by measuring the absorbance at 490nm. Asa control, cells killed with 25% DMSO were measured. To determine the background values, DMEM and DMEM with 25% DMSO was also measured. Depicted is the mean from three technical replicates with standard deviation.
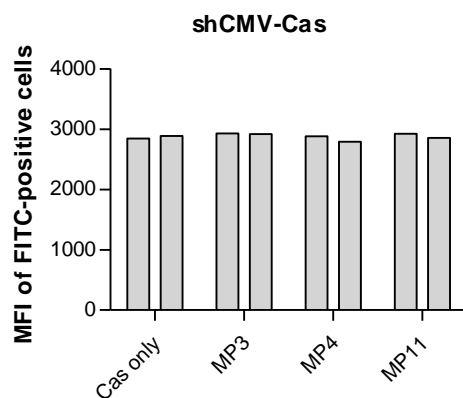
shCMV-Cas

Figure 5.3: Mean fluorescence intensity of HIV-1 infected anti-p24 stained human primary CD4$^+$ T cells pre-treated with gRNA multiplexing vectors and shCMV-Cas9. Mean fluorescence intensity of FITC-positive cells. CD4$^+$ T cells from one donor were activated three days and then transduced with AAV6 encoding gRNA multiplexing vectors and a Cas9 expressing vector. As control cells were only transduced with a Cas9 encoding AAV6. Two days later the cells were infected with HIV-1 NL4-3. Three days post infection the cells were fixed, stained with a FITC-labeled anti-p24 antibody and analyzed with flow cytometry. N=1.
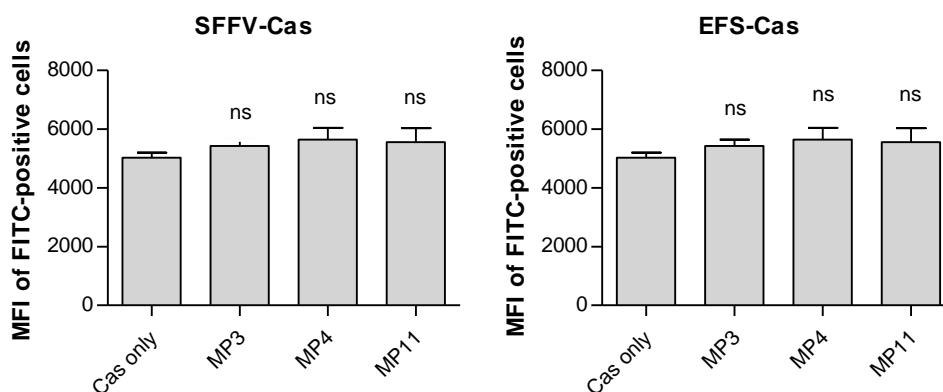

SFFV-Cas **EFS-Cas**

Figure 5.4: Mean fluorescence intensity of HIV-1 infected anti-p24 stained human primary CD4$^+$ T cells pre-treated with gRNA multiplexing vectors and SSFV- or EFS-Cas9. Mean fluorescence intensity of FITC-positive cells. CD4$^+$ T cells from one donor were activated three days and then transduced with AAV6 encoding gRNA multi-plexing vectors and a Cas9 expressing vector. As control cells were only transduced with a Cas9 encoding AAV6. Two days later the cells were infected with HIV-1 NL4-3. Three days post infection the cells were fixed, stained with a FITC-labeled anti-p24 antibody and analyzed with flow cytometry. N=3.
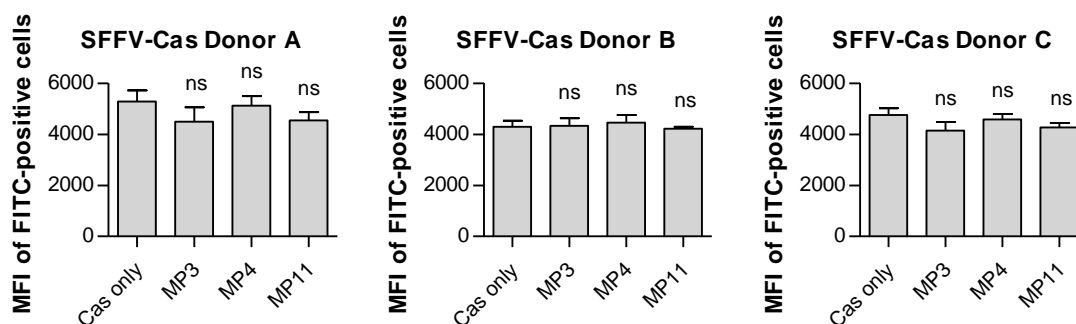
119

Figure 5.5: Mean fluorescence intensity of HIV-1 infected anti-p24 stained human primary CD4+ T cells pre-treated with gRNA multiplexing vectors and SSFV-Cas9. Mean fluorescence intensity of FITC-positive cells. CD4+ T cells from three donors were activated three days and then transduced with AAV6 encoding gRNA multiplexing vectors and a Cas9 expressing vector. As control cells were only transduced with a Cas9 encoding AAV6. Two days later the cells were infected with HIV-1 NL4-3. Three days post infection the cells were fixed, stained with a FITC-labeled anti-p24 antibody and analyzed with flow cytometry. N=4.

Table 5.1: Sequences of the gRNAs used in this work.

Name	Sequence (5´→3´)	Length (nt)
g1	AGAACTACACACCAGGGCCA	20
g2	GATATCCACTGACCTTTGGA	20
g3	AGAGAGAAGTGTTAGAGTGG	20
g4	GCCTGGGCGGGACTGGGGAG	20
g5	GGTTAGACCAGATCTGAGCC	20
g6	GGGAGCTCTCTGGCTAACTA	20
g7	GCCCGTCTGTTGTGTGACTC	20
g8	GTACTCCGGATGCAGCTCTC	20
g9	GATTTTCCACACTGACTAAA	20
gag	GAGGCTAGAAGGAGAGAGAT	20
p17	GATGGGTGCGAGAGCGT	17
p24_1	GACAGCATGTCAGGGAG	17
p24_2	AGAAATGATGACAGCATGTC	20
int3	GGGATTGGGGGGGTACAGTGC	20
int4	AAGCTCCTCTGGAAAGGTGA	20
int5	GATTATGGAAAACAGATGGC	20

120

6. References

1.   Gallo RC, Sarin PS, Gelmann EP, Robert-Guroff M, Richardson E, Kalyanaraman VS, Mann D, Sidhu GD, Stahl RE, Zolla-Pazner S, Leibowitch J, Popovic M: Isolation of human T-cell leukemia virus in acquired immune deficiency syndrome (AIDS). Science 220, 865–7 (1983)

2.   Barré-Sinoussi F, Chermann JC, Rey F, Nugeyre MT, Chamaret S, Gruest J, Dauguet C, Axler-Blin C, Vézinet-Brun F, Rouzioux C, Rozenbaum W, Montagnier L: Isolation of a T-lymphotropic retrovirus from a patient at risk for acquired immune deficiency syndrome (AIDS). Science 220, 868–71 (1983)

3.   Li G, De Clercq E: HIV Genome-Wide Protein Associations: a Review of 30 Years of Research. Microbiol Mol Biol Rev 80, 679–731 (2016)

4.   Fanales-Belasio E, Raimondo M, Suligoi B, Buttò S: HIV virology and pathogenetic mechanisms of infection: a brief overview. Ann Ist Super Sanita 46, 5–14 (2010)

5.   Wilen CB, Tilton JC, Doms RW: HIV: cell binding and entry. Cold Spring Harb Perspect Med 2, (2012)

6.   Hu W-S, Hughes SH: HIV-1 reverse transcription. Cold Spring Harb Perspect Med 2, (2012)

7.   Lusic M, Siliciano RF: Nuclear landscape of HIV-1 infection and integration. Nat Rev Microbiol 15, 69–82 (2017)

8.   Karn J, Stoltzfus CM: Transcriptional and posttranscriptional regulation of HIV-1 gene expression. Cold Spring Harb Perspect Med 2, a006916 (2012)

9.   Feng S, Holland EC: HIV-1 tat trans-activation requires the loop sequence within tar. Nature 334, 165–7 (1988)

10.   Roy S, Delling U, Chen CH, Rosen CA, Sonenberg N: A bulge structure in HIV-1 TAR RNA is required for Tat binding and Tat-mediated trans-activation. Genes Dev 4, 1365–73 (1990)

11.   Kao SY, Calman AF, Luciw PA, Peterlin BM: Anti-termination of transcription within the long terminal repeat of HIV-1 by tat gene product. Nature 330, 489–93

12.   Feinberg MB, Baltimore D, Frankel AD: The role of Tat in the human immunodeficiency virus life cycle indicates a primary effect on transcriptional elongation. Proc Natl Acad Sci U S A 88, 4045–9 (1991)

13.   Malim MH, Hauber J, Le SY, Maizel J V, Cullen BR: The HIV-1 rev trans-activator acts through a structured target sequence to activate nuclear export of unspliced viral mRNA. Nature 338, 254–7 (1989)

14.   Jacks T, Power MD, Masiarz FR, Luciw PA, Barr PJ, Varmus HE: Characterization of ribosomal frameshifting in HIV-1 gag-pol expression. Nat 1988 3316153 331, 280 (1988)

15. Franzusoff A, Volpe AM, Josse D, Pichuantes S, Wolf JR: Biochemical and genetic definition of the cellular protease required for HIV-1 gp160 processing. J Biol Chem 270, 3154–9 (1995)

16. Decroly E, Vandenbranden M, Ruysschaert JM, Cogniaux J, Jacob GS, Howard SC, Marshall G, Kompelli A, Basak A, Jean F: The convertases furin and PC1 can both cleave the human immunodeficiency virus (HIV)-1 envelope glycoprotein gp160 into gp120 (HIV-1 SU) and gp41 (HIV-I TM). J Biol Chem 269, 12240–7 (1994)

17. Harrison GP, Lever AM: The human immunodeficiency virus type 1 packaging signal and major splice donor region have a conserved stable secondary structure. J Virol 66, 4144–53 (1992)

18. Göttlinger HG, Dorfman T, Sodroski JG, Haseltine WA: Effect of mutations affecting the p6 gag protein on human immunodeficiency virus particle release. Proc Natl Acad Sci U S A 88, 3195–9 (1991)

19. Martin-Serrano J, Zang T, Bieniasz PD: HIV-1 and Ebola virus encode small peptide motifs that recruit Tsg101 to sites of particle assembly to facilitate egress. Nat Med 7, 1313–9 (2001)

20. Peng C, Ho BK, Chang TW, Chang NT: Role of human immunodeficiency virus type 1-specific protease in core protein maturation and viral infectivity. J Virol 63, 2550–6 (1989)

21. Göttlinger HG, Sodroski JG, Haseltine WA: Role of capsid precursor processing and myristoylation in morphogenesis and infectivity of human immunodeficiency virus type 1. Proc Natl Acad Sci U S A 86, 5781–5 (1989)

22. Kaplan AH, Zack JA, Knigge M, Paul DA, Kempf DJ, Norbeck DW, Swanstrom R: Partial inhibition of the human immunodeficiency virus type 1 protease results in aberrant virus assembly and the formation of noninfectious particles. J Virol 67, 4050–5 (1993)

23. Mattei S, Tan A, Glass B, Müller B, Kräusslich H-G, Briggs JAG: High-resolution structures of HIV-1 Gag cleavage mutants determine structural switch for virus maturation. Proc Natl Acad Sci U S A 115, E9401–E9410 (2018)

24. James JS: Saquinavir (Invirase): first protease inhibitor approved--reimbursement, information hotline numbers. AIDS Treat News 1–2 (1995)

25. Gulick RM, Mellors JW, Havlir D, Eron JJ, Gonzalez C, McMahon D, Richman DD, Valentine FT, Jonas L, Meibohm A, Emini EA, Chodakewitz JA: Treatment with indinavir, zidovudine, and lamivudine in adults with human immunodeficiency virus infection and prior antiretroviral therapy. N Engl J Med 337, 734–9 (1997)

26. Hammer SM, Squires KE, Hughes MD, Grimes JM, Demeter LM, Currier JS, Eron JJ, Feinberg JE, Balfour HH, Deyton LR, Chodakewitz JA, Fischl MA: A controlled trial of two nucleoside analogues plus indinavir in persons with human immunodeficiency virus infection and CD4 cell counts of 200 per cubic millimeter or less. AIDS Clinical Trials Group 320 Study Team. N Engl J Med 337, 725–33 (1997)

27. Harrison KM, Song R, Zhang X: Life expectancy after HIV diagnosis based on national HIV surveillance data from 25 states, United States. J Acquir Immune Defic Syndr 53, 124–30 (2010)

28.	Palella FJ, Delaney KM, Moorman AC, Loveless MO, Fuhrer J, Satten GA, Aschman DJ, Holmberg SD: Declining morbidity and mortality among patients with advanced human immunodeficiency virus infection. HIV Outpatient Study Investigators. N Engl J Med 338, 853–860 (1998)

29.	Davey RT, Bhat N, Yoder C, Chun TW, Metcalf JA, Dewar R, Natarajan V, Lempicki RA, Adelsberger JW, Miller KD, Kovacs JA, Polis MA, Walker RE, Falloon J, Masur H, Gee D, Baseler M, Dimitrov DS, Fauci AS, Lane HC: HIV-1 and T cell dynamics after interruption of highly active antiretroviral therapy (HAART) in patients with a history of sustained viral suppression. Proc Natl Acad Sci U S A 96, 15109–15114 (1999)

30.	Zhang L, Chung C, Hu BS, He T, Guo Y, Kim AJ, Skulsky E, Jin X, Hurley A, Ramratnam B, Markowitz M, Ho DD: Genetic characterization of rebounding HIV-1 after cessation of highly active antiretroviral therapy. J Clin Invest 106, 839–45 (2000)

31.	Chun TW, Finzi D, Margolick J, Chadwick K, Schwartz D, Siliciano RF: In vivo fate of HIV-1-infected T cells: quantitative analysis of the transition to stable latency. Nat Med 1, 1284–90 (1995)

32.	Sengupta S, Siliciano RF: Targeting the Latent Reservoir for HIV-1. Immunity 48, 872–895 (2018)

33.	Bukrinsky MI, Stanwick TL, Dempsey MP, Stevenson M: Quiescent T lymphocytes as an inducible virus reservoir in HIV-1 infection. Science 254, 423–7 (1991)

34.	Zack JA, Arrigo SJ, Weitsman SR, Go AS, Haislip A, Chen IS: HIV-1 entry into quiescent primary lymphocytes: molecular analysis reveals a labile, latent viral structure. Cell 61, 213–22 (1990)

35.	Zhou Y, Zhang H, Siliciano JD, Siliciano RF: Kinetics of human immunodeficiency virus type 1 decay following entry into resting CD4+ T cells. J Virol 79, 2199–210 (2005)

36.	Böhnlein E, Lowenthal JW, Siekevitz M, Ballard DW, Franza BR, Greene WC: The same inducible nuclear proteins regulates mitogen activation of both the interleukin-2 receptor-alpha gene and type 1 HIV. Cell 53, 827–36 (1988)

37.	Molitor JA, Walker WH, Doerre S, Ballard DW, Greene WC: NF-kappa B: a family of inducible and differentially expressed enhancer-binding proteins in human T cells. Proc Natl Acad Sci U S A 87, 10028–32 (1990)

38.	Gao WY, Cara A, Gallo RC, Lori F: Low levels of deoxynucleotides in peripheral blood lymphocytes: a strategy to inhibit human immunodeficiency virus type 1 replication. Proc Natl Acad Sci U S A 90, 8925–8 (1993)

39.	Nabel G, Baltimore D: An inducible transcription factor activates expression of human immunodeficiency virus in T cells. Nat 1987 3266114 326, 711 (1987)

40.	Kinoshita S, Chen BK, Kaneshima H, Nolan GP: Host control of HIV-1 parasitism in T cells by the nuclear factor of activated T cells. Cell 95, 595–604 (1998)

41.	Lin X, Irwin D, Kanazawa S, Huang L, Romeo J, Yen TSB, Peterlin BM: Transcriptional profiles of latent human immunodeficiency virus in infected individuals: effects of Tat on the host and reservoir. J Virol 77, 8227–36 (2003)

42. Laughlin MA, Zeichner S, Kolson D, Alwine JC, Seshamma T, Pomerantz RJ, Gonzalez-Scarano F: Sodium butyrate treatment of cells latently infected with HIV-1 results in the expression of unspliced viral RNA. Virology 196, 496–505 (1993)

43. Van Lint C, Emiliani S, Ott M, Verdin E: Transcriptional activation and chromatin remodeling of the HIV-1 promoter in response to histone acetylation. EMBO J 15, 1112–20 (1996)

44. Kauder SE, Bosque A, Lindqvist A, Planelles V, Verdin E: Epigenetic regulation of HIV-1 latency by cytosine methylation. PLoS Pathog 5, e1000495 (2009)

45. Blazkova J, Trejbalova K, Gondois-Rey F, Halfon P, Philibert P, Guiguen A, Verdin E, Olive D, Van Lint C, Hejnar J, Hirsch I: CpG methylation controls reactivation of HIV from latency. PLoS Pathog 5, e1000554 (2009)

46. Siliciano JD, Kajdas J, Finzi D, Quinn TC, Chadwick K, Margolick JB, Kovacs C, Gange SJ, Siliciano RF: Long-term follow-up studies confirm the stability of the latent reservoir for HIV-1 in resting CD4+ T cells. Nat Med 9, 727–8 (2003)

47. Churchill MJ, Deeks SG, Margolis DM, Siliciano RF, Swanstrom R: HIV reservoirs: what, where and how to target them. Nat Rev Microbiol 2015 141 14, 55 (2015)

48. Josefsson L, von Stockenstrom S, Faria NR, Sinclair E, Bacchetti P, Killian M, Epling L, Tan A, Ho T, Lemey P, Shao W, Hunt PW, Somsouk M, Wylie W, Douek DC, Loeb L, Custer J, Hoh R, Poole L, Deeks SG, Hecht F, Palmer S: The HIV-1 reservoir in eight patients on long-term suppressive antiretroviral therapy is stable with few genetic changes over time. Proc Natl Acad Sci U S A 110, E4987–96 (2013)

49. von Stockenstrom S, Odevall L, Lee E, Sinclair E, Bacchetti P, Killian M, Epling L, Shao W, Hoh R, Ho T, Faria NR, Lemey P, Albert J, Hunt P, Loeb L, Pilcher C, Poole L, Hatano H, Somsouk M, Douek D, Boritz E, Deeks SG, Hecht FM, Palmer S: Longitudinal Genetic Characterization Reveals That Cell Proliferation Maintains a Persistent HIV Type 1 DNA Pool During Effective HIV Therapy. J Infect Dis 212, 596–607 (2015)

50. Imamichi H, Natarajan V, Adelsberger JW, Rehm CA, Lempicki RA, Das B, Hazen A, Imamichi T, Lane HC: Lifespan of effector memory CD4+ T cells determined by replication-incompetent integrated HIV-1 provirus. AIDS 28, 1091–9 (2014)

51. Maldarelli F, Wu X, Su L, Simonetti FR, Shao W, Hill S, Spindler J, Ferris AL, Mellors JW, Kearney MF, Coffin JM, Hughes SH: HIV latency. Specific HIV integration sites are linked to clonal expansion and persistence of infected cells. Science 345, 179–83 (2014)

52. Wagner TA, McLaughlin S, Garg K, Cheung CYK, Larsen BB, Styrchak S, Huang HC, Edlefsen PT, Mullins JI, Frenkel LM: HIV latency. Proliferation of cells with HIV integrated into cancer genes contributes to persistent infection. Science 345, 570–3 (2014)

53. Ikeda T, Shibata J, Yoshimura K, Koito A, Matsushita S: Recurrent HIV-1 integration at the BACH2 locus in resting CD4+ T cell populations during effective highly active antiretroviral therapy. J Infect Dis 195, 716–25 (2007)

54. Bosque A, Famiglietti M, Weyrich AS, Goulston C, Planelles V: Homeostatic proliferation fails to efficiently reactivate HIV-1 latently infected central memory CD4+ T cells. PLoS Pathog 7, e1002288 (2011)

55. Vandergeeten C, Fromentin R, DaFonseca S, Lawani MB, Sereti I, Lederman MM, Ramgopal M, Routy J-P, Sékaly R-P, Chomont N: Interleukin-7 promotes HIV persistence during antiretroviral therapy. Blood 121, 4321–9 (2013)

56. Katlama C, Lambert-Niclot S, Assoumou L, Papagno L, Lecardonnel F, Zoorob R, Tambussi G, Clotet B, Youle M, Achenbach CJ, Murphy RL, Calvez V, Costagliola D, Autran B, EraMune-01 study team: Treatment intensification followed by interleukin-7 reactivates HIV without reducing total HIV DNA: a randomized trial. AIDS 30, 221–30 (2016)

57. Glesby MJ: Cardiovascular Complications of HIV Infection. Top Antivir Med 24, 127–131 (2017)

58. Wyatt CM: Kidney Disease and HIV Infection. Top Antivir Med 25, 13–16 (2017)

59. Tang MW, Shafer RW: HIV-1 antiretroviral resistance: scientific principles and clinical applications. Drugs 72, e1–25 (2012)

60. Lehrman G, Hogue IB, Palmer S, Jennings C, Spina CA, Wiegand A, Landay AL, Coombs RW, Richman DD, Mellors JW, Coffin JM, Bosch RJ, Margolis DM: Depletion of latent HIV-1 infection in vivo: a proof-of-concept study. Lancet (London, England) 366, 549–55

61. Rasmussen TA, Tolstrup M, Brinkmann CR, Olesen R, Erikstrup C, Solomon A, Winckelmann A, Palmer S, Dinarello C, Buzon M, Lichterfeld M, Lewin SR, Østergaard L, Søgaard OS: Panobinostat, a histone deacetylase inhibitor, for latent-virus reactivation in HIV-infected patients on suppressive antiretroviral therapy: a phase 1/2, single group, clinical trial. Lancet HIV 1, e13–e21 (2014)

62. Søgaard OS, Graversen ME, Leth S, Olesen R, Brinkmann CR, Nissen SK, Kjaer AS, Schleimann MH, Denton PW, Hey-Cunningham WJ, Koelsch KK, Pantaleo G, Krogsgaard K, Sommerfelt M, Fromentin R, Chomont N, Rasmussen TA, Østergaard L, Tolstrup M: The Depsipeptide Romidepsin Reverses HIV-1 Latency In Vivo. PLoS Pathog 11, e1005142 (2015)

63. Williams SA, Chen L-F, Kwon H, Fenard D, Bisgrove D, Verdin E, Greene WC: Prostratin antagonizes HIV latency by activating NF-kappaB. J Biol Chem 279, 42008–17 (2004)

64. Blazkova J, Chun T-W, Belay BW, Murray D, Justement JS, Funk EK, Nelson A, Hallahan CW, Moir S, Wender PA, Fauci AS: Effect of histone deacetylase inhibitors on HIV production in latently infected, resting CD4(+) T cells from infected individuals receiving effective antiretroviral therapy. J Infect Dis 206, 765–9 (2012)

65. Archin NM, Liberty AL, Kashuba AD, Choudhary SK, Kuruc JD, Crooks AM, Parker DC, Anderson EM, Kearney MF, Strain MC, Richman DD, Hudgens MG, Bosch RJ, Coffin JM, Eron JJ, Hazuda DJ, Margolis DM: Administration of vorinostat disrupts HIV-1 latency in patients on antiretroviral therapy. Nature 487, 482–5 (2012)

66. Douek DC: HIV Infection: Advances Toward a Cure. Top Antivir Med 25, 121–125 (2018)

67. Hütter G, Nowak D, Mossner M, Ganepola S, Müssig A, Allers K, Schneider T, Hofmann J, Kücherer C, Blau O, Blau IW, Hofmann WK, Thiel E: Long-term control of HIV by CCR5 Delta32/Delta32 stem-cell transplantation. N Engl J Med 360, 692–8 (2009)

68. Allers K, Hütter G, Hofmann J, Loddenkemper C, Rieger K, Thiel E, Schneider T: Evidence for the cure of HIV infection by CCR5Δ32/Δ32 stem cell transplantation. Blood 117, 2791–9 (2011)

69. Samson M, Libert F, Doranz BJ, Rucker J, Liesnard C, Farber CM, Saragosti S, Lapoumeroulie C, Cognaux J, Forceille C, Muyldermans G, Verhofstede C, Burtonboy G, Georges M, Imai T, Rana S, Yi Y, Smyth RJ, Collman RG, Doms RW, Vassart G, Parmentier M: Resistance to HIV-1 infection in caucasian individuals bearing mutant alleles of the CCR-5 chemokine receptor gene. Nature 382, 722–5 (1996)

70. Haworth KG, Peterson CW, Kiem H-P: CCR5-edited gene therapies for HIV cure: Closing the door to viral entry. Cytotherapy 19, 1325–1338 (2017)

71. Karpinski J, Hauber I, Chemnitz J, Schäfer C, Paszkowski-Rogacz M, Chakraborty D, Beschorner N, Hofmann-Sieber H, Lange UC, Grundhoff A, Hackmann K, Schrock E, Abi-Ghanem J, Pisabarro MT, Surendranath V, Schambach A, Lindner C, van Lunzen J, Hauber J, Buchholz F: Directed evolution of a recombinase that excises the provirus of most HIV-1 primary isolates with high specificity. Nat Biotechnol [Epub ahead of print], doi: 10.1038/nbt.3467 (2016)

72. Ebina H, Kanemura Y, Misawa N, Sakuma T, Kobayashi T, Yamamoto T, Koyanagi Y: A high excision potential of TALENs for integrated DNA of HIV-based lentiviral vector. PLoS One 10, e0120047 (2015)

73. Kishida T, Ejima A, Mazda O: Specific Destruction of HIV Proviral p17 Gene in T Lymphoid Cells Achieved by the Genome Editing Technology. Front Microbiol 7, 1001 (2016)

74. Strong CL, Guerra HP, Mathew KR, Roy N, Simpson LR, Schiller MR: Damaging the Integrated HIV Proviral DNA with TALENS. PLoS One 10, e0125652 (2015)

75. Ji H, Lu P, Liu B, Qu X, Wang Y, Jiang Z, Yang X, Zhong Y, Yang H, Pan H, Zhao L, Xu J, Lu H, Zhu H: Zinc-Finger Nucleases Induced by HIV-1 Tat Excise HIV-1 from the Host Genome in Infected and Latently Infected Cells. Mol Ther Nucleic Acids 12, 67–74 (2018)

76. Okee M, Bayiyana A, Musubika C, Joloba ML, Ashaba-Katabazi F, Bagaya B, Wayengera M: In Vitro Transduction and Target-Mutagenesis Efficiency of HIV-1 pol Gene Targeting ZFN and CRISPR/Cas9 Delivered by Various Plasmids and/or Vectors: Toward an HIV Cure. AIDS Res Hum Retroviruses 34, 88–102 (2018)

77. Kaminski R, Bella R, Yin C, Otte J, Ferrante P, Gendelman HE, Li H, Booze R, Gordon J, Hu W, Khalili K: Excision of HIV-1 DNA by gene editing: a proof-of-concept in vivo study. Gene Ther 23, 690–5 (2016)

78. Yin C, Zhang T, Qu X, Zhang Y, Putatunda R, Xiao X, Li F, Xiao W, Zhao H, Dai S, Qin X, Mo X, Young W-B, Khalili K, Hu W: In Vivo Excision of HIV-1 Provirus by saCas9 and Multiplex Single-Guide RNAs in Animal Models. Mol Ther 25, 1168–1186 (2017)

79. Bella R, Kaminski R, Mancuso P, Young W-B, Chen C, Sariyer R, Fischer T, Amini S, Ferrante P, Jacobson JM, Kashanchi F, Khalili K: Removal of HIV DNA by CRISPR from Patient Blood Engrafts in Humanized Mice. Mol Ther Nucleic Acids 12, 275–282 (2018)

80. Mojica FJM, Díez-Villaseñor C, García-Martínez J, Soria E: Intervening sequences of regularly spaced prokaryotic repeats derive from foreign genetic elements. J Mol Evol 60, 174–82 (2005)

81. Bolotin A, Quinquis B, Sorokin A, Ehrlich SD: Clustered regularly interspaced short palindrome repeats (CRISPRs) have spacers of extrachromosomal origin. Microbiology 151, 2551–61 (2005)

82. Pourcel C, Salvignol G, Vergnaud G: CRISPR elements in Yersinia pestis acquire new repeats by preferential uptake of bacteriophage DNA, and provide additional tools for evolutionary studies. Microbiology 151, 653–63 (2005)

83. Jinek M, Chylinski K, Fonfara I, Hauer M, Doudna JA, Charpentier E: A programmable dual-RNA-guided DNA endonuclease in adaptive bacterial immunity. Science 337, 816–21 (2012)

84. Gasiunas G, Barrangou R, Horvath P, Siksnys V: Cas9-crRNA ribonucleoprotein complex mediates specific DNA cleavage for adaptive immunity in bacteria. Proc Natl Acad Sci 109, E2579–E2586 (2012)

85. Haft DH, Selengut J, Mongodin EF, Nelson KE: A guild of 45 CRISPR-associated (Cas) protein families and multiple CRISPR/Cas subtypes exist in prokaryotic genomes. PLoS Comput Biol 1, e60 (2005)

86. Makarova KS, Haft DH, Barrangou R, Brouns SJJ, Charpentier E, Horvath P, Moineau S, Mojica FJM, Wolf YI, Yakunin AF, van der Oost J, Koonin E V: Evolution and classification of the CRISPR-Cas systems. Nat Rev Microbiol 9, 467–77 (2011)

87. Koonin E V, Makarova KS, Zhang F: Diversity, classification and evolution of CRISPR-Cas systems. Curr Opin Microbiol 37, 67–78 (2017)

88. Deltcheva E, Chylinski K, Sharma CM, Gonzales K, Chao Y, Pirzada ZA, Eckert MR, Vogel J, Charpentier E: CRISPR RNA maturation by trans-encoded small RNA and host factor RNase III. Nature 471, 602–7 (2011)

89. Deveau H, Barrangou R, Garneau JE, Labonté J, Fremaux C, Boyaval P, Romero DA, Horvath P, Moineau S: Phage response to CRISPR-encoded resistance in Streptococcus thermophilus. J Bacteriol 190, 1390–400 (2008)

90. Hsu PD, Scott DA, Weinstein JA, Ran FA, Konermann S, Agarwala V, Li Y, Fine EJ, Wu X, Shalem O, Cradick TJ, Marraffini LA, Bao G, Zhang F: DNA targeting specificity of RNA-guided Cas9 nucleases. Nat Biotechnol 31, 827–32 (2013)

91. Boch J, Scholze H, Schornack S, Landgraf A, Hahn S, Kay S, Lahaye T, Nickstadt A, Bonas U: Breaking the code of DNA binding specificity of TAL-type III effectors. Science 326, 1509–12 (2009)

92. Christian M, Cermak T, Doyle EL, Schmidt C, Zhang F, Hummel A, Bogdanove AJ, Voytas DF: Targeting DNA double-strand breaks with TAL effector nucleases. Genetics 186, 757–61 (2010)

93. Miller J, McLachlan AD, Klug A: Repetitive zinc-binding domains in the protein transcription factor IIIA from Xenopus oocytes. EMBO J 4, 1609–14 (1985)

94. Kim YG, Cha J, Chandrasegaran S: Hybrid restriction enzymes: zinc finger fusions to Fok I cleavage domain. Proc Natl Acad Sci U S A 93, 1156–60 (1996)

95. Cong L, Ran FA, Cox D, Lin S, Barretto R, Habib N, Hsu PD, Wu X, Jiang W, Marraffini LA, Zhang F: Multiplex genome engineering using CRISPR/Cas systems. Science 339, 819–23 (2013)

96.: Fundamental CRISPR-Cas9 tools and current applications in microbial systems. Synth Syst Biotechnol 2, 219–225 (2017)

97. Wyman C, Kanaar R: DNA Double-Strand Break Repair: All's Well that Ends Well. Annu Rev Genet 40, 363–383 (2006)

98. Kato T, Hara S, Goto Y, Ogawa Y, Okayasu H, Kubota S, Tamano M, Terao M, Takada S: Creation of mutant mice with megabase-sized deletions containing custom-designed breakpoints by means of the CRISPR/Cas9 system. Sci Rep 7, (2017)

99. Korablev AN, Serova IA, Serov OL: Generation of megabase-scale deletions, inversions and duplications involving the Contactin-6 gene in mice by CRISPR/Cas9 technology. BMC Genet 18, (2017)

100. Wu X, Scott DA, Kriz AJ, Chiu AC, Hsu PD, Dadon DB, Cheng AW, Trevino AE, Konermann S, Chen S, Jaenisch R, Zhang F, Sharp PA: Genome-wide binding of the CRISPR endonuclease Cas9 in mammalian cells. Nat Biotechnol 32, 670–6 (2014)

101. Duan J, Lu G, Xie Z, Lou M, Luo J, Guo L, Zhang Y: Genome-wide identification of CRISPR/Cas9 off-targets in human genome. Cell Res 24, 1009–12 (2014)

102. Kuscu C, Arslan S, Singh R, Thorpe J, Adli M: Genome-wide analysis reveals characteristics of off-target sites bound by the Cas9 endonuclease. Nat Biotechnol 32, 677–83 (2014)

103. Tsai SQ, Zheng Z, Nguyen NT, Liebers M, Topkar V V, Thapar V, Wyvekens N, Khayter C, Iafrate AJ, Le LP, Aryee MJ, Joung JK: GUIDE-seq enables genome-wide profiling of off-target cleavage by CRISPR-Cas nucleases. Nat Biotechnol 33, 187–197 (2015)

104. Wang X, Wang Y, Wu X, Wang J, Wang Y, Qiu Z, Chang T, Huang H, Lin R-J, Yee J-K: Unbiased detection of off-target cleavage by CRISPR-Cas9 and TALENs using integrase-defective lentiviral vectors. Nat Biotechnol 33, 175–8 (2015)

105. Paulis M, Castelli A, Lizier M, Susani L, Lucchini F, Villa A, Vezzoni P: A pre-screening FISH-based method to detect CRISPR/Cas9 off-targets in mouse embryonic stem cells. Sci Rep 5, 12327 (2015)

106. Jiang W, Bikard D, Cox D, Zhang F, Marraffini LA: RNA-guided editing of bacterial genomes using CRISPR-Cas systems. Nat Biotechnol 31, 233–9 (2013)

107. Mali P, Aach J, Stranges PB, Esvelt KM, Moosburner M, Kosuri S, Yang L, Church GM: CAS9 transcriptional activators for target specificity screening and paired nickases for cooperative genome engineering. Nat Biotechnol 31, 833–8 (2013)

108. Pattanayak V, Lin S, Guilinger JP, Ma E, Doudna JA, Liu DR: High-throughput profiling of off-target DNA cleavage reveals RNA-programmed Cas9 nuclease specificity. Nat Biotechnol 31, 839–43 (2013)

109. Ran FA, Cong L, Yan WX, Scott DA, Gootenberg JS, Kriz AJ, Zetsche B, Shalem O, Wu X, Makarova KS, Koonin E V, Sharp PA, Zhang F: In vivo genome editing using Staphylococcus aureus Cas9. Nature 520, 186–91 (2015)

110. Sternberg SH, Redding S, Jinek M, Greene EC, Doudna JA: DNA interrogation by the CRISPR RNA-guided endonuclease Cas9. Nature 507, 62–7 (2014)

111. Fu Y, Sander JD, Reyon D, Cascio VM, Joung JK: Improving CRISPR-Cas nuclease specificity using truncated guide RNAs. Nat Biotechnol 32, 279–284 (2014)

112. Kim D, Bae S, Park J, Kim E, Kim S, Yu HR, Hwang J, Kim J-I, Kim J-S: Digenome-seq: genome-wide profiling of CRISPR-Cas9 off-target effects in human cells. Nat Methods 12, 237–43, 1 p following 243 (2015)

113. Kleinstiver BP, Pattanayak V, Prew MS, Tsai SQ, Nguyen NT, Zheng Z, Keith Joung J: High-fidelity CRISPR–Cas9 nucleases with no detectable genome-wide off-target effects. Nature 529, 490–495 (2016)

114. Slaymaker IM, Gao L, Zetsche B, Scott DA, Yan WX, Zhang F: Rationally engineered Cas9 nucleases with improved specificity. Science 351, 84–8 (2016)

115. Ran FA, Hsu PD, Lin C-Y, Gootenberg JS, Konermann S, Trevino AE, Scott DA, Inoue A, Matoba S, Zhang Y, Zhang F: Double nicking by RNA-guided CRISPR Cas9 for enhanced genome editing specificity. Cell 154, 1380–9 (2013)

116. Guilinger JP, Thompson DB, Liu DR: Fusion of catalytically inactive Cas9 to FokI nuclease improves the specificity of genome modification. Nat Biotechnol 32, 577–582 (2014)

117. Wyvekens N, Topkar V V, Khayter C, Joung JK, Tsai SQ: Dimeric CRISPR RNA-Guided FokI-dCas9 Nucleases Directed by Truncated gRNAs for Highly Specific Genome Editing. Hum Gene Ther 26, 425–31 (2015)

118. Liang X, Potter J, Kumar S, Zou Y, Quintanilla R, Sridharan M, Carte J, Chen W, Roark N, Ranganathan S, Ravinder N, Chesnut JD: Rapid and highly efficient mammalian cell engineering via Cas9 protein transfection. J Biotechnol 208, 44–53 (2015)

119. Wang M, Zuris JA, Meng F, Rees H, Sun S, Deng P, Han Y, Gao X, Pouli D, Wu Q, Georgakoudi I, Liu DR, Xu Q: Efficient delivery of genome-editing proteins using bioreducible lipid nanoparticles. Proc Natl Acad Sci U S A 113, 2868–73 (2016)

120. Lee K, Conboy M, Park HM, Jiang F, Kim HJ, Dewitt MA, Mackley VA, Chang K, Rao A, Skinner C, Shobha T, Mehdipour M, Liu H, Huang W-C, Lan F, Bray NL, Li S, Corn JE, Kataoka K, Doudna JA, Conboy I, Murthy N: Nanoparticle delivery of Cas9 ribonucleoprotein and donor DNA in vivo induces homology-directed DNA repair. Nat Biomed Eng 1, 889–901 (2017)

121. Nelson CE, Hakim CH, Ousterout DG, Thakore PI, Moreb EA, Castellanos Rivera RM, Madhavan S, Pan X, Ran FA, Yan WX, Asokan A, Zhang F, Duan D, Gersbach CA: In vivo genome editing improves muscle function in a mouse model of Duchenne muscular dystrophy. Science 351, 403–7 (2016)

122. Kim S, Kim D, Cho SW, Kim J, Kim J-S: Highly efficient RNA-guided genome editing in human cells via delivery of purified Cas9 ribonucleoproteins. Genome Res 24, 1012–9 (2014)

123. Hashimoto M, Takemoto T: Electroporation enables the efficient mRNA delivery into the mouse zygotes and facilitates CRISPR/Cas9-based genome editing. Sci Rep 5, 11315 (2015)

124. Niu Y, Shen B, Cui Y, Chen Y, Wang J, Wang L, Kang Y, Zhao X, Si W, Li W, Xiang AP, Zhou J, Guo X, Bi Y, Si C, Hu B, Dong G, Wang H, Zhou Z, Li T, Tan T, Pu X, Wang F, Ji S, Zhou Q, Huang X, Ji W, Sha J: Generation of gene-modified cynomolgus monkey via Cas9/RNA-mediated gene targeting in one-cell embryos. Cell 156, 836–43 (2014)

125. Chang N, Sun C, Gao L, Zhu D, Xu X, Zhu X, Xiong J-W, Xi JJ: Genome editing with RNA-guided Cas9 nuclease in Zebrafish embryos. Cell Res 23, 465–472 (2013)

126. Crispo M, Mulet AP, Tesson L, Barrera N, Cuadro F, dos Santos-Neto PC, Nguyen TH, Crénéguy A, Brusselle L, Anegón I, Menchaca A: Efficient Generation of Myostatin Knock-Out Sheep Using CRISPR/Cas9 Technology and Microinjection into Zygotes. PLoS One 10, e0136690 (2015)

127. Zhen S, Hua L, Liu Y-H, Gao L-C, Fu J, Wan D-Y, Dong L-H, Song H-F, Gao X: Harnessing the clustered regularly interspaced short palindromic repeat (CRISPR)/CRISPR-associated Cas9 system to disrupt the hepatitis B virus. Gene Ther 22, 404–12 (2015)

128. Xue W, Chen S, Yin H, Tammela T, Papagiannakopoulos T, Joshi NS, Cai W, Yang G, Bronson R, Crowley DG, Zhang F, Anderson DG, Sharp PA, Jacks T: CRISPR-mediated direct mutation of cancer genes in the mouse liver. Nature 514, 380–4 (2014)

129. Yin H, Xue W, Chen S, Bogorad RL, Benedetti E, Grompe M, Koteliansky V, Sharp PA, Jacks T, Anderson DG: Genome editing with Cas9 in adult mice corrects a disease mutation and phenotype. Nat Biotechnol 32, 551–3 (2014)

130. Jiang C, Mei M, Li B, Zhu X, Zu W, Tian Y, Wang Q, Guo Y, Dong Y, Tan X: A non-viral CRISPR/Cas9 delivery system for therapeutically targeting HBV DNA and pcsk9 in vivo. Cell Res 27, 440 (2017)

131. Sun W, Ji W, Hall JM, Hu Q, Wang C, Beisel PDCL, Gu PDZ: Efficient Delivery of CRISPR-Cas9 for Genome Editing via Self-Assembled DNA Nanoclews. Angew Chem Int Ed Engl 54, 12029 (2015)

132. Lino CA, Harper JC, Carney JP, Timlin JA: Delivering CRISPR: a review of the challenges and approaches. Drug Deliv 25, 1234–1257 (2018)

133. Sakuma T, Barry MA, Ikeda Y: Lentiviral vectors: basic to translational. Biochem J 443, 603–18 (2012)

134. Colella P, Ronzitti G, Mingozzi F: Emerging Issues in AAV-Mediated In Vivo Gene Therapy. Mol Ther Methods Clin Dev 8, 87–104 (2018)

135. Büning H, Huber A, Zhang L, Meumann N, Hacker U: Engineering the AAV capsid to optimize vector-host-interactions. Curr Opin Pharmacol 24, 94–104 (2015)

136. ATCHISON RW, CASTO BC, HAMMON WM: ADENOVIRUS-ASSOCIATED DEFECTIVE VIRUS PARTICLES. Science 149, 754–6 (1965)

137. Srivastava A, Lusby EW, Berns KI: Nucleotide sequence and organization of the adeno-associated virus 2 genome. J Virol 45, 555–64 (1983)

138. Bleker S, Sonntag F, Kleinschmidt JA: Mutational analysis of narrow pores at the fivefold symmetry axes of adeno-associated virus type 2 capsids reveals a dual role in genome packaging and activation of phospholipase A2 activity. J Virol 79, 2528–40 (2005)

139. Im DS, Muzyczka N: The AAV origin binding protein Rep68 is an ATP-dependent site-specific endonuclease with DNA helicase activity. Cell 61, 447–57 (1990)

140. Im DS, Muzyczka N: Partial purification of adeno-associated virus Rep78, Rep52, and Rep40 and their biochemical characterization. J Virol 66, 1119–28 (1992)

141. King JA, Dubielzig R, Grimm D, Kleinschmidt JA: DNA helicase-mediated packaging of adeno-associated virus type 2 genomes into preformed capsids. EMBO J 20, 3282–91 (2001)

142. Buller RM, Rose JA: Characterization of adenovirus-associated virus-induced polypeptides in KB cells. J Virol 25, 331–8 (1978)

143. Johnson FB, Ozer HL, Hoggan MD: Structural proteins of adenovirus-associated virus type 3. J Virol 8, 860–63 (1971)

144. Rose JA, Maizel J V, Inman JK, Shatkin AJ: Structural proteins of adenovirus-associated viruses. J Virol 8, 766–70 (1971)

145. Sonntag F, Schmidt K, Kleinschmidt JA: A viral assembly factor promotes AAV2 capsid formation in the nucleolus. Proc Natl Acad Sci U S A 107, 10220–5 (2010)

146. Naumer M, Sonntag F, Schmidt K, Nieto K, Panke C, Davey NE, Popa-Wagner R, Kleinschmidt JA: Properties of the adeno-associated virus assembly-activating protein. J Virol 86, 13038–48 (2012)

147. Mietzsch M, Broecker F, Reinhardt A, Seeberger PH, Heilbronn R: Differential adeno-associated virus serotype-specific interaction patterns with synthetic heparins and other glycans. J Virol 88, 2991–3003 (2014)

148. Uhrig S, Coutelle O, Wiehe T, Perabo L, Hallek M, Büning H: Successful target cell transduction of capsid-engineered rAAV vectors requires clathrin-dependent endocytosis. Gene Ther 19, 210–8 (2012)

149. Bantel-Schaal U, Braspenning-Wesch I, Kartenbeck J: Adeno-associated virus type 5 exploits two different entry pathways in human embryo fibroblasts. J Gen Virol 90, 317–22 (2009)

150. Nonnenmacher M, Weber T: Adeno-associated virus 2 infection requires endocytosis through the CLIC/GEEC pathway. Cell Host Microbe 10, 563–76 (2011)

151. Bantel-Schaal U, Hub B, Kartenbeck J: Endocytosis of adeno-associated virus type 5 leads to accumulation of virus particles in the Golgi compartment. J Virol 76, 2340–9 (2002)

152. Pajusola K, Gruchala M, Joch H, Lüscher TF, Ylä-Herttuala S, Büeler H: Cell-type-specific characteristics modulate the transduction efficiency of adeno-associated virus type 2 and restrain infection of endothelial cells. J Virol 76, 11530–40 (2002)

153. Johnson JS, Li C, DiPrimio N, Weinberg MS, McCown TJ, Samulski RJ: Mutagenesis of adeno-associated virus type 2 capsid protein VP1 uncovers new roles for basic amino acids in trafficking and cell-specific transduction. J Virol 84, 8888–902 (2010)

154. Johnson JS, Samulski RJ: Enhancement of adeno-associated virus infection by mobilizing capsids into and out of the nucleolus. J Virol 83, 2632–44 (2009)

155. Sonntag F, Bleker S, Leuchs B, Fischer R, Kleinschmidt JA: Adeno-associated virus type 2 capsids with externalized VP1/VP2 trafficking domains are generated prior to passage through the cytoplasm and are maintained until uncoating occurs in the nucleus. J Virol 80, 11040–54 (2006)

156. Kotin RM, Menninger JC, Ward DC, Berns KI: Mapping and direct visualization of a region-specific viral DNA integration site on chromosome 19q13-qter. Genomics 10, 831–4 (1991)

157. Samulski RJ, Zhu X, Xiao X, Brook JD, Housman DE, Epstein N, Hunter LA: Targeted integration of adeno-associated virus (AAV) into human chromosome 19. EMBO J 10, 3941–50 (1991)

158. Linden RM, Ward P, Giraud C, Winocour E, Berns KI: Site-specific integration by adeno-associated virus. Proc Natl Acad Sci U S A 93, 11288–94 (1996)

159. Samulski RJ, Muzyczka N: AAV-Mediated Gene Therapy for Research and Therapeutic Purposes. Annu Rev Virol 1, 427–51 (2014)

160. Wistuba A, Kern A, Weger S, Grimm D, Kleinschmidt JA: Subcellular compartmentalization of adeno-associated virus type 2 assembly. J Virol 71, 1341–52 (1997)

161. Xiao X, Li J, Samulski RJ: Production of high-titer recombinant adeno-associated virus vectors in the absence of helper adenovirus. J Virol 72, 2224–32 (1998)

162. Matsushita T, Elliger S, Elliger C, Podsakoff G, Villarreal L, Kurtzman GJ, Iwaki Y, Colosi P: Adeno-associated virus vectors can be efficiently produced without helper virus. Gene Ther 5, 938–45 (1998)

163. Grimm D, Kern A, Rittner K, Kleinschmidt JA: Novel tools for production and purification of recombinant adenoassociated virus vectors. Hum Gene Ther 9, 2745–60 (1998)

164. Wright JF: Manufacturing and characterizing AAV-based vectors for use in clinical studies. Gene Ther 15, 840–8 (2008)

165. Clément N, Grieger JC: Manufacturing of recombinant adeno-associated viral vectors for clinical trials. Mol Ther Methods Clin Dev 3, 16002 (2016)

166. Ferrari FK, Samulski T, Shenk T, Samulski RJ: Second-strand synthesis is a rate-limiting step for efficient transduction by recombinant adeno-associated virus vectors. J Virol 70, 3227–34 (1996)

167. Fisher KJ, Gao GP, Weitzman MD, DeMatteo R, Burda JF, Wilson JM: Transduction with recombinant adeno-associated virus for gene therapy is limited by leading-strand synthesis. J Virol 70, 520–32 (1996)

168. McCarty DM, Monahan PE, Samulski RJ: Self-complementary recombinant adeno-associated virus (scAAV) vectors promote efficient transduction independently of DNA synthesis. Gene Ther 8, 1248–54 (2001)

169. Dong JY, Fan PD, Frizzell RA: Quantitative analysis of the packaging capacity of recombinant adeno-associated virus. Hum Gene Ther 7, 2101–12 (1996)

170. Hermonat PL, Quirk JG, Bishop BM, Han L: The packaging capacity of adeno-associated virus (AAV) and the potential for wild-type-plus AAV gene therapy vectors. FEBS Lett 407, 78–84 (1997)

171. Wu Z, Yang H, Colosi P: Effect of genome size on AAV vector packaging. Mol Ther 18, 80–6 (2010)

172. Trapani I, Colella P, Sommella A, Iodice C, Cesi G, de Simone S, Marrocco E, Rossi S, Giunti M, Palfi A, Farrar GJ, Polishchuk R, Auricchio A: Effective delivery of large genes to the retina by dual AAV vectors. EMBO Mol Med 6, 194–211 (2014)

173. Pryadkina M, Lostal W, Bourg N, Charton K, Roudaut C, Hirsch ML, Richard I: A comparison of AAV strategies distinguishes overlapping vectors for efficient systemic delivery of the 6.2 kb Dysferlin coding sequence. Mol Ther Methods Clin Dev 2, 15009 (2015)

174. Zhong L, Li B, Mah CS, Govindasamy L, Agbandje-McKenna M, Cooper M, Herzog RW, Zolotukhin I, Warrington KH, Weigel-Van Aken KA, Hobbs JA, Zolotukhin S, Muzyczka N, Srivastava A: Next generation of adeno-associated virus 2 vectors: Point mutations in tyrosines lead to high-efficiency transduction at lower doses. Proc Natl Acad Sci 105, 7827–7832 (2008)

175. Song L, Kauss MA, Kopin E, Chandra M, Ul-Hasan T, Miller E, Jayandharan GR, Rivers AE, Aslanidi G V, Ling C, Li B, Ma W, Li X, Andino LM, Zhong L, Tarantal AF, Yoder MC, Wong KK, Tan M, Chatterjee S, Srivastava A: Optimizing the transduction efficiency of capsid-modified AAV6 serotype vectors in primary human hematopoietic stem cells in vitro and in a xenograft mouse model in vivo. Cytotherapy 15, 986–98 (2013)

176. Münch RC, Muth A, Muik A, Friedel T, Schmatz J, Dreier B, Trkola A, Plückthun A, Büning H, Buchholz CJ: Off-target-free gene delivery by affinity-purified receptor-targeted viral vectors. Nat Commun 6, 6246 (2015)

177. Cideciyan A V, Aleman TS, Boye SL, Schwartz SB, Kaushal S, Roman AJ, Pang J-J, Sumaroka A, Windsor EAM, Wilson JM, Flotte TR, Fishman GA, Heon E, Stone EM, Byrne BJ, Jacobson SG, Hauswirth WW: Human gene therapy for RPE65 isomerase deficiency activates the retinoid cycle of vision but with slow rod kinetics. Proc Natl Acad Sci U S A 105, 15112–7 (2008)

178. Nathwani AC, Tuddenham EGD, Rangarajan S, Rosales C, McIntosh J, Linch DC, Chowdary P, Riddell A, Pie AJ, Harrington C, O'Beirne J, Smith K, Pasi J, Glader B, Rustagi P, Ng CYC, Kay MA, Zhou J, Spence Y, Morton CL, Allay J, Coleman J, Sleep S, Cunningham JM, Srivastava D, Basner-Tschakarjan E, Mingozzi F, High KA, Gray JT, Reiss UM, Nienhuis AW, Davidoff AM: Adenovirus-Associated Virus Vector–Mediated Gene Transfer in Hemophilia B. http://dx.doi.org/101056/NEJMoa1108046 [Epub ahead of print], doi: 10.1056/NEJMOA1108046 (2011)

179. Miller DG, Wang P-R, Petek LM, Hirata RK, Sands MS, Russell DW: Gene targeting in vivo by adeno-associated virus vectors. Nat Biotechnol 24, 1022–6 (2006)

180. Paulk NK, Wursthorn K, Wang Z, Finegold MJ, Kay MA, Grompe M: Adeno-associated virus gene repair corrects a mouse model of hereditary tyrosinemia in vivo. Hepatology 51, 1200–8 (2010)

181. Li H, Malani N, Hamilton SR, Schlachterman A, Bussadori G, Edmonson SE, Shah R, Arruda VR, Mingozzi F, Wright JF, Bushman FD, High KA: Assessing the potential for AAV vector genotoxicity in a murine model. Blood 117, 3311–9 (2011)

182. Chirmule N, Xiao W, Truneh A, Schnell MA, Hughes J V, Zoltick P, Wilson JM: Humoral immunity to adeno-associated virus type 2 vectors following administration to murine and nonhuman primate muscle. J Virol 74, 2420–5 (2000)

183. Zaiss AK, Muruve DA: Immune responses to adeno-associated virus vectors. Curr Gene Ther 5, 323–31 (2005)

184. Nathwani AC, Reiss UM, Tuddenham EGD, Rosales C, Chowdary P, McIntosh J, Della Peruta M, Lheriteau E, Patel N, Raj D, Riddell A, Pie J, Rangarajan S, Bevan D, Recht M, Shen Y-M, Halka KG, Basner-Tschakarjan E, Mingozzi F, High KA, Allay J, Kay MA, Ng CYC, Zhou J, Cancio M, Morton CL, Gray JT, Srivastava D, Nienhuis AW, Davidoff AM: Long-Term Safety and Efficacy of Factor IX Gene Therapy in Hemophilia B. http://dx.doi.org/101056/NEJMoa1407309 [Epub ahead of print], doi: 10.1056/NEJMOA1407309 (2014)

185. Niemeyer GP, Herzog RW, Mount J, Arruda VR, Tillson DM, Hathcock J, van Ginkel FW, High KA, Lothrop CD: Long-term correction of inhibitor-prone hemophilia B dogs treated with liver-directed AAV2-mediated factor IX gene therapy. Blood 113, 797–806 (2009)

186. Li C, Narkbunnam N, Samulski RJ, Asokan A, Hu G, Jacobson LJ, Manco-Johnson MJ, Monahan PE, Joint Outcome Study Investigators: Neutralizing antibodies against adeno-associated virus examined prospectively in pediatric patients with hemophilia. Gene Ther 19, 288–94 (2012)

187. Boutin S, Monteilhet V, Veron P, Leborgne C, Benveniste O, Montus MF, Masurier C: Prevalence of serum IgG and neutralizing factors against adeno-associated virus (AAV) types 1, 2, 5, 6, 8, and 9 in the healthy population: implications for gene therapy using AAV vectors. Hum Gene Ther 21, 704–12 (2010)

188. Jordan A, Bisgrove D, Verdin E: HIV reproducibly establishes a latent infection after acute infection of T cells in vitro. EMBO J 22, 1868–77 (2003)

189. Northrop JP, Ullman KS, Crabtree GR: Characterization of the nuclear and cytoplasmic components of the lymphoid-specific nuclear factor of activated T cells (NF-AT) complex. J Biol Chem 268, 2917–23 (1993)

190. Pear WS, Nolan GP, Scott ML, Baltimore D: Production of high-titer helper-free retroviruses by transient transfection. Proc Natl Acad Sci U S A 90, 8392–6 (1993)

191. Charneau P, Alizon M, Clavel F: A second origin of DNA plus-strand synthesis is required for optimal human immunodeficiency virus replication. J Virol 66, 2814–20 (1992)

192. Harada S, Koyanagi Y, Yamamoto N: Infection of HTLV-III/LAV in HTLV-I-carrying cells MT-2 and MT-4 and application in a plaque assay. Science 229, 563–6 (1985)

193. Joseph AM, Ladha JS, Mojamdar M, Mitra D: Human immunodeficiency virus-1 Nef protein interacts with Tat and enhances HIV-1 gene expression. FEBS Lett 548, 37–42 (2003)

194. Lampe M, Briggs JAG, Endress T, Glass B, Riegelsberger S, Kräusslich H-G, Lamb DC, Bräuchle C, Müller B: Double-labelled HIV-1 particles for study of virus-cell interaction. Virology 360, 92–104 (2007)

195. Adachi A, Gendelman HE, Koenig S, Folks T, Willey R, Rabson A, Martin MA: Production of acquired immunodeficiency syndrome-associated retrovirus in human and nonhuman cells transfected with an infectious molecular clone. J Virol 59, 284–91 (1986)

196. Ran FA, Hsu PD, Wright J, Agarwala V, Scott DA, Zhang F: Genome engineering using the CRISPR-Cas9 system. Nat Protoc 8, 2281–2308 (2013)

197. Sander JD, Maeder ML, Reyon D, Voytas DF, Joung JK, Dobbs D: ZiFiT (Zinc Finger Targeter): an updated zinc finger engineering tool. Nucleic Acids Res 38, W462–8 (2010)

198. Sander JD, Zaback P, Joung JK, Voytas DF, Dobbs D: Zinc Finger Targeter (ZiFiT): an engineered zinc finger/target site design tool. Nucleic Acids Res 35, W599–605 (2007)

199. ter Brake O, Konstantinova P, Ceylan M, Berkhout B: Silencing of HIV-1 with RNA interference: a multiple shRNA approach. Mol Ther 14, 883–92 (2006)

200. Cho SW, Kim S, Kim Y, Kweon J, Kim HS, Bae S, Kim J-S: Analysis of off-target effects of CRISPR/Cas-derived RNA-guided endonucleases and nickases. Genome Res 24, 132–41 (2014)

201. Senís E, Fatouros C, Große S, Wiedtke E, Niopek D, Mueller A-K, Börner K, Grimm D: CRISPR/Cas9-mediated genome engineering: An adeno-associated viral (AAV) vector toolbox. Biotechnol J 9, 1402–12 (2014)

202. Chen B, Gilbert LA, Cimini BA, Schnitzbauer J, Zhang W, Li G-W, Park J, Blackburn EH, Weissman JS, Qi LS, Huang B: Dynamic imaging of genomic loci in living human cells by an optimized CRISPR/Cas system. Cell 155, 1479–91 (2013)

203. Bannwarth S, Gatignol A: HIV-1 TAR RNA: the target of molecular interactions between the virus and its host. Curr HIV Res 3, 61–71 (2005)

204. Brady J, Kashanchi F: Tat gets the "green" light on transcription initiation. Retrovirology 2, 69 (2005)

205. Börner K, Hermle J, Sommer C, Brown NP, Knapp B, Glass B, Kunkel J, Torralba G, Reymann J, Beil N, Beneke J, Pepperkok R, Schneider R, Ludwig T, Hausmann M, Hamprecht F, Erfle H, Kaderali L, Kräusslich H-G, Lehmann MJ: From experimental setup to bioinformatics: an RNAi screening platform to identify host factors involved in HIV-1 replication. Biotechnol J 5, 39–49 (2010)

206. Bieniasz PD, Cullen BR: Multiple blocks to human immunodeficiency virus type 1 replication in rodent cells. J Virol 74, 9868–77 (2000)

207. Lenasi T, Contreras X, Peterlin BM: Transcriptional interference antagonizes proviral gene expression to promote HIV latency. Cell Host Microbe 4, 123–33 (2008)

208. Frauwirth KA, Thompson CB: Activation and inhibition of lymphocytes by costimulation. J Clin Invest 109, 295–9 (2002)

209. Chilson OP, Boylston AW, Crumpton MJ: Phaseolus vulgaris phytohaemagglutinin (PHA) binds to the human T lymphocyte antigen receptor. EMBO J 3, 3239–45 (1984)

210. Roychoudhury P, De Silva Feelixge H, Reeves D, Mayer BT, Stone D, Schiffer JT, Jerome KR: Viral diversity is an obligate consideration in CRISPR/Cas9 designs for targeting the HIV reservoir. BMC Biol 16, 75 (2018)

211. Wang G, Zhao N, Berkhout B, Das AT: CRISPR-Cas9 can inhibit HIV-1 replication but NHEJ repair facilitates virus escape. Mol Ther 24, 522–6 (2016)

212. Mefferd AL, Bogerd HP, Irwan ID, Cullen BR: Insights into the mechanisms underlying the inactivation of HIV-1 proviruses by CRISPR/Cas. Virology 520, 116–126 (2018)

213. Ophinni Y, Inoue M, Kotaki T, Kameoka M: CRISPR/Cas9 system targeting regulatory genes of HIV-1 inhibits viral replication in infected T-cell cultures. Sci Rep 8, 7784 (2018)

214. Yin C, Zhang T, Li F, Yang F, Putatunda R, Young W-B, Khalili K, Hu W, Zhang Y: Functional screening of guide RNAs targeting the regulatory and structural HIV-1 viral genome for a cure of AIDS. AIDS 30, 1163–74 (2016)

215. Zhu W, Lei R, Le Duff Y, Li J, Guo F, Wainberg MA, Liang C: The CRISPR/Cas9 system inactivates latent HIV-1 proviral DNA. Retrovirology 12, 22 (2015)

216. Liao H-K, Gu Y, Diaz A, Marlett J, Takahashi Y, Li M, Suzuki K, Xu R, Hishida T, Chang C-J, Esteban CR, Young J, Izpisua Belmonte JC: Use of the CRISPR/Cas9 system as an intracellular defense against HIV-1 infection in human cells. Nat Commun 6, 6413 (2015)

217. Wang G, Zhao N, Berkhout B, Das AT: A Combinatorial CRISPR-Cas9 Attack on HIV-1 DNA Extinguishes All Infectious Provirus in Infected T Cell Cultures. Cell Rep 17, 2819–2826 (2016)

218. Lebbink RJ, de Jong DCM, Wolters F, Kruse EM, van Ham PM, Wiertz EJHJ, Nijhuis M: A combinational CRISPR/Cas9 gene-editing approach can halt HIV replication and prevent viral escape. Sci Rep 7, 41968 (2017)

219. Uusi-Mäkelä MIE, Barker HR, Bäuerlein CA, Häkkinen T, Nykter M, Rämet M: Chromatin accessibility is associated with CRISPR-Cas9 efficiency in the zebrafish (Danio rerio). PLoS One 13, e0196238 (2018)

220. Wright A V, Sternberg SH, Taylor DW, Staahl BT, Bardales JA, Kornfeld JE, Doudna JA: Rational design of a split-Cas9 enzyme complex. Proc Natl Acad Sci U S A 112, 2984–9 (2015)

221. Hu W, Kaminski R, Yang F, Zhang Y, Cosentino L, Li F, Luo B, Alvarez-Carbonell D, Garcia-Mesa Y, Karn J, Mo X, Khalili K: RNA-directed gene editing specifically eradicates latent and prevents new HIV-1 infection. Proc Natl Acad Sci U S A 111, 11461–11466 (2014)

222. Kaminski R, Chen Y, Fischer T, Tedaldi E, Napoli A, Zhang Y, Karn J, Hu W, Khalili K: Elimination of HIV-1 Genomes from Human T-lymphoid Cells by CRISPR/Cas9 Gene Editing. Sci Rep 6, 22555 (2016)

223. Wang Z, Pan Q, Gendron P, Zhu W, Guo F, Cen S, Wainberg MA, Liang C: CRISPR/Cas9-Derived Mutations Both Inhibit HIV-1 Replication and Accelerate Viral Escape. Cell Rep 15, 481–489 (2016)

224. Ueda S, Ebina H, Kanemura Y, Misawa N, Koyanagi Y: Anti-HIV-1 potency of the CRISPR/Cas9 system insufficient to fully inhibit viral replication. Microbiol Immunol 60, 483–96 (2016)

225. Yoder KE, Bundschuh R: Host Double Strand Break Repair Generates HIV-1 Strains Resistant to CRISPR/Cas9. Sci Rep 6, 29530 (2016)

226. Zhao N, Wang G, Das AT, Berkhout B: Combinatorial CRISPR-Cas9 and RNA Interference Attack on HIV-1 DNA and RNA Can Lead to Cross-Resistance. Antimicrob Agents Chemother 61, (2017)

227. Wang Z, Wang W, Cui YC, Pan Q, Zhu W, Gendron P, Guo F, Cen S, Witcher M, Liang C: HIV-1 Employs Multiple Mechanisms To Resist Cas9/Single Guide RNA Targeting the Viral Primer Binding Site. J Virol 92, JVI.01135–18 (2018)

228. Gao Z, Herrera-Carrillo E, Berkhout B: RNA Polymerase II Activity of Type 3 Pol III Promoters. Mol Ther Nucleic Acids 12, 135–145 (2018)

229. Wang G, Zhao N, Berkhout B, Das AT: CRISPR-Cas9 Can Inhibit HIV-1 Replication but NHEJ Repair Facilitates Virus Escape. Mol Ther 24, 522–6 (2016)

230. Jordan A, Bisgrove D, Verdin E: HIV reproducibly establishes a latent infection after acute infection of T cells in vitro. EMBO J 22, 1868–77 (2003)

231. Canver MC, Bauer DE, Dass A, Yien YY, Chung J, Masuda T, Maeda T, Paw BH, Orkin SH: Characterization of genomic deletion efficiency mediated by clustered regularly interspaced short palindromic repeats (CRISPR)/Cas9 nuclease system in mammalian cells. J Biol Chem 289, 21312–24 (2014)

232. Bauer DE, Canver MC, Orkin SH: Generation of genomic deletions in mammalian cell lines via CRISPR/Cas9. J Vis Exp e52118 (2015)

233. Ebina H, Misawa N, Kanemura Y, Koyanagi Y: Harnessing the CRISPR/Cas9 system to disrupt latent HIV-1 provirus. Sci Rep 3, 2510 (2013)

234. Gao Z, Harwig A, Berkhout B, Herrera-Carrillo E: Mutation of nucleotides around the +1 position of type 3 polymerase III promoters: The effect on transcriptional activity and start site usage. Transcription 8, 275–287 (2017)

235. Ellis BL, Hirsch ML, Barker JC, Connelly JP, Steininger RJ, Porteus MH: A survey of ex vivo/in vitro transduction efficiency of mammalian primary cells and cell lines with Nine natural adeno-associated virus (AAV1-9) and one engineered adeno-associated virus serotype. Virol J 10, 74 (2013)

236. Wang J, DeClercq JJ, Hayward SB, Li PW-L, Shivak DA, Gregory PD, Lee G, Holmes MC: Highly efficient homology-driven genome editing in human T cells by combining zinc-finger nuclease mRNA and AAV6 donor delivery. Nucleic Acids Res 44, e30 (2016)

237. Kandathil AJ, Sugawara S, Balagopal A: Are T cells the only HIV-1 reservoir? Retrovirology 13, 86 (2016)

238. Jones S, Peng PD, Yang S, Hsu C, Cohen CJ, Zhao Y, Abad J, Zheng Z, Rosenberg SA, Morgan RA: Lentiviral vector design for optimal T cell receptor gene expression in the transduction of peripheral blood lymphocytes and tumor-infiltrating lymphocytes. Hum Gene Ther 20, 630–40 (2009)

239. Halbert CL, Alexander IE, Wolgamot GM, Miller AD: Adeno-associated virus vectors transduce primary cells much less efficiently than immortalized cells. J Virol 69, 1473–9 (1995)

240. Ling C, Bhukhai K, Yin Z, Tan M, Yoder MC, Leboulch P, Payen E, Srivastava A: High-Efficiency Transduction of Primary Human Hematopoietic Stem/Progenitor Cells by AAV6 Vectors: Strategies for Overcoming Donor-Variation and Implications in Genome Editing. Sci Rep 6, 35495 (2016)

241. Chun TW, Carruth L, Finzi D, Shen X, DiGiuseppe JA, Taylor H, Hermankova M, Chadwick K, Margolick J, Quinn TC, Kuo YH, Brookmeyer R, Zeiger MA, Barditch-Crovo P, Siliciano RF: Quantification of latent tissue reservoirs and total body viral load in HIV-1 infection. Nature 387, 183–8 (1997)

242. Finzi D, Hermankova M, Pierson T, Carruth LM, Buck C, Chaisson RE, Quinn TC, Chadwick K, Margolick J, Brookmeyer R, Gallant J, Markowitz M, Ho DD, Richman DD, Siliciano RF: Identification of a reservoir for HIV-1 in patients on highly active antiretroviral therapy. Science 278, 1295–300 (1997)

243. Mailler E, Bernacchi S, Marquet R, Paillart J-C, Vivet-Boudou V, Smyth RP: The Life-Cycle of the HIV-1 Gag-RNA Complex. Viruses 8, (2016)

244. Robinson HL: New hope for an AIDS vaccine. Nat Rev Immunol 2, 239–50 (2002)

245. Gebre M, Nomburg JL, Gewurz BE: CRISPR-Cas9 Genetic Analysis of Virus-Host Interactions. Viruses 10, (2018)

246. Herrmann A-K, Grimm D: High-Throughput Dissection of AAV-Host Interactions: The Fast and the Curious. J Mol Biol 430, 2626–2640 (2018)

7. Acknowledgements

In general I am very thankful to all members of the Kräusslich, Grimm and Müller groups for creating a very good working atmosphere.

Especially, I want to thank my running mates Susann Kummer and Annika Flemming for all the fun runs after work which let me forget stressful lab days. I really miss that!

A big thanks to the members of the Erfle lab Jürgen Beneke, Ruben Bulkescher and Nina Beil. You made the time in Bioquant so much fun! A special thanks to Ruben for his helpful corrections of the manuscript.

A very special thanks goes to Julia Fakhiri and Vilmante Zitkute, my best friends during my time in Heidelberg. If you have crazy friends you have everything! I will never forget all the wonderful evenings with you.

Furthermore, I want to thank my new colleges in Tübingen for the warm welcome and for their understanding which made it much easier to write the thesis and work in parallel.

I am deeply thankful to Flo for being there during the last months. Thank you for your understanding and support. You made the hard times so much easier!

Finally, I thank my parents and my brother for supporting me during the whole studies and for always being there! I could not imagine having a better family!